

Report of Investigations 2006-2  
Version 1.0.1

**BEDROCK GEOLOGIC MAP OF THE LIBERTY BELL  
AREA, FAIRBANKS A-4 QUADRANGLE, BONNIFIELD  
MINING DISTRICT, ALASKA**

by

J.E. Athey, R.J. Newberry, M.B. Werdon,  
L.K. Freeman, R.L. Smith, and D.J. Szumigala



**Published by**

STATE OF ALASKA  
DEPARTMENT OF NATURAL RESOURCES

DIVISION OF GEOLOGICAL & GEOPHYSICAL SURVEYS

**2006**

**Report of Investigations 2006-2**  
Version 1.0.1

**BEDROCK GEOLOGIC MAP OF THE LIBERTY BELL  
AREA, FAIRBANKS A-4 QUADRANGLE, BONNIFIELD  
MINING DISTRICT, ALASKA**

by

J.E. Athey, R.J. Newberry, M.B. Werdon,  
L.K. Freeman, R.L. Smith, and D.J. Szumigala

2006

This DGGS Report of Investigations is a final report of scientific research.  
It has received technical review and may be cited as an agency publication.



STATE OF ALASKA  
Frank Murkowski, *Governor*

DEPARTMENT OF NATURAL RESOURCES  
Mike Menge, *Commissioner*

DIVISION OF GEOLOGICAL & GEOPHYSICAL SURVEYS  
Robert F. Swenson, *Acting State Geologist and Acting Director*

Division of Geological & Geophysical Surveys publications can be inspected at the following locations. Address mail orders to the Fairbanks office.

Alaska Division of Geological  
& Geophysical Surveys  
3354 College Road  
Fairbanks, Alaska 99709-3707

University of Alaska Anchorage Library  
3211 Providence Drive  
Anchorage, Alaska 99508

Elmer E. Rasmuson Library  
University of Alaska Fairbanks  
Fairbanks, Alaska 99775-1005

Alaska Resource Library  
and Information Services (ARLIS)  
3150 C Street, Suite 100  
Anchorage, Alaska 99503

Alaska State Library  
State Office Building, 8th Floor  
333 Willoughby Avenue  
Juneau, Alaska 99811-0571

This publication released by the Division of Geological & Geophysical Surveys was produced and printed in Fairbanks, Alaska at a cost of \$23 per copy. Publication is required by Alaska Statute 41, "to determine the potential of Alaskan land for production of metals, minerals, fuels, and geothermal resources; the location and supplies of groundwater and construction materials; the potential geologic hazards to buildings, roads, bridges, and other installations and structures; and shall conduct such other surveys and investigations as will advance knowledge of the geology of Alaska."

## CONTENTS

Abstract .....	1
Introduction .....	2
Discussion of geology .....	3
Lithologic studies and interpretation .....	3
Quaternary units .....	3
Tertiary sedimentary rocks .....	3
Paleozoic units .....	12
Totatlanika Schist .....	12
Keivy Peak Formation .....	13
Structure .....	18
Mineralization and Cretaceous intrusions .....	20
Unit descriptions .....	24
Tertiary sedimentary rocks .....	24
Tertiary–Cretaceous igneous rocks .....	26
Paleozoic units .....	27
Acknowledgments .....	30
References cited .....	31

## TABLES

Table 1. Clustered items shown with their corresponding distance coefficients .....	5
2. Normalized major point-count parameters of Tertiary sandstone .....	8
3. Qualitative comparison of montmorillonite and kaolinite content in Nenana Gravel and Usibelli Group clays .....	11
4. Pollen samples from random outcrop locations in the Tertiary Usibelli Group .....	11
5. Interpreted <sup>40</sup> Ar/ <sup>39</sup> Ar ages for selected samples from the Liberty Bell area, Fairbanks A-4 Quadrangle .....	14
6. Placer gold composition from Little Moose Creek .....	22

## FIGURES

Figure 1. Location figure showing the map and airborne geophysical survey areas in relation to rural communities, transportation systems, and utilities .....	2
2. Dendrogram showing statistical distance between samples (or degree of dissimilarity) versus groupings of similarly composed Tertiary sandstone .....	5
3. Tectonic provenance for Usibelli Group and Nenana Gravel sandstone clasts .....	9
4. Paleocurrent directions measured from cross-beds in the Liberty Bell area .....	10
5. Summary of SHRIMP U-Pb ages from Paleozoic rocks collected in the Alaska Range Foothills .....	13
6. Discriminant analysis of metasedimentary and meta-igneous rocks from the Liberty Bell area .....	16
7. Tectonic setting for igneous and meta-igneous rocks from the Liberty Bell area as indicated by trace-element discrimination diagrams .....	19
8. Gridded ore-element data from rock samples in the Liberty Bell Mine area .....	21
9. Typical(?) gold composition patterns for Interior Alaskan intrusion-related deposits .....	23

## APPENDICES

Appendix A.	Geochemical analyses of Paleozoic samples .....	35
B.	<sup>40</sup> Ar/ <sup>39</sup> Ar analyses .....	47
C.	Grain-mount petrology of Tertiary samples .....	59
D.	Clay compositions of Tertiary samples .....	71
E.	Palynology .....	75
F.	Energy and geochemical analyses of coal and coal ash .....	83
G.	Alaska Resource Data File occurrences in the southern half of the Fairbanks A-4 Quadrangle .....	95

## SHEET

(in envelope)

Bedrock geologic map of the Liberty Bell area, Fairbanks A-4 Quadrangle, Bonnifield mining district, Alaska

# BEDROCK GEOLOGIC MAP OF THE LIBERTY BELL AREA, FAIRBANKS A-4 QUADRANGLE, BONNIFIELD MINING DISTRICT, ALASKA

by

Jennifer E. Athey<sup>1</sup>, Rainer J. Newberry<sup>2</sup>, Melanie B. Werdon<sup>1</sup>,  
Lawrence K. Freeman<sup>1</sup>, Robin L. Smith<sup>1</sup>, and David J. Szumigala<sup>1</sup>

## Abstract

The geology of the Liberty Bell area, located in the northern Alaska Range foothills, comprises Devonian metasedimentary and meta-igneous rocks of the Totatlanika Schist and Keevy Peak formations, Cretaceous and Tertiary igneous rocks, and overlying unconsolidated Tertiary sedimentary rocks of the Usibelli Group and the younger Nenana Gravel. Broad folds and high-angle faults form and expose east–west-trending bands of Paleozoic and Tertiary rocks across the map area. Ore-element geochemistry and geologic mapping suggest the east–west-oriented faults are reactivated (latest apparent movement is reverse on north-dipping [57–90°] faults in the Liberty Bell Mine area); northeast- and northwest-trending structures may be activated fracture sets. Thrust faults postulated to accommodate north-directed compression from active uplift of the Alaska Range were not recognized in the map area, but they may be present at depth.

Tertiary Usibelli Group and Nenana Gravel outcrops commonly contain interbedded sand and gravel with no distinctive lithologies within or between the formations. A petrographic study of sand composition yielded data that can be used to classify the formations. Sand from the Nenana Gravel contains a diverse population of unstable rock fragment compositions while the Usibelli Group sand contains a higher percentage of stable rock fragments. The percentage of stable rock fragments increases down-section in the Usibelli Group. This relationship is also recognized by previous workers in the Suntrana Creek area to the south, where a similar geologic section exists. Paleotopographic differences may be responsible for discrepancies in the Usibelli Group between the Suntrana Creek section and the Liberty Bell area units, including contrasting paleocurrent directions (south- versus west-directed), the absence of the Grubstake Formation, and coarsening of the Lignite Creek Formation to the north.

Bedrock units California Creek and Moose Creek (members of the Totatlanika Schist) and the Keevy Peak Formation are composed of metasedimentary and lesser meta-igneous rocks. The similar-looking rocks can be distinguished with a combination of trace-element compositions ( $\text{Nb} + \text{Y} < 50$  ppm = metasedimentary;  $\text{Nb} + \text{Y} > 50$  ppm = meta-igneous), modal composition, and relict textures (embayed crystals, graded bedding, grain sorting, etc.) as seen on cut surfaces or in thin sections. The Keevy Peak Formation is composed of graphitic quartzite and metamorphosed quartz wacke. The California Creek Member is primarily composed of metamorphosed arkosic wacke and other minor metasedimentary rocks, but it also contains metamorphosed, generally hypabyssal, granitic intrusions and rare metabasite. The Moose Creek Member previously mapped in the Fairbanks A-4 Quadrangle is a metamorphosed granitic intrusion indistinguishable from the meta-igneous units within the California Creek Member.

An east–west-trending band of metasedimentary (quartzite, graphitic quartzite, and metawacke) and meta-igneous (metamorphosed felsic and mafic intrusions and flows[?]) rocks mapped within the California Creek member hosts the Liberty Bell Mine, the major plutonic-related gold deposit in the area. Mineralization occurs as pyrrhotite ± gold ± arsenopyrite + actinolite + biotite skarn (metasomatized carbonate-altered metabasite) and arsenopyrite ± gold ± bismuth minerals ± stibnite ± tourmaline + quartz veins and replacements. A positive aeromagnetic anomaly (8 by 5.5 km) and the extent of hornfels and hydrothermal alteration suggest the Liberty Bell Mine area is underlain by a large pluton. This body is expressed on the surface by granite and granodiorite dikes with consistent <sup>40</sup>Ar/<sup>39</sup>Ar and K-Ar ages of approximately 92–93 Ma. A comparison of placer gold fineness (~830), estimated temperature of mineral assemblage formation (300–350° C), and extent of hornfels with other plutonic-related deposits in Interior Alaska suggests that the pluton is emplaced approximately 300–1,200 m below the surface. Given the depth of the pluton, viable exploration targets in the mine area include replacement/skarn and structurally controlled mineralization, both of which are documented at Liberty Bell.

<sup>1</sup>Alaska Division of Geological & Geophysical Surveys, 3354 College Rd., Fairbanks, Alaska 99709-3707  
Email for Jennifer Athey: Jennifer\_Athey@dnr.state.ak.us

<sup>2</sup>Department of Geology & Geophysics, University of Alaska, P.O. Box 755780, Fairbanks, Alaska 99775-5780

## INTRODUCTION

This booklet accompanies *Bedrock geologic map of the Liberty Bell area, Fairbanks A-4 Quadrangle, Bonnifield mining district, Alaska*, a 1:50,000-scale map covering the southern half of the Fairbanks A-4 Quadrangle. The booklet contains unit descriptions and supporting information. The map area covers the southern 340 square km of the Liberty Bell airborne geophysical survey (Burns and others, 2002). This project is part of the State's Airborne Geophysical/Geological Mineral Inventory program, which seeks to delineate mineral zones on Alaska state lands that: (1) have major economic value; (2) can be developed in the short term to provide high-quality jobs for Alaska; and (3) will provide diversification of the State's economic base. New geologic mapping in historic mining areas such as the western Bonnifield district that incorporates interpretation of high-quality geophysical data will provide information that could lead to renewed exploration and mine development.

The Liberty Bell map area is located 96 km southwest of Fairbanks and 320 km north of Anchorage (fig. 1). The map area is situated in the western half of the Bonnifield mining district, which extends across the north flank of the Alaska Range for approximately 65 km. Approximately 85,000 ounces of placer gold have been mined from the region since 1903 (Szumigala and Hughes, 2005), with most production between the

Totatlanika River and Ferry, Alaska. Eleven placer gold mines (three active) and eight metallic lode occurrences are located in the map area (Freeman and Schaefer, 2001). The Liberty Bell gold mine is the major lode occurrence known in the mining district. The Liberty Bell property has an announced potential of 250,000 ounces of gold, with inferred resources of 1,240,000 tons at an average grade of 0.1 ounces of gold per ton at the Mine Zone (Freeman and Schaefer, 2001). The map area also covers the northern edge of the Nenana coal basin. Tertiary units contain coal resources and the possibility of shallow natural gas. Mineral, shallow natural gas, and coal targets within the map area have recently been selected or are actively being explored by industry.

The western part of the mining district is highly accessible, with extensive infrastructure for mineral development (fig. 1). Alaska's main ground transportation corridor between Anchorage and Fairbanks, containing the Parks Highway and Alaska Railroad, runs 8 km west of the western edge of the study area. A well maintained, 16-km-long dirt road (informally known as the Ferry Road) and numerous spur trails exist between the Liberty Bell Mine near the center of the map area and Ferry. In addition, two high-voltage interties, which run parallel to the Parks Highway and railroad corridors, connect the Healy Power Plant (located 19 km south of the map area) to the power grid that provides electricity to Fairbanks, Anchorage, and numerous railbelt communities.

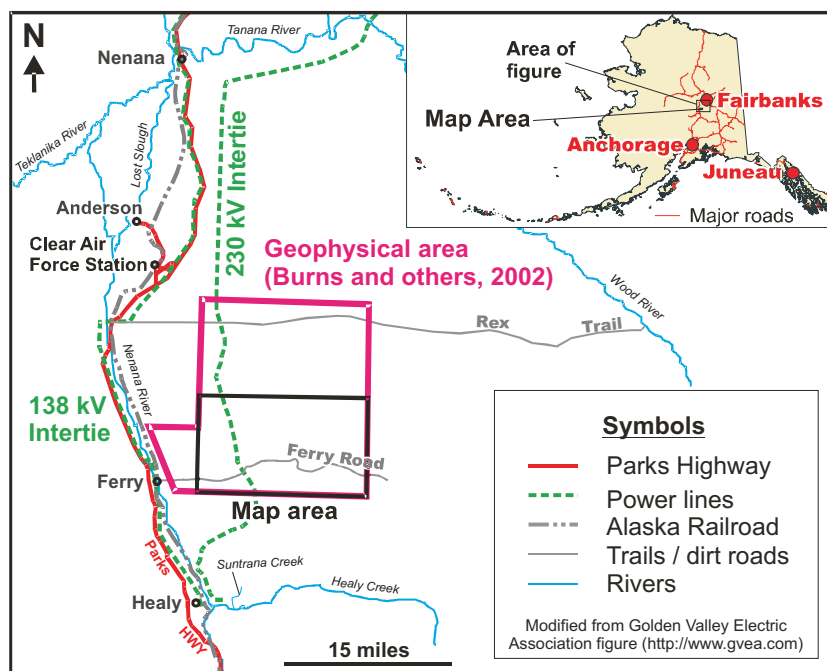


Figure 1. Location figure showing the map and airborne geophysical survey areas in relation to rural communities, transportation systems, and utilities.

During July 2005, personnel from the Alaska Division of Geological & Geophysical Surveys (DGGS) and the University of Alaska Fairbanks spent approximately 105 person days conducting field work in the Liberty Bell area. A variety of data were used to create the geologic map. Total field magnetic and electromagnetic geophysical data (Burns and others, 2002) aided our bedrock mapping, especially in areas covered by vegetation and unconsolidated Quaternary deposits. For example, our interpretation of the geophysical data reveals locations of pyrrhotite-bearing hornfels, burned coal and sedimentary units, and structures that would otherwise remain undetected by conventional surface mapping methods.

Preliminary interpretation of air photos allowed identification of linear features that were utilized in the structural interpretation. Air photos used in this study include color-infrared photographs at a scale of approximately 1:63,360 that were taken in August 1981. These linear features were identified during a simultaneous surficial-geologic study being conducted by DGGS in the field area largely from interpretation of aerial photography, revision of historical data, and limited field work. From this additional study, we anticipate the completion of a comprehensive-geologic and a surficial-geologic map in winter 2006. The comprehensive geologic map will depict Paleozoic bedrock geology, covered by Tertiary and Quaternary units.

Geologic units are defined by field observations and analysis of samples collected at more than 1,405 stations in 2005. Paleozoic rocks and younger, unmetamorphosed igneous rocks were primarily defined by chemical composition, examination of hand samples, and petrography. Approximately 280 samples were analyzed for major-and minor-oxide and trace elements by a commercial analytical laboratory (Athey and others, 2005) and the University of Alaska Fairbanks (appendix A). These data are used to suggest possible protoliths of metamorphosed and altered rocks, identify types of alteration, and assign trace-element indicated tectonic settings to igneous and meta-igneous rocks. Unit descriptions are also based on the petrographic examination and modal analysis of 169 thin sections. Six  $^{40}\text{Ar}/^{39}\text{Ar}$  ages (table 5; appendix B) were used to constrain timing of igneous events, mineralization, and metamorphism in the Liberty Bell Mine area. (Liberty Bell Mine area is defined as the western, rounded portion of the area outlined on sheet 1 as underlain by the subsurface pluton [see 'Map Symbols']; area is outlined in figure 'Location Map of the Liberty Bell Mine area and hill VABM Coal' on sheet 1. The area coincides with a donut-shaped, aeromagnetic high [Burns and others, 2002]). Tertiary units were differentiated by a combination of field observations, cluster analysis of sand grain composition, clay composition, and palynology. Sixty

grain mounts of Tertiary sand were point-counted (appendix C) in order to compare sand composition. Clay compositions were determined by X-ray diffraction for 65 samples of unconsolidated rock (appendix D). Pollen was identified and counted in 15 samples of fine-grained Tertiary sedimentary rock and coal (appendix E).

To evaluate the mineral-resource potential of the Liberty Bell area, 116 samples of visibly mineralized rock, or rock exhibiting features associated with mineralization, were analyzed for geochemical trace elements (Athey and others, 2005). To evaluate the energy-resource potential of the Liberty Bell area, 21 coal samples were analyzed for energy values (proximate and ultimate analyses, BTU, etc.) and trace elements of their ash (appendix F). The composition of a placer gold sample was determined by X-ray fluorescence (table 6). Historical and mineral industry data were incorporated into the data set wherever possible. Locations and descriptions of Alaska Resource Data File occurrences (Freeman and Schafer, 2001) are compiled in appendix G. Unpublished mapping conducted in 1994 by DGGS personnel, geologic maps created by mineral exploration companies, and industry geochemical data were utilized in this study (Freeman and others, 1987; Puchner and Freeman, 1988; Galey and others, 1993; Bidwell, 1994; DGGS, 1994). We especially thank the Blair family, Wallace O. Turner, II, and Jim Roland for allowing us to compile and publish industry geologic information held by them, which greatly enhanced the quality of our map and interpretations.

## **DISCUSSION OF GEOLOGY**

---

### **LITHOLOGIC STUDIES AND INTERPRETATIONS**

#### **QUATERNARY UNITS**

A diverse suite of Quaternary materials, including glacial, alluvial, landslide, fan, and swamp deposits, discontinuously overlie older units in the area. Placer deposits of unknown age (Holocene or Pleistocene) and character are also located throughout the map area, which suggests that multiple sources of lode gold are exposed and shedding detritus. The placer gold has two morphologies, one is smooth and rounded, probably reworked from older Quaternary placers or possibly from Tertiary units, and the other is pristine gold presumably eroded from nearby lode sources (R.W. Flanders, oral commun., 2005).

#### **TERTIARY SEDIMENTARY ROCKS**

Tertiary Nenana gravel and sand derived from the post-Middle Miocene uplift of the Alaska Range (Plafker and others, 1992) overlies older, poorly lithified, Tertiary continental clastic rocks of the coal-bearing Usibelli

Group. The Usibelli Group unconformably overlies Paleozoic metamorphic rocks. Wahrhaftig and others (1969) separated the Usibelli Group into five formations: Grubstake, Lignite Creek, Suntrana, Sanctuary, and Healy Creek (youngest to oldest, respectively). In the map area, two of the five Usibelli Group formations, the Grubstake and Sanctuary Formations, were not recognized. The Suntrana Formation south of the map area contains known surface-mineable coal reserves in excess of 100 million tons that are currently being processed at the Usibelli Coal Mine east of Healy (<http://www.usibelli.com/>).

Tertiary outcrops were mapped by comparison to the Suntrana Creek section, located 15 km south of the map area, where the entire Usibelli Group and a large portion of the Nenana Gravel are exposed (Wahrhaftig, 1987). Unlike the excellent exposures of the Tertiary section in the Suntrana Creek area, Tertiary units in the map area are poorly exposed and crop out in about 2 percent of the map area; outcrops average ~5 m in width and ~5 m in height. No unit is completely exposed at any location in the map area, which severely hinders correlating units between locations. Because outcrops are rare and gravel lag deposits are common on the surface, Tertiary samples were collected in pits at least 0.3 meters deep, and commonly 0.5 to more than a meter deep. Also unlike the Suntrana Creek section, the Tertiary stratigraphic section in the map area is rarely complete. Entire formations are frequently missing from the section, possibly from deposition on an irregular topographic surface and differential erosion.

Lack of exposures, complete sections, and marker units such as the distinctive shale units, Grubstake and Sanctuary Formations, hindered the authors' ability to confidently assign a particular formation to a field station. In order to refine or confirm the identity of the Tertiary units, field calls were supplemented by cluster analysis of sand modal compositions and comparison of sand compositions, clay compositions, and pollen taxa with other data sets from the same units. Future study of the Tertiary units could include additional coal energy and ash trace-element analyses and comparison of these compositions to more comprehensive data sets.

Sixty grain mounts of unconsolidated sandstone were point-counted to determine sand composition using the methodology of Decker (1985) and the "traditional" methodology of Ingersoll and others (1984). Hierarchical cluster classification was used to combine the samples into groups in a relatively unbiased manner. Davis (1986) describes hierarchical cluster analysis as an iterative process where similar samples are successively joined together. A matrix is computed for the total number of samples ( $n$ ), which contains coefficients of similarity (referred to here as coefficients of statistical distance) for each pair of samples. The pair with the

lowest distance coefficient is more similar than any other pair in the data set; these samples are grouped together into a 'cluster.' A new mean value is computed for the new cluster, and the matrix is recomputed for ' $n - 1$ ' individual samples and one cluster. The process is repeated until all individual samples are combined into the minimum number of clusters requested. Clusters are then arranged on a dendrogram vertically according to their similarity to other clusters, and the general value of the distance coefficients used for joining the clusters are also displayed. For the current project, the cluster analyses for the 60 grain mounts were calculated using the computer program SPSS and an algorithm using the between-group (average) linkage method where the interval measured is the squared Euclidean distance. The program was instructed to arrange all individual samples into 15 through 2 clusters; since only four geologic units (Nenana Gravel, Lignite Creek, Suntrana, and Healy Creek Formations) were expected to cluster from the individual samples, it was assumed that a maximum of 15 clusters would capture the significant variability in the data set.

This cluster analysis was performed on various permutations of the point-counted sand composition components quartz, feldspar, sedimentary rock fragments, volcanic rock fragments, metamorphic rock fragments, plutonic rock fragments, detrital minerals, and undetermined grains. To determine which analysis was the best fit to the data, individual cluster members (where the samples were grouped into 15 through 2 clusters for each analysis) were plotted on the map and visually compared with the field-mapped Tertiary unit polygons. The following method and variables were used in the analysis that produced cluster results that most closely matched the expected formations: totals of quartz, feldspar, sedimentary rock fragments, volcanic rock fragments, metamorphic rock fragments, plutonic rock fragments, detrital minerals, and undetermined grains were normalized to 100 percent, and all components except detrital minerals and undetermined grains were selected as variables. Only this best-fit analysis will be discussed here.

The dendrogram (fig. 2) shows the results of the best cluster analysis achieved (table 1). The cluster analysis confirmed that most of the Tertiary unit field determinations were correct. Approximately 85 percent (50 of 60) of the samples were assigned by the cluster analysis to their field-determined formation. Samples that were mapped as a different unit from the one in which they were grouped in the cluster analysis were changed on the map to reflect their assigned cluster analysis formation (except sample 2005JEA249A, see details below). The cluster analysis is interpreted to have combined 57 of the 60 samples into seven main clusters, including two Healy Creek Formation subgroups (H1 and H2), Suntrana Formation group (S), two Lignite Creek Forma-

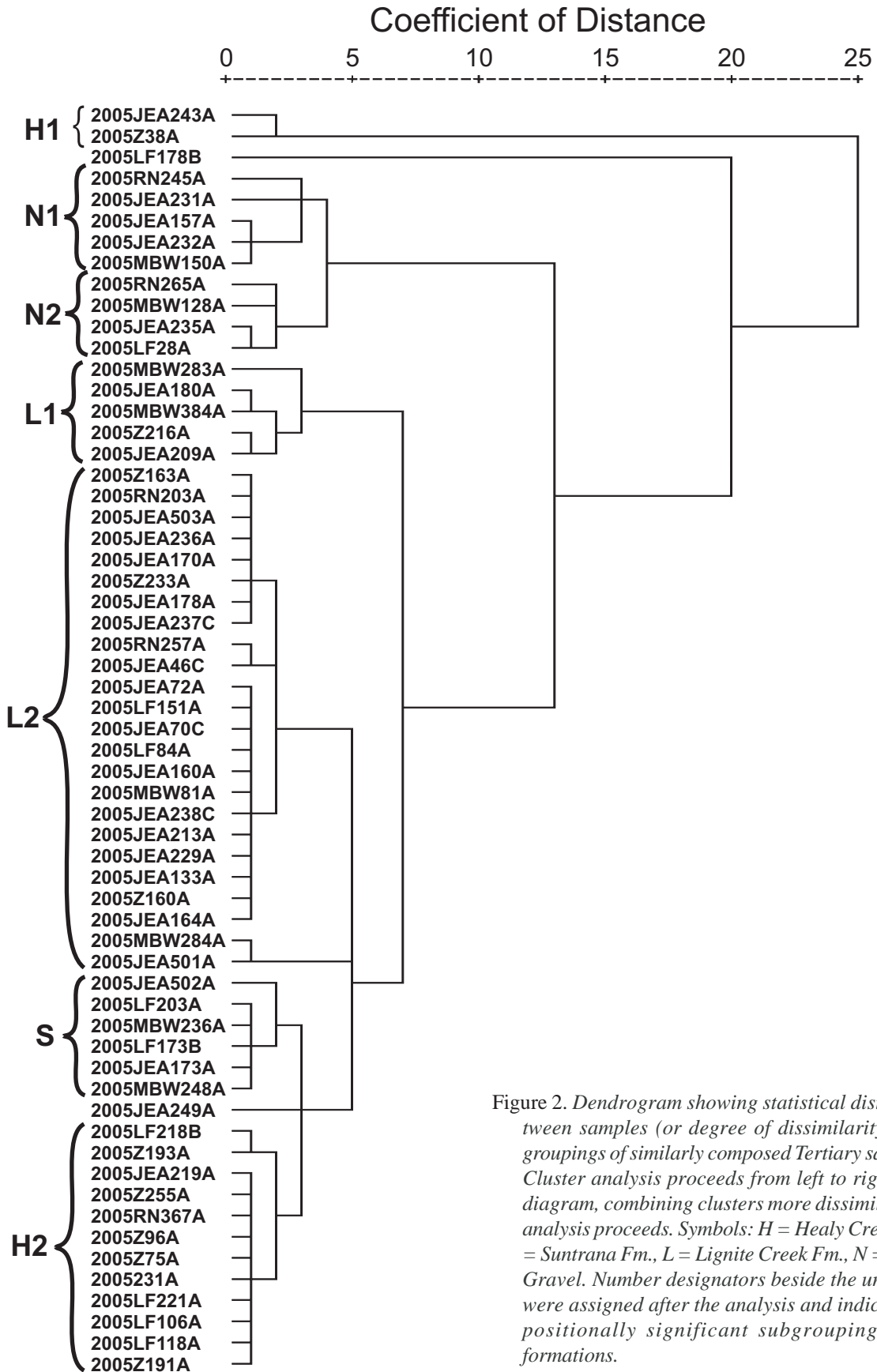


Figure 2. Dendrogram showing statistical distance between samples (or degree of dissimilarity) versus groupings of similarly composed Tertiary sandstone. Cluster analysis proceeds from left to right on the diagram, combining clusters more dissimilar as the analysis proceeds. Symbols: H = Healy Creek Fm., S = Suntrana Fm., L = Lignite Creek Fm., N = Nenana Gravel. Number designators beside the unit letters were assigned after the analysis and indicate compositionally significant subgroupings of the formations.

tion subgroups (L1 and L2), and two Nenana Gravel subgroups (N1 and N2). The Healy Creek subgroup H1 contains only two members, but the samples' unique compositions appear to have a geologic basis. Cluster H1 and adjacent sample 2005LF178B (fig. 2) will be discussed below. The cluster analysis subgroupings of these formations reflect significant compositional differences in the grain mounts; none of those compositional differences (or subgroupings) were recognized in the field.

Strong homogeneity is apparent for samples within clusters H2, S, N2, and 22 of 24 samples that clustered early into the L2 cluster. These clusters each formed around a distance coefficient of 2 (table 1). Sand modal compositions of S and H2 in particular are very similar; S and H2, the first two units to combine into one cluster (SH2), joined at a distance coefficient of 3. Sample 2005JEA249A combined with cluster H2 before the S and H2 clusters merged. This sample, a silicified conglomerate with a high percentage of metamorphic clasts, was difficult to point count. In this particular case, the sample was left in the Suntrana Formation as it was origi-

nally mapped, because its field-determined formation was considered more reliable than its formation suggested by statistical analysis. In contrast with these relatively homogeneous clusters, the L1 and N1 subgroups show more variation in sand modal composition.

As the cluster analysis progressed, the remaining main subgroups (L1, L2, N1, and N2) each formed before any other units combined. L2 and L1 were added at distance coefficients 5 and 7, respectively, to the SH2 cluster. Excluding cluster H1 and sample 2005LF178B at the top of the dendrogram (fig. 2), all of the Usibelli Group clusters combined around a distance coefficient of 7. The order of clustering indicates that L2 is more similar in composition to the combination of Healy Creek and Suntrana Formations than it is to the rest of the Lignite Formation. The Nenana Gravel subgroup N2 clustered at a distance coefficient of 2, N1 clustered at 3, and N1 and N2 combined into one cluster around 4; thus, the data suggest the Nenana Gravel is more homogeneous than the Usibelli Group as a whole (coefficient of 7). The Nenana Gravel subgroups remain distinct from the

Table 1. *Clustered items shown with their corresponding distance coefficients for the last 17 clusters formed. For example, line one can be read as "Most of L2 clustered at a distance coefficient of about 2 and that cluster was one of 17 clusters grouped in the data set." Symbols: H = Healy Creek Fm., S = Suntrana Fm., L = Lignite Creek Fm., N = Nenana Gravel. Number designators beside the unit letters were assigned after the analysis and indicate compositionally significant subgroupings of the formations. Specific sample numbers are in parentheses. See figure 2 for the dendrogram of the full hierarchical classification.*

<b>New Cluster Formed</b>	<b>Approximate Coefficient of Distance</b>	<b>Number of Clusters</b>
Most of L2	2	17
N2	2	16
S	2	15
H2	2	14
H1	2	13
(2005JEA249A) joins H2	3	12
S joins H2	3	11
(2005JEA231A) joins N1	3	10
(2005RN245A) joins N1	3	9
(2005MBW283A) joins L1	3	8
N2 joins N1 to form Nenana Gravel	4	7
L2	5	6
SH2 joins L2	5	5
L1 joins L2SH2 to form most of Usibelli Group	7	4
Nenana Gravel joins Usibelli Group	13	3
(2005LF178B) joins Nenana Gravel + Usibelli Group	20	2
H1 joins all other samples	25	1

Usibelli Group until a distance value of 13, indicating that the sand modal composition of the Nenana Gravel is fairly different from the composition of the Usibelli Group.

Determining which cluster groupings are significant is largely subjective. As the analysis continues joining clusters, increasingly heterogeneous samples are combined to a point where the combined samples are not, in reality, related. Sudden increases in the distance coefficients indicate dissimilar groups are being joined that should really be left as separate clusters. An example of this is the fusion of sample 2005LF178B and H1 with the rest of the clusters at distance coefficients 20 and 25, respectively. Correct placement of sample 2005LF178B, a partially fused (coal-fired), quartz-rich sandstone, within the cluster hierarchy is problematic due to poor sample conditions making grain identification and counting difficult. The sample is considered to be from the Suntrana Formation, its field-mapped unit. Samples in H1 were mapped as Healy Creek Formation. Although the H1 cluster appears to be markedly different from any other samples in the data set (possibly reflecting poor data quality or errors), the two samples in this cluster, while containing extraordinarily high amounts of metamorphic rock fragments, have proportionally similar sand compositions to H2. A possible geologic explanation for this composition is discussed below.

In summary (excluding cluster H1 and sample 2005LF178B), the sand compositions of Healy Creek (H2), Suntrana, and most of the Lignite Creek (L2) Formations in the Usibelli Group are homogenous, and the formations are similar to each other. The sand compositions of the rest of the Lignite Creek Formation (L1) and the Nenana Gravel are more heterogeneous, and these formations are less similar to the bulk of the Usibelli Group. Lignite Creek 1, however, is still more similar to the Usibelli Group than it is to the Nenana Gravel. Given that the Nenana Gravel is compositionally distinct from the Usibelli Group, it is most similar to the Lignite Creek Formation and least similar to the Healy Creek Formation.

Sandstone compositions in the Tertiary section show several trends (table 2). Nenana Gravel is more compositionally heterogeneous than the Usibelli Group formations, and homogeneity progressively increases down-section. The dendrogram (fig. 2) shows this trend through its vertical arrangement of groups (except subgroup H1 and sample 2005LF178B), which approximates the formations in the stratigraphic section. The vertical arrangement of subgroups within a formation, however, does not necessarily have stratigraphic significance, but represents variations within the unit. Nenana Gravel ( $Q_{26}F_{11}L_{63}; Qm_{16}F_{11}Lt_{73}$ ) contains more lithics and less total quartz, monocrystalline quartz, and polycrystalline quartz than the Usibelli Group ( $Q_{53}F_{12}L_{35}; Qm_{36}F_{12}Lt_{52}$ ) (fig. 3). Healy Creek has more polycrystalline quartz than

any of the other units, probably due to incorporation of fragments from the underlying Paleozoic rocks and other Yukon–Tanana terrane metamorphic rocks. The Nenana Gravel contains more sedimentary rock fragments (and non-chert sedimentary rock fragments;  $LS_{65}LP_{14}Lm_{22}$ ) and plutonic rock fragments than the Usibelli Group ( $LS_{38}LP_{10}Lm_{53}$ ), and these lithics decrease progressively in abundance down-section through the entire Tertiary section. N2 contains almost twice as much chert as N1, and about three times as much chert as any formation in the Usibelli Group. Through the whole section, differences in the amounts of feldspar and volcanic rock fragments between units are subtle, and near the 95 percent confidence of the data (estimated confidence; Van der Plas and Tobi, 1965). While sedimentary and plutonic rock fragments increase progressively up-section, metamorphic rock fragments are more prevalent in the Usibelli Group. The increase of total quartz (Q), and especially polycrystalline quartz (Qp), in sandstones from the lower Usibelli Group suggests derivation from the nearby metamorphic rocks. In addition, subgroups L1 and H1 both contain large, immature populations of metamorphic rock fragments that are texturally and compositionally similar to the metasedimentary and meta-igneous units in the map area; these subgroupings are at least partially locally derived (basal conglomerates?). Lignite Creek and Healy Creek both unconformably overlie Paleozoic bedrock in a significant portion of the map area.

Sandstone compositions and related data from the Suntrana Creek section (Ridgway and others, 1999) are similar to sandstone compositions in the map area, supporting the correlation between the two areas (fig. 3). Because this study used the “traditional” point-counting method (Ingersoll and others, 1984; Decker, 1985) and Ridgway and others (1999) primarily reported data counted with the Gazzi–Dickinson method, most of the data are not directly comparable. Data from this study will have lower total quartz, feldspar, and detrital minerals counts and higher lithics counts than data from Ridgway and others (1999) (Ingersoll and others, 1984). Even so, most of the trends mentioned above hold true for both data sets. Ridgway and others (1999) also show that Nenana Gravel is lithic-rich and quartz-poor, and that these components progressively decrease and increase in abundance, respectively, down-section. Ridgway and others (1999) reported that feldspar and volcanic rock fragments increase in abundance progressively higher in the section, but they did not mention this same trend in sedimentary rock fragments.

The differences in lithic and total quartz contents between formations are readily apparent in figure 3. The high percentage of unstable lithics in Nenana Gravel suggests a sediment source area such as an undissected arc, transitional arc, or recycled orogen having a diverse composition but high percentage of quartz–feldspar-

bearing rocks (Dickinson and others, 1983). Evidence such as abundant conglomerate clasts from the Cantwell Formation and north-directed paleocurrent data (fig. 4) indicates the Alaska Range and rocks to the south are the source of the Nenana Gravel (Wahrhaftig, 1987). The high total quartz and moderate lithic content of the Usibelli Group suggests that it is sourced from a recycled orogen composed of sediments, metamorphic rocks, and lesser volcanic and plutonic rocks (Dickinson and others, 1983). The paleocurrent directions of the Lignite Creek and Suntrana Formations in the field area are predominately westward (fig. 4; Wahrhaftig and others, 1969), while

they are south-directed in the Suntrana Creek area (Wahrhaftig and others, 1969; Ridgway and others, 1999). The change in paleocurrent direction may coincide with the northern extent of the Grubstake Formation and a change in Lignite Creek facies from coal-bearing to coarser-grained, non-coal bearing. This facies change and the northern extent of the Grubstake Formation are mapped by Wahrhaftig and others (1969) as cutting through the southwestern quarter of the map area. These lithologic discontinuities may be related to differences in paleotopography between this area and the Suntrana Creek area to the south. Wahrhaftig and others (1969)

Table 2. *Normalized major point-count parameters of Tertiary sandstone. Formations, but not necessarily their subgroupings, are arranged in stratigraphic order. Raw normalized parameters: Qm = monocrystalline quartz, Qp = polycrystalline quartz, F = total feldspar, Lv = volcanic rock fragments, C = chert, Lm = metamorphic rock fragments, Lp = plutonic rock fragments. Calculated normalized parameters: Q = Qp + Qm + quartz undifferentiated, Ls = sedimentary rock fragments + C. Abbreviation s.d. = standard deviation of 2σ (Van Der Plas and Tobi, 1965), n = number of samples. See appendix C for raw data.*

Unit	%Q	%Qm	%Qp	%F	%Lv	%Ls	%C	%Lm	%Lp
<b>Nenana Gravel Summary</b>	<b>26.3</b>	<b>16.6</b>	<b>9.7</b>	<b>11.1</b>	<b>9.0</b>	<b>34.6</b>	<b>23.0</b>	<b>11.7</b>	<b>7.3</b>
<b>Nenana Gravel 1</b>									
n = 5									
average	31.0	20.9	10.2	11.8	9.9	27.3	18.0	10.8	9.1
s.d.	5.7	5.1	3.8	4.0	3.8	5.6	4.8	3.9	3.5
<b>Nenana Gravel 2</b>									
n = 4									
average	20.3	11.2	9.0	8.2	7.8	43.8	29.3	12.8	5.0
s.d.	5.1	4.0	3.5	3.4	3.2	6.2	5.7	4.1	2.5
<b>Usibelli Group Summary</b>	<b>54.9</b>	<b>37.0</b>	<b>17.9</b>	<b>12.7</b>	<b>4.7</b>	<b>10.5</b>	<b>7.3</b>	<b>14.6</b>	<b>2.7</b>
<b>Lignite Creek 1</b>									
n = 5									
average	43.0	25.3	17.7	8.7	3.5	12.5	9.4	31.2	1.1
s.d.	4.2	5.5	4.8	3.4	2.0	4.1	3.5	5.8	1.4
<b>Lignite Creek 2</b>									
n = 24									
average	48.7	32.6	16.1	16.7	7.7	12.2	8.4	10.2	4.5
s.d.	6.3	5.8	4.6	4.6	3.1	4.8	3.5	3.8	2.4
<b>Lignite Creek Fm. Summary</b>	<b>47.7</b>	<b>31.3</b>	<b>16.4</b>	<b>15.3</b>	<b>7.0</b>	<b>12.3</b>	<b>8.6</b>	<b>13.9</b>	<b>3.9</b>
<b>Suntrana Fm.</b>									
n = 6									
average	64.6	50.7	14.0	15.3	3.8	9.8	6.1	5.5	1.0
s.d.	6.0	6.3	4.4	4.6	2.1	3.8	3.0	2.8	1.3
<b>Healy Creek 1</b>									
n = 2									
average	19.6	11.2	8.3	9.8	0.4	6.1	5.2	64.1	0.0
s.d.	5.0	4.0	3.5	3.8	0.8	3.0	2.8	6.1	0.0
<b>Healy Creek 2</b>									
n = 13									
average	71.7	47.2	24.5	6.4	0.5	7.6	5.4	12.9	1.0
s.d.	5.7	6.3	5.4	3.1	0.9	3.4	2.9	4.2	1.3
<b>Healy Creek Fm. Summary</b>	<b>64.8</b>	<b>42.4</b>	<b>22.4</b>	<b>6.8</b>	<b>0.5</b>	<b>7.4</b>	<b>5.3</b>	<b>19.8</b>	<b>0.9</b>

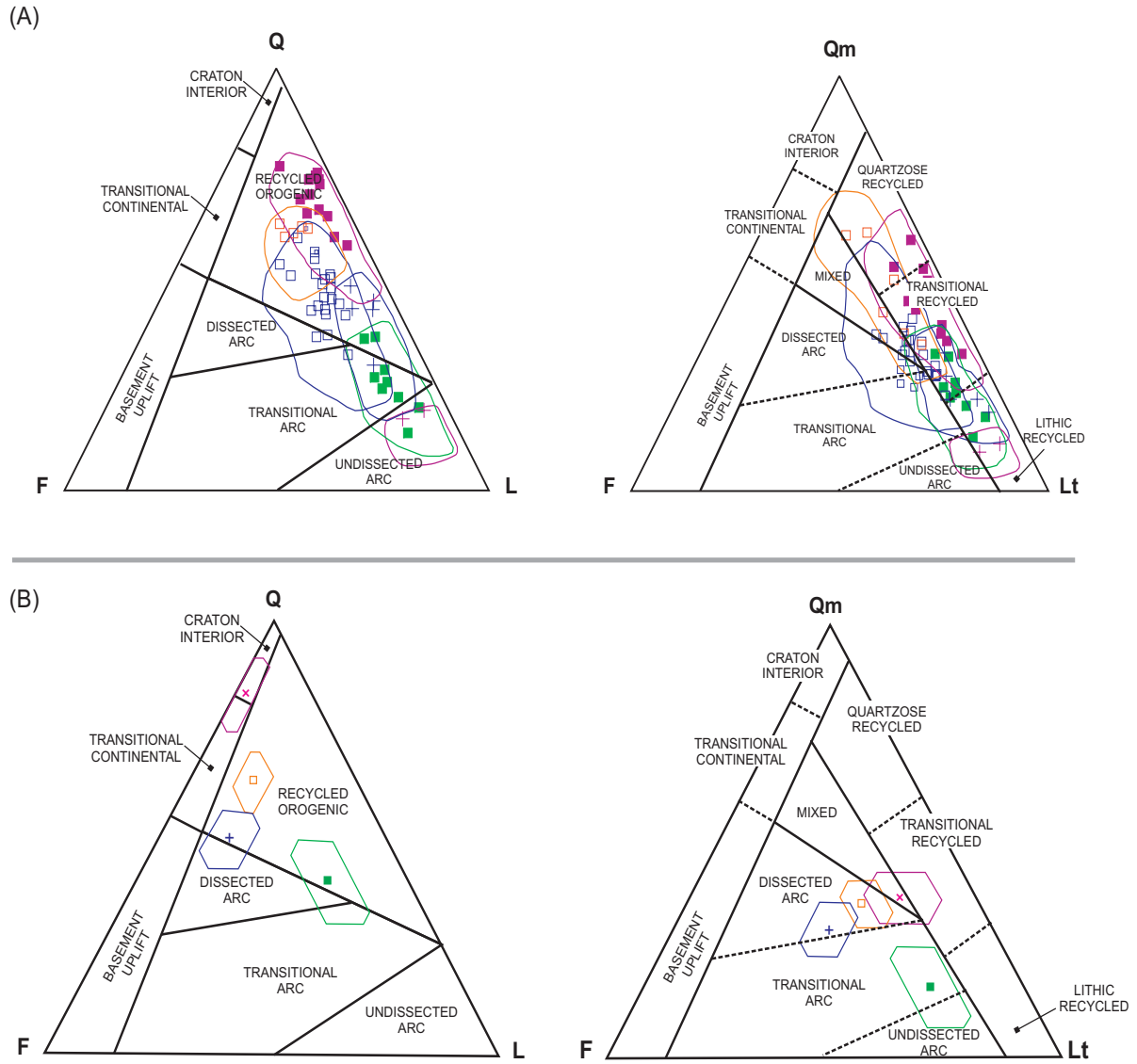


Figure 3. Tectonic provenance for Usibelli Group and Nenana Gravel sandstone clasts from this study (A) and Ridgway and others (1999; B). (A) Standard deviation error for this study is from Van Der Plas and Tobi (1965). Tectonic provenance diagrams are modified from Dickinson and others (1983). See table 2 for grain parameters not listed here. Parameters:  $D$  = detrital minerals. Calculated parameters:  $L = L_v + L_s + L_m + L_p + D$ ;  $L_t = Q_p + L$ . Parameter 'L' in this study includes detrital minerals, because some samples contain a significant amount of mica grains between 0.0625–2.0 mm in diameter. Amounts of other detrital minerals are negligible. See appendix C for raw data. (B) Average modal compositions of Tertiary sandstone from Ridgway and others (1999). Polygons represent one standard deviation about the means. Tectonic provenance diagrams are from Dickinson and others (1983). Grain parameters are as shown above except detrital minerals 'D' are not included in calculated parameters 'L' or 'L<sub>t</sub>'.

This study	Ridgway and others, 1999
<span style="border: 1px solid green; padding: 2px;">■ Nenana Gravel</span>	<span style="border: 1px solid green; padding: 2px;">■ Nenana Gravel</span>
<span style="border: 1px solid blue; padding: 2px;">+ Lignite Creek 1</span> <span style="border: 1px solid blue; padding: 2px;">□ Lignite Creek 2</span>	<span style="border: 1px solid blue; padding: 2px;">+ Lignite Creek</span>
<span style="border: 1px solid orange; padding: 2px;">□ Suntrana</span>	<span style="border: 1px solid orange; padding: 2px;">□ Suntrana</span>
<span style="border: 1px solid pink; padding: 2px;">+ Healy Creek 1</span> <span style="border: 1px solid pink; padding: 2px;">■ Healy Creek 2</span>	<span style="border: 1px solid pink; padding: 2px;">x Healy Creek</span>

reported that bedding in the Nenana Gravel and the Lignite Creek Formation is almost parallel in the southern Fairbanks A-4 Quadrangle. Because, in this area, Lignite Creek contains up to 5 percent Cantwell Formation conglomerate and the compositions of Lignite Creek and Nenana Gravel are similar (figs. 2 and 3), we infer that the Nenana Gravel may be in paraconformable contact with the underlying Lignite Creek Formation. A portion of the Lignite Creek Formation may represent a mixing zone of sediment from the Yukon–Tanana terrane and Alaska Range, arriving from the east. A mixing zone in the Lignite Creek Formation would suggest that uplift of the Alaska Range started before the deposition of the Nenana Gravel in this section of the Alaska Range foothills. Wahrhaftig and others (1969) suggest a similar scenario for deposition of the Grubstake Formation, because it also contains clasts of Cantwell Formation and is lithologically more similar to the Nenana Gravel than the rest of the Usibelli Group.

Qualitative measurements of kaolinite and montmorillonite and tentative presence of chlorite in the clay fractions of Tertiary sedimentary rocks were compared with a similar study conducted in the Nenana coal basin along Lignite and Healy creeks (Triplehorn, 1976). Sixty-five samples with a significant amount of fine-grained material were analyzed. The clay composition of the units

appears to be an effective geologic mapping tool in the Tertiary units. According to Triplehorn (1976), the Usibelli Group can essentially be divided into two sections based on its kaolinite and montmorillonite content (table 3). (No data are available for comparison with the Nenana Gravel samples from this study.) We find three groups of differing clay compositions that track closely with the clay percentages suggested by Triplehorn (1976; table 3; appendix D). Our data and data from Triplehorn (1976) indicate the Healy Creek Formation has the lowest montmorillonite content and that kaolinite content decreases up-section. Triplehorn (1976) suggests that montmorillonite is weathering from volcanic glass (possibly from ash, flows, or intrusions in the subsurface) and kaolinite is weathering from feldspar. The increase in montmorillonite composition up-section may indicate increasing contributions of a volcanic source area. In the map area, the prevalent, underlying arkosic metawacke would be an excellent source for the feldspar, and, hence, the kaolinite.

Fifteen samples were collected for palynology from random exposures in the Usibelli Group with no definite lithologic correlation between sites, except as assigned from geologic mapping and other data. Two hundred pollen grains were identified and counted per sample, and samples were also scanned for unusual grains or

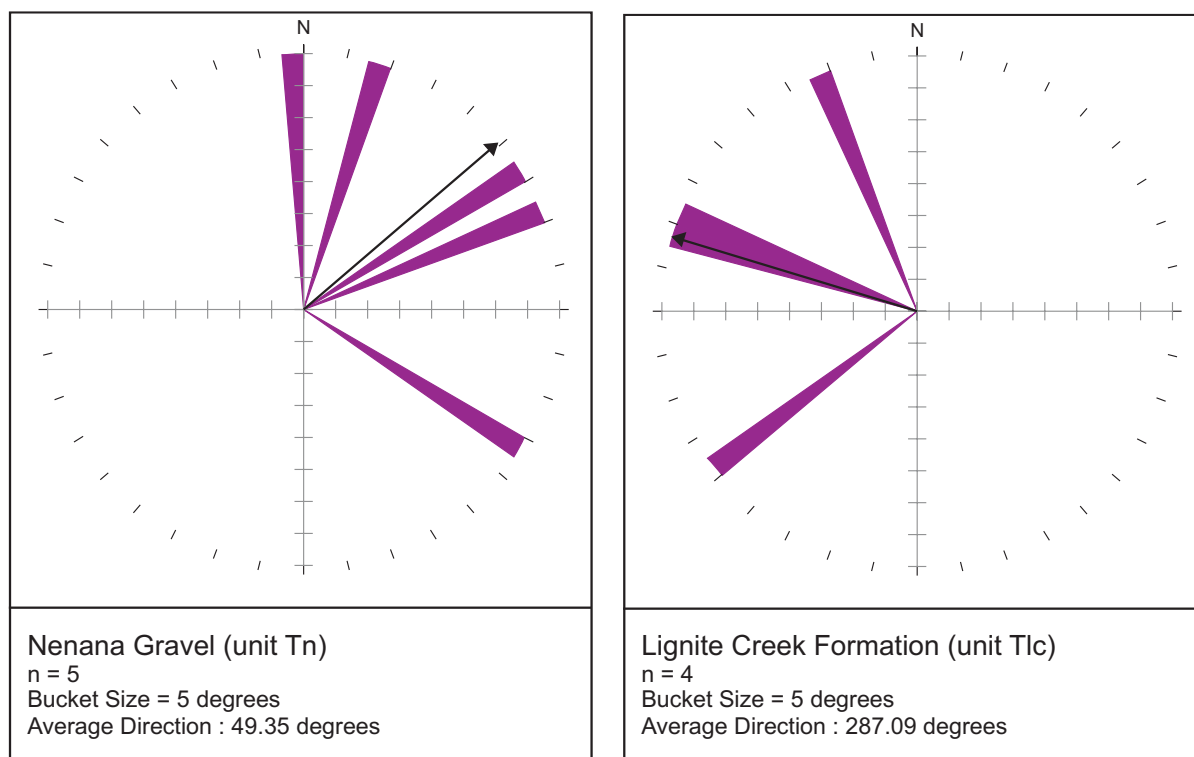


Figure 4. Paleocurrent directions measured from cross-beds in the Liberty Bell area. Note: n = number of samples measured.

Table 3. *Qualitative comparison of montmorillonite and kaolinite content in Nenana Gravel and Usibelli Group clays. Data from this study and Triplehorn (1976). Very small, small, moderate, large, and very large refer to amounts of either montmorillonite or kaolinite in the sample. See appendix D for compositional data from individual samples.*

Unit	Triplehorn (1976)		This study		This study other mineral(s)
	montmorillonite	kaolinite	montmorillonite	kaolinite	
Nenana Gravel	no data	no data	small to moderate	small to moderate	possible chlorite and zeolite
Lignite Creek Fm.	moderate to large	moderate to large	small to moderate	small to moderate	possible chlorite and zeolite
Suntrana Fm.	moderate to large	moderate to large	small to moderate	moderate to very large	possible chlorite
Sanctuary Fm.	small	very large	no data	no data	no data
Healy Creek Fm.	none to small	very large	none to small	moderate to very large	more possible chlorite

Table 4. *Pollen samples from random outcrop locations in the Tertiary Usibelli Group. Samples of fine-grained sedimentary rock and coal were collected. Samples are arranged in pseudo-stratigraphic order. The vertical organization of samples is primarily based on comparison with taxa of samples collected from the Usibelli Group and their inferred climatic conditions (Wahrhaftig and others, 1969; Leopold and Liu, 1994). Samples were adjusted in the pseudo-section according to their spatial locations within formations and comparison of their flora. See appendix E for raw data and taxa included in each summarized category.*

Map Location	Unit	Climate Inferred	Sample Number	Cool - (alder + birch)				Undrft. angiosperm (flowering tree)				Reworked		
				Warm	Cool	Wet	Algal	Fern	Moss	Fungal	Weed			
P1	Lignite Creek Fm.	cool	2005JEA160C	9	182	175	1	0	3	5	1	0	1	0
P2	Lignite Creek Fm.	warm	2005JEA237A	32	111	63	5	4	47	1	3	0	1	0
P3	Suntrana Fm.	moderate	2005MBW415A	14	162	82	6	0	1	15	7	1	0	1
P4	Suntrana Fm.	moderate	2005Z235A	0	153	100	39	0	0	5	42	0	0	0
P5	Suntrana Fm.	moderate	2005Z165B	7	161	75	1	0	26	2	4	1	0	0
P6	Suntrana Fm.	moderate	2005Z171B	18	106	81	2	0	70	1	5	0	0	1
P7	Healy Creek Fm.	cool	2005LF124A	11	174	122	1	0	5	3	7	0	0	0
P8	Healy Creek Fm.	cool	2005Z47B	9	189	182	1	0	2	0	1	0	0	0
P9	Healy Creek Fm.	cool	2005MBW232A	2	177	145	2	1	14	3	3	1	0	0
P10	Healy Creek Fm.	moderate	2005MBW144A	8	168	40	6	0	10	7	7	0	0	0
P11	Healy Creek Fm.	warm	2005JEA210C	38	134	113	5	2	17	3	3	2	0	1
P12	Healy Creek Fm.	warm	2005LF105A	53	121	82	7	0	18	1	8	0	0	0
P13	Healy Creek Fm.	warm	2005Z36C	98	67	14	3	2	6	26	2	0	0	0
P14	Healy Creek Fm.	unknown	2005LF217D	1	0	0	0	0	2	0	0	0	0	0
P15	Healy Creek Fm.	unknown	2005Z229A	0	0	0	0	0	8	0	0	0	0	0

flora not represented in the official count. Pollen grains are well preserved and thermally immature. Three samples did not contain enough pollen for a complete count; two samples were essentially barren, but one sample contained 76 grains and was included in the calculations. In order to arrange the samples within the pseudo-section, pollen counts were normalized to 200, pollen with climatic and environmental significance were summarized, and samples were visually compared to each other and data from Leopold and Liu (1994; table 4). Climatic conditions in the Miocene were variable (Leopold and Liu, 1994; Ridgway and others, 1999), and all of the flora indicated from pollen in the samples existed throughout the Miocene (R.L. Ravn, written commun., 2006). In the absence of a comparative vertical succession of palynological data, the data from these samples cannot be presently used as a tool for geologic mapping. In conjunction with other data, the flora do suggest climatic conditions related to temperature or topography and environmental conditions such as wet swamp versus dry deciduous forest.

Lower Healy Creek Formation is characterized by pollen from thermophilous tree taxa of a mixed deciduous–conifer forest, and pollen from upper Healy Creek Formation suggests a cooler climate (Leopold and Liu, 1994). Wahrhaftig and others (1969) noted Late Oligocene (later reinterpreted to be Early Oligocene; Leopold and Liu, 1994) exotic pollen taxa *Eucommia*, *Engelhardtia* type, *Gynkaletes*, and *Orbiculapollis* in a sample from lower Healy Creek Formation near the junction of Rex and California creeks. Wolfe and Tanai (1987) extend the age of the Rex Creek samples into the Late Eocene. Pollen grains from these older taxa, however, were not seen in any samples from this study. Instead, our samples from the Healy Creek Formation contain pollen from a variety of warm- (including tropical fern *Osmunda*) and cool-loving (including pine, spruce, and juniper) flora, and these samples are arranged in the pseudo-section from warm-loving to cool-loving progressively up-section. A pollen assemblage primarily of thermophiles and lesser conifers indicates the Suntrana Formation was deposited in a warm environment (Leopold and Liu, 1994). Each of our Suntrana Formation samples contain a mixture of pollen from warm- and cool-loving flora, which suggests a temperate climate for this unit. Although the Lignite Creek Formation is characterized by cool-loving flora (Leopold and Liu, 1994), high counts of elm pollen from one Lignite Creek sample suggest a warmer climate. The sample was probably collected from lower in the section. High counts of pine, juniper, and spruce pollen from a sample probably collected higher in the section indicate a cool climate.

## PALEOZOIC UNITS

Wahrhaftig (1968, 1970a–f) mapped greenschist-facies meta-igneous and metasedimentary rocks in the region and assigned them to the Totatlanika Schist and Keevy Peak Formation. Wahrhaftig described the Totatlanika Schist as being dominantly of volcanic origin and the Keevy Peak Formation as being dominantly of sedimentary origin, although each unit contains a variety of rock types. These two units crop out in the map area and unconformably underlie Quaternary and Tertiary strata. U-Pb SHRIMP zircon data indicate the two formations are Late Devonian to Early Mississippian in age (fig. 5; Dusel-Bacon and others, 2004). A white-mica sample from the lower Totatlanika Schist, sampled as far away as possible from any observed intrusions, exhibited an  $^{40}\text{Ar}/^{39}\text{Ar}$  plateau age of  $152.8 \pm 1.0$  Ma (map location A6; table 5). This age presumably approximates the age of the latest regional metamorphism. The Keevy Peak Formation and the five members of the Totatlanika Schist are arranged below in the stratigraphic order proposed by Wahrhaftig (1968). Previously mapped lithologies and their interpreted protoliths are from Wahrhaftig (1968) unless otherwise referenced.

### TOTATLANIKA SCHIST

**Sheep Creek Member**—Thinly bedded dark gray and light gray slate. Quartz–feldspar–sericite schist with preserved bedding and crossbedding (meta-arkose). Purple and pale green slates composed of chlorite, sericite, epidote, and minor quartz (tuffaceous protolith). Fine-grained graphitic schist with 60 percent quartz and 40 percent graphite. Banded chert (Wahrhaftig, 1970d). Lenticular bodies of rhyolite schist (shallow, sill-like intrusions) occur within Mystic Creek and Sheep Creek Members.

**Mystic Creek Member**—Fine-grained purple, green, and yellow (and black [graphitic?]; Wahrhaftig, 1970a, 1970d) schist with 10–20 percent relict phenocrysts of beta-quartz, albite, and orthoclase in a fine-grained foliated matrix of quartz, feldspar, sericite, chlorite, hematite, and stilpnomelane (metarhyolite). Thin fossiliferous limestone beds.

**Chute Creek Member**—Dark green chlorite–zoisite (or epidote)–actinolite–albite–biotite schist with rare relict pyroxene and plagioclase (greenschist facies, metamorphosed mafic volcanic rocks).

**California Creek Member**—White- to buff-weathering, gray quartz–orthoclase–sericite schist and gneiss, with mixed coarse- and medium-grained phases. Coarse-grained facies contains 2.5 to 25

mm K-feldspar augen and smaller quartz in gray to greenish-gray matrix of sericite, chlorite, quartz, feldspar, and calcite. Euhedral to broken anhedral augen. Medium-grained facies contains flattened to sharply angular quartz < feldspar (orthoclase and albite) grains up to 2 mm in diameter in a foliated groundmass of sericite, orthoclase, and quartz. Interpreted as felsic meta-igneous rocks (Gilbert and Bundtzen, 1979). Includes thin, interbedded layers of black carbonaceous schist and slate. (Present in map area.)

**Moose Creek Member**—Black graphitic schist, dark green chloritic schist (metavolcanic), and yellow quartz–orthoclase schist and gneiss. Unit is lenticular and tectonically disturbed. (Present in map area.)

**KEEVEY PEAK FORMATION**

Located stratigraphically below the Totatlanika Schist. Unit contains gray–green–purple slate, quartz–sericite schist, graphitic schist, graphitic quartzite, calcareous schist, quartz–feldspar metawacke (“grit”), and stretched conglomerate. The Keevey Peak Formation is located unconformably on the Healy Schist (Birch Creek Schist of former usage; Wahrhaftig, 1968; Newberry and others, 1997).

Wahrhaftig (1970c) mapped the lower two members, Moose Creek and California Creek, in the Liberty Bell map area. He described the lower member (Moose Creek) as primarily containing yellow quartz–orthoclase schist and gneiss in contrast to the aerially extensive and stratigraphically younger California Creek Member, which hosts the Liberty Bell gold deposit and contains gray quartz–orthoclase–sericite schist and gneiss (Wahrhaftig, 1970c). Wahrhaftig considered the contact between the members as unconformable. Both units have been suggested to have a crystal-rich pyroclastic (felsic igneous) protolith (Capps, 1912; Wahrhaftig, 1968; Gilbert and Bundtzen, 1979). Instead, our mapping shows that the bulk of the California Creek Member is of sedimentary origin (unit Daw), instead of igneous origin, and was intruded by plugs, dikes, sills, and possibly flows of now-metamorphosed granite (unit Dg) and rhyolite (and rare dacite; units Dr and Dar). Conversely, the Moose Creek Member does have an igneous protolith but likely represents a larger, metamorphosed granite body identical to the ones intruding the California Creek Member. Further discussion of the Moose Creek Member is located below.

The metasedimentary and meta-igneous rocks appear similar in outcrop. A combination of chemical data (major- and minor-oxide and trace elements), modal petrographic data, and textural observations made on hand

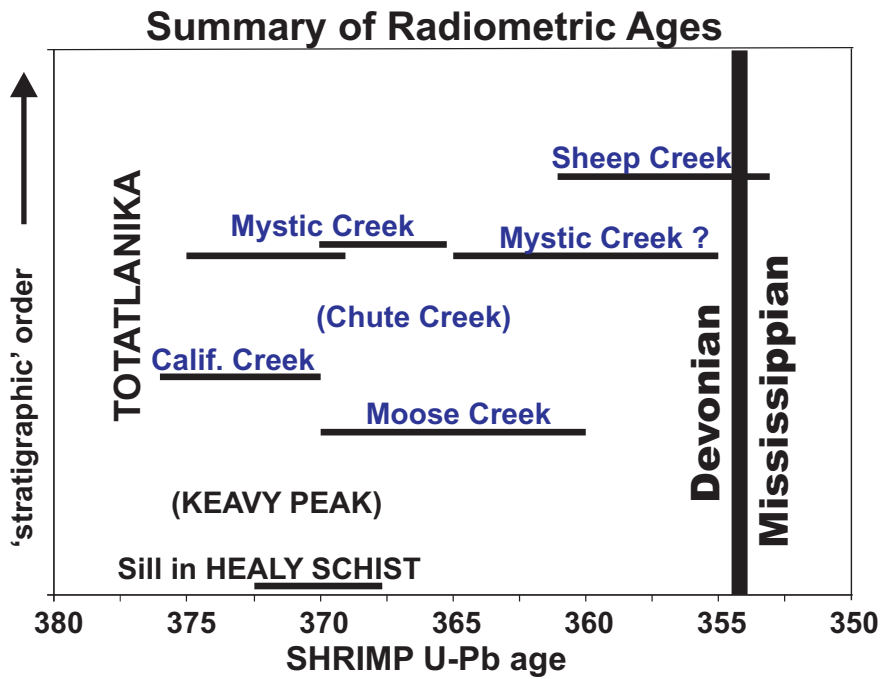


Figure 5. Summary of SHRIMP U-Pb ages from Paleozoic rocks collected in the Alaska Range Foothills. Age data from Dusel-Bacon and others (2004).

Table 5. Interpreted  $^{40}\text{Ar}/^{39}\text{Ar}$  ages for selected samples from the Liberty Bell area, Fairbanks A-4 Quadrangle. Except where noted with an asterisk, location coordinates were collected using a hand-held GPS unit (no differential correction was applied), and coordinates are presented in latitude and longitude (based on the NAD27 Alaska datum) and in UTM coordinates (based on the Clark 1866 spheroid, NAD27 datum, UTM zone 6 projection). Asterisk denotes locations collected using the NAD83 datum. Plateau is defined as 3 or more consecutive fractions with a Mean Square Weighted Deviation (MSWD) < ~2.5 and more than ~50%  $^{39}\text{Ar}$  release. Ages are plateau unless specified otherwise. Reset ages are indicated with an 'r'. **Bold:** preferred age for each sample (ages reported at  $\pm 1$  sigma). See appendix B for methodology, spectra, and detailed analyses.

Sample Number	Map Location	Latitude	Longitude	UTM Easting	UTM Northing	Description	Mineral Analyzed	Integrated Age (Ma)	Plateau or other age (Ma)	Plateau Information
2005LF197B	---	64.09851	-148.778564	413318	7109006	Baked clay, age of coal bed fire	whole rock	-0	---	---
2005JDDS01	---	63.976417*	-148.688528*	417460*	7095332*	Hornblende adakite volcanic flow(?)	hornblende 1	---	---	Poor heating schedule, insufficient sample size
							hornblende 2	0.139 $\pm$ 0.260	0.793 $\pm$ 0.253	3 fractions, 61% $^{39}\text{Ar}$ released, MSWD = 0.1
							hornblende 3	0.981 $\pm$ 0.109	1.007 $\pm$ 0.105	3 fractions, 92% $^{39}\text{Ar}$ released, MSWD = 0.2
							hornblende 4	0.895 $\pm$ 0.091	1.103 $\pm$ 0.107	3 fractions, 73% $^{39}\text{Ar}$ released, MSWD = 0.3
							hornblende 5	0.807 $\pm$ 0.153	0.920 $\pm$ 0.180	2 fractions, 78% $^{39}\text{Ar}$ released, MSWD = 1.3
							hornblende 6	0.881 $\pm$ 0.123	1.065 $\pm$ 0.139	3 fractions, 83% $^{39}\text{Ar}$ released, MSWD = 0.1
							hornblende 7	1.090 $\pm$ 0.111	1.022 $\pm$ 0.174	2 fractions, 50% $^{39}\text{Ar}$ released, MSWD = 0.6
							<b>1.026 <math>\pm</math> 0.057</b> Weighted average		6 sample average	MSWD = 0.4
2005RN269A	A1	63.999983	-148.570176	423202	7097762	Dacite volcanic flow	biotite	37.4 $\pm$ 0.3	<b>37.4 <math>\pm</math> 0.3</b>	11 fractions, 99% $^{39}\text{Ar}$ released, MSWD = 0.2
2005MBW71A (a)	A2	64.042658	-148.943428	405095	7103019	Granodiorite dike	hornblende 1	88.7 $\pm$ 0.6	90.4 $\pm$ 0.5 (some Ar loss?) 30 r	7 fractions, 89% $^{39}\text{Ar}$ released, MSWD = 0.7
2005MBW71A (b)							hornblende 2	91.9 $\pm$ 0.5	<b>91.6 <math>\pm</math> 0.5</b>	6 fractions, 88% $^{39}\text{Ar}$ released, MSWD = 0.4
2005Z239A	A3	64.073466	-148.788838	412759	7106230	Arkosic metawacke, fine grained biotite in mats, age of hornfels	biotite	91.1 $\pm$ 0.5	<b>92.0 <math>\pm</math> 0.5</b> 50 r	11 fractions, 93% $^{39}\text{Ar}$ released, MSWD = 0.3

Table 5. Interpreted  $^{40}\text{Ar}/^{39}\text{Ar}$  ages for selected samples from the Liberty Bell area, Fairbanks A-4 Quadrangle. Except where noted with an asterisk, location coordinates were collected using a hand-held GPS unit (no differential correction was applied), and coordinates are presented in latitude and longitude (based on the NAD27 Alaska datum) and in UTM coordinates (based on the Clark 1866 spheroid, NAD27 datum, UTM zone 6 projection). Asterisk denotes locations collected using the NAD83 datum. Plateau is defined as 3 or more consecutive fractions with a Mean Square Weighted Deviation (MSWD) < ~2.5 and more than ~50%  $^{39}\text{Ar}$  release. Ages are plateau unless specified otherwise. Reset ages are indicated with an 'r'. **Bold:** preferred age for each sample (ages reported at  $\pm 1$  sigma). See appendix B for methodology, spectra, and detailed analyses—continued.

Sample Number	Map Location	Latitude	Longitude	UTM Easting	UTM Northing	Description	Mineral Analyzed	Integrated Age (Ma)	Plateau or other age (Ma)	Plateau Information
2005JEA30A	A4	64.029306	-148.946368	404906	7101536	Granodiorite, secondary biotite, subparallel to foliation, 2.4-m-thick dike	biotite	92.4 $\pm$ 0.5	<b>92.9 <math>\pm</math> 0.5</b> 60 r	9 fractions, 95% $^{39}\text{Ar}$ released, MSWD = 0.5
2005MBW218A (a)	A5	64.056122	-148.577207	423013	7104025	Gabbro dike	biotite 1	92.5 $\pm$ 0.5	<b>95.5 <math>\pm</math> 0.5</b> 30 r	9 fractions, 80% $^{39}\text{Ar}$ released, MSWD = 1.7
2005MBW218A (b)							biotite 2	92.2 $\pm$ 0.5	<b>95.6 <math>\pm</math> 0.5</b> 20 r	10 fractions, 79% $^{39}\text{Ar}$ released, MSWD = 1.6
2005JEA184A	A6	64.040527	-148.527137	425415	7102228	Arkosic metawacke, age of metamorphism	white mica	149.8 $\pm$ .08	<b>152.8 <math>\pm</math> 1.0</b> 125 r	5 fractions, 69% $^{39}\text{Ar}$ released, MSWD = 0.4

samples and thin sections are necessary to differentiate these rocks. The best discriminant is Nb + Y (fig. 6). Meta-igneous rocks typically contain Nb + Y > 50 ppm; metasedimentary rocks typically contain Nb + Y < 50 ppm. Alteration is a complicating factor in the Liberty Bell Mine area. Altered samples commonly contain elevated SiO<sub>2</sub>, which may dilute the trace-element content of the rocks. Samples containing 40–60 ppm Nb + Y are differentiated based on other chemistry, texture, and modal composition. Meta-igneous rocks tend to be more massive and less well foliated because they contain less mica. Relict quartz and feldspar phenocrysts are randomly scattered throughout the sample, and are usually euhedral to subhedral. The ratio of feldspar to quartz crystals is 3:2 to 2:1. Quartz crystals are frequently embayed; this texture is less common in the metasedimentary rocks. Meta-igneous rocks tend to have lower TiO<sub>2</sub> contents than the metasedimentary rocks. In metasedimentary rocks, relict textures such as graded bedding and grain sorting are common in hand sample and in outcrop. Metasedimentary rocks may contain sedimentary and igneous lithic fragments, and a variety of quartz types, including white, smoky, and clear quartz. Quartz and feldspar clasts are more rounded than euhedral.

Within the metasedimentary unit Daw described above, we recognize metamorphosed arkosic wacke, and minor feldspathic and quartz wacke. The presence of euhedral grains suggests the sediments have not undergone significant traction transport (D.L. LePain, oral commun., 2006). The presence of more than a thousand meters of graphitic quartzite and graphitic schist interbedded with the Devonian section (Warhaftig, 1968) suggests the rocks were deposited in a subaqueous environment. Due to the homogeneous composition (quartz + feldspar) of unit Daw and presence of occasional euhedral and embayed crystals, it is probably sourced in felsic igneous rocks and may be volcanoclastic. Primary textures of volcanoclastic grains could be retained for a long distance (tens to hundreds of km) if transported in a subaqueous environment (K.F. Bull, oral commun., 2006). Future study of the Paleozoic rocks would include additional dating of metasedimentary and meta-igneous rocks.

The Keevy Peak Formation contains graphitic quartzite (unit Dgq) and phyllitic, metamorphosed quartz wacke and minor feldspathic wacke and quartz arenite (unit Dqw). Locally exposed, thinly bedded, cyclic, size-graded meta-arenite–phyllitic metawacke layers suggest in part a deep-water, turbidite origin. For units Dqw and

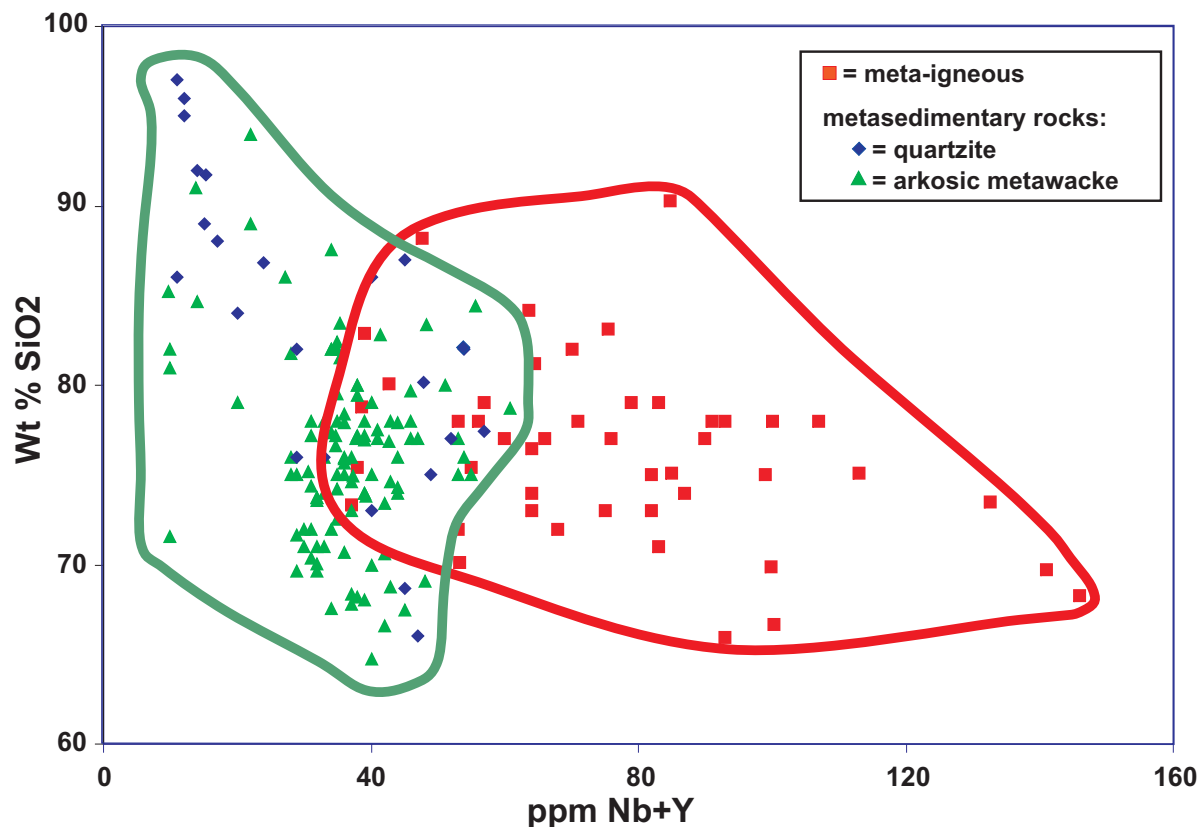


Figure 6. *Discriminant analysis of metasedimentary and meta-igneous rocks from the Liberty Bell area. Data from this study (appendix A) and Athey and others (2005).*

Daw, definitions of wacke (or “grit” in the Keevy Peak Formation in Wahrhaftig [1968]) and arenite are modified from Williams and others (1982) and Pettijohn and others (1987). Sandstone with >15 percent matrix of clay and fine silt is defined as wacke, and sandstone containing <15 percent matrix is arenite. Sandstone with <10 percent detrital feldspar grains in which quartz is the dominant detrital grain is referred to as quartz arenite or quartz wacke, depending on the abundance of detrital silt and clay. Wacke with >10 and <25 percent feldspar is referred to as feldspathic wacke; if detrital feldspar component is >25 percent, the rock is called an arkosic wacke.

Shallowly emplaced and (or) extrusive meta-igneous rocks are located throughout the map area. Textures range from an aphyric metarhyolite (flow?; unit Dar) at the head of Spruce and Cody creeks to fine- and medium-grained porphyritic metarhyolite (unit Dr) to megacrystic metagranite with potassium feldspar crystals 3 cm in length along the northern edge of the map (unit Dg). Chemical and textural data indicate that the metagranite and metarhyolite bodies intruding the California Creek Member are indistinguishable from the rocks mapped as Moose Creek Member schist and gneiss by Wahrhaftig (1970c). We interpret the variable thickness of the Moose Creek Member (Wahrhaftig, 1968) as a result of its igneous nature, and suggest that the remaining Moose Creek lithologies, mafic metavolcanic schist and graphitic schist (Wahrhaftig, 1968), be reassigned to the California Creek Member and Keevy Peak Formation, respectively.

In contrast, we have identified a group of mixed lithologies, historically mapped as a part of the California Creek Member (Wahrhaftig, 1970c), that appear to have stratigraphic significance. This group, consisting of metarhyolite (unit Dr), metagranite (unit Dg), metabasite (unit Db), fine-grained quartzite (unit Dq), and graphitic quartzite (Dgq), is interfoliated in no particular order within the topographically (and stratigraphically?) lower section of the arkosic metawacke (unit Daw). The group is approximately 100–200 m thick and traceable across the area for at least 25 km. This group is equivalent to the “Liberty Bell Mine sequence” of Freeman and others (1987). Due to the abnormally high carbonate content in altered metabasite (unit Db), this group is the preferred ore host in the Liberty Bell area.

The combination of mostly felsic (units Dr, Dg, and Dar) and occasionally mafic (unit Db) lithologies indicates an ancient, bimodal volcanic system. These units display within-plate trace-element compositions (fig. 7). The bimodal chemistry, elevated concentration of high-field-strength and rare-earth elements, and presence of carbon-rich basinal sediments suggest that these rocks formed in an extensional tectonic setting such as a rift

environment like those in the Red Sea and Gulf of California (this study, Dusel-Bacon and others, 2004). Volcanogenic massive sulfide (VMS) deposits are associated with deep-water structures such as submarine caldera and rift zones, and both the Totatlanika Schist and Keevy Peak Formation host VMS occurrences (commonly containing galena + sphalerite ± chalcocopyrite ± pyrite in the Alaska Range foothills; Newberry and others, 1997). Because the meta-igneous and meta-sedimentary “Liberty Bell Mine sequence” (Freeman and others, 1987) only contains anomalous metals where hornfelsed in the Liberty Bell Mine area, mineralization at the Liberty Bell Mine is likely pluton-related and not associated with VMS.

No stratabound base-metal sulfide occurrences were located in the California Creek Member, Moose Creek Member, or Keevy Peak Formation during the recent mapping project. The closest VMS occurrence is located about 11 km southeast of the map area (Freeman and Schaefer, 2001; Ellis and others, 2004) in the Keevy Peak Formation (Wahrhaftig, 1970e). The most notable VMS prospects in the Bonnifield mining district, Red Mountain/Dry Creek and WTF, are hosted within the uppermost section of the Totatlanika Schist, Mystic Creek, and Sheep Creek members, respectively (Newberry and others, 1997). The geotectonic paleoenvironment of the lower members of the Totatlanika Schist may have been incompatible with the development of VMS mineralization. The Keevy Peak Formation and oldest members of the Totatlanika Schist can be interpreted as sedimentary deposits formed during an early stage of rift basin development and beginning or peripheral stage of more extensive volcanism. Keevy Peak graphitic quartzite (unit Dgq) may represent the deepening of the basin with occasional influx of quartz-rich sediment (unit Dqw). Carbonate alteration of basalts (unit Db) from heated saline water not long after emplacement would be consistent with an extensional setting. The rift basin in its early stage could either be marine or saline lake, but a corral fossil *Syringopora* collected in marble from the Mystic Creek Member (located stratigraphically up-section; Wahrhaftig, 1968) indicates the basin was marine by the time that member was deposited. Greater but intermittent amounts of limestone were deposited in the Mystic Creek Member sediments (Wahrhaftig, 1968), suggesting an increase in heat, and by extension, in volcanism. (Heating marine water can decrease the solubility of calcite; heat from volcanic activity could allow limestone deposition at significant water depth.) Bimodal volcanic rocks do appear in greater amounts higher in the stratigraphic section. The Chute Creek Member, located stratigraphically above the California Creek Member, contains metamorphosed mafic volcanic rocks, and the two youngest members, Sheep Creek and Mystic Creek,

contain rocks possibly of felsic volcanic origin (Wahrhaftig, 1968). The absence of volcanogenic massive sulfide prospects in the lower portion of the Totatlanika Schist may be a result of the scarcity of volcanic rocks; the center of the ancient volcanic system was possibly tens to hundreds of kilometers away, and (or) it occurred later (higher in the stratigraphic section).

## STRUCTURE

Seismic activity related to movement on the Denali Fault and the poorly understood Northern Foothills thrust (informal name; Thoms, 2000; Ridgway and others, 2002; Bemis, 2004) is hazardous to important Alaskan infrastructure traversing the Alaska Range foothills, and national defense facilities located nearby. One of the objectives of DGGS's Liberty Bell project was to collect data that could help provide a better understanding of the regional tectonic framework. In the Liberty Bell area, a complex system of dormant and active faults and folds displaces the geologic units and mineralization. At least four episodes of structural deformation (Freeman and others, 1987) are present in the Liberty Bell area. Poor exposures, especially in poorly consolidated Tertiary formations, hampered the identification of faults in the field. Through the interpretation of linear features in electromagnetic and magnetic geophysical data (Burns and others, 2002) and aerial photography, in conjunction with detailed surficial and bedrock mapping, we recognize three sets of high-angle faults (northwest-, northeast-, and east-west-trending) and area-wide folding with axes primarily directed east-west. Faults were inferred where differing lithologies formed a contact relationship that could not be more simply explained by folding or normal intrusive or stratigraphic relations. Faults were also inferred from areas of intense silicification, clay gouge zones, and geomorphologic features such as boggy swales and linear drainages.

There are several reports of recent faulting in the map area. Freeman and others (1987) reported fractures in Quaternary alluvial bench sediments along Eva Creek. A possible scarp was located on a Paleozoic/Tertiary fault just south of hill VABM Coal (this study). An unsuccessful attempt to physically locate a possible fault scarp crossing pediment gravel (identified from aerial photography) was made by D.S.P. Stevens (oral commun., 2005). Recent regional studies suggest that the northern Alaska Range foothills are actively undergoing compression, resulting in a wedge-shaped fold and thrust fault belt propagating north from the Alaska Range (Thoms, 2000; Ridgway and others, 2002; Bemis, 2004). Previous to this study, data from the Liberty Bell area utilized in regional studies have primarily involved interpretation of aerial photography and Wahrhaftig's (1970c) mapping. Our ground-truth geologic mapping

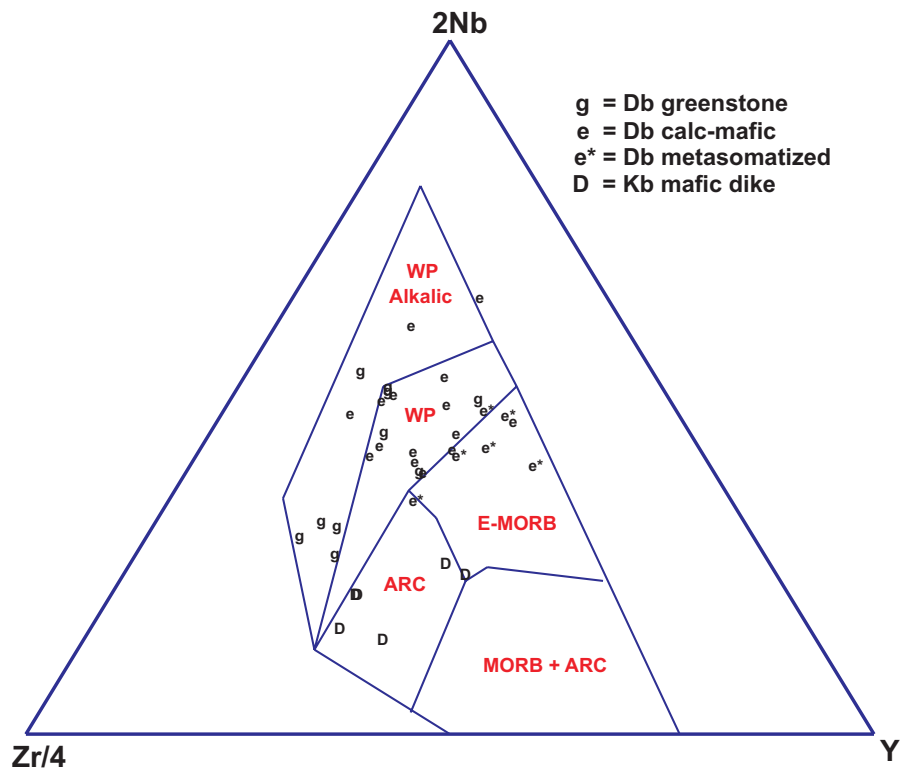
found no evidence of thrust faults. If present, the near-surface expression of a basement-involved, regional structural system may be either active in conjunction with, superimposed on, or possibly reactivating high-angle faults. Wahrhaftig (1970c) mapped a thrust fault that defined the contact between California Creek Member and "Moose Creek Member." Due to reinterpretation of the Devonian units presented in this report, this fault is relocated to the south and redefined as high-angle. The extension of Wahrhaftig's (1970c) thrust fault and another postulated thrust fault located just north of hill VABM Coal (Bemis, 2004) primarily run along the unconformity between Devonian arkosic metawacke (unit Daw) and the Healy Creek Formation (unit Thc). At the location of the postulated thrust north of hill VABM Coal and on the eastern edge of the map, Freeman and others (1987) noted a fault dipping 50° to the south in a trench. The fault is described as a 2-meter-wide gouge zone composed of clay and crushed unit Daw. Offset was not determined as identical lithologies were juxtaposed by the fault.

Young folding, however, is documented in the map area. East-west-trending folds involving the Tertiary sedimentary rocks are common. Some of the anticline and syncline pairs may be parasitic folds indicating larger, regional structures. Freeman and others (1987) noted large-scale, east-northeast-trending, commonly asymmetrical folds plunging 10° to the west, and state that Eva Creek flows down the axis of one of these synclines. Regionally, Wahrhaftig (1987) noted that the Nenana Gravel was deformed into irregular box folds with amplitudes of 0.6–1.8 km and wavelengths of 8–16 km. Our cross-section shows where we interpret these major structures to cross the map area.

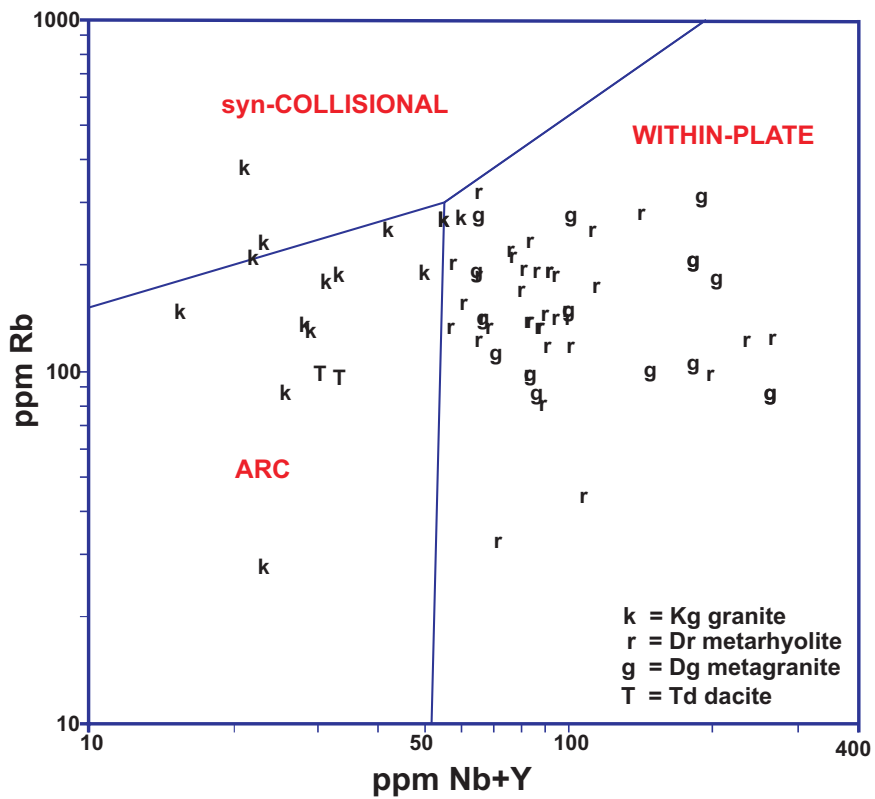
In the Liberty Bell Mine area, foliation and bedding measurements indicate a dome-like structure that is truncated by the Eva Creek fault (informal name) on its north side. There are several possible ways (and combinations of ways) this dome-like structure could have formed. Due to lack of surface and subsurface data, we can only speculate on the correct model. (1) Dome-like

Figure 7 (right). *Tectonic setting for igneous and meta-igneous rocks from the Liberty Bell area as indicated by trace-element discrimination diagrams. (A) Mafic igneous and meta-igneous rocks from the Liberty Bell area plotted on Nb-Zr-Y discrimination diagram for basalts. Diagram after Meschede (1986). (B) Felsic igneous and meta-igneous rocks from the Liberty Bell area plotted on Rb vs. Nb + Y discrimination diagram for rhyolites. Diagram after Pearce and others (1984). Note: WP = within-plate, MORB = mid-ocean ridge basalt, E-MORB = extensional, mid-ocean ridge basalt.*

(A)



(B)



structure is related to regional folding caused by compression of Devonian and Tertiary units in the vicinity of a subsurface pluton (assumed to be Cretaceous) that possibly acts as a doorstep and is not deformed, although the less competent units deform around it. (2) Devonian units were deformed into the dome shape during the intrusion of the subsurface pluton, and subparallel bedding in the Tertiary units is a coincidence and unrelated to the dome-like structure. Tertiary units are in angular unconformity with Devonian units at depth and truncate against them. (3) Dome-like structure is the result of egg-crate style folding, where regional east-west folds meet an earlier north-south fold (proposed by Freeman and others [1987], who also noted this feature). Aeromagnetic data suggest a large intrusive body underlies this area, consequently, we prefer some combination of models 1 and 2. The underlying pluton is discussed in more detail below (p. 22).

The majority of faults on the map displace the Nenana Gravel and (or) Usibelli Group, indicating some movement on these faults must be of middle Tertiary age or younger. The relative timing of these faults is unclear. The northwest-, northeast-, and east-west-trending faults do not terminate in any particular pattern, which suggests that they all might have been (or are still) part of the same structural system. The northwest- and northeast-trending faults may be activated fracture sets. Where Tertiary units are offset by these faults, the faults appear to have significant movement. Where these faults occur within homogeneous Paleozoic rocks, it is difficult to determine if significant movement has occurred. For instance, in the California Creek canyon, where continuous exposures of bedrock allow for detailed observation of structures, several cross-cutting faults were noted. These faults are expressed as heavily iron-stained, silicified shear zones ranging from 0.75 up to about 5 m wide with highly fractured rock and rock flour. We assume that shear zones of this magnitude have had significant movement along them.

The east-west-trending faults may be reactivated, and at least several hundred meters of vertical offset is suspected along them. The two parallel, east-west-trending faults in the southeast corner of the map area juxtapose the older Keevy Peak Formation against the California Creek Member of the Totatlanika Schist. The east-west-trending Eva Creek high-angle (57–90°) fault displaces mineralization and hornfels in the Liberty Bell Mine area. The Eva Creek fault is composed of several subparallel splays. The dip and dip direction of the longest strand is unknown; geologic mapping indicates that the southern side of the fault is down-thrown. Its trace at a scale of 1:50,000 does not appear to be topographically controlled, and therefore the longest strand is probably a high-angle fault. Freeman and others (1987) noted a 70°, north-dipping splay with reverse motion (south-

side-down) immediately south of the longest strand. Approximately 120+ m of offset is indicated from drill results. Conversely, plots of ore-element concentrations from rock samples suggest that relative movement on the Eva Creek fault is south-side-up. Te and Cu, elements found more proximal to plutons in hydrothermal systems, are concentrated south of the fault while Sb, Pb, and Zn, elements found more distal to plutons in hydrothermal systems, are more concentrated to the north of the fault (fig. 8). This elemental evidence suggests a possible vertical offset of more than 300 meters. Either the Eva Creek fault was reactivated later within a different stress regime or the fault is actually composed of several en echelon faults with different directions and amounts of offset. This fault is important because it offsets a magnetic high mapped as pyrrhotite-bearing hornfels and the ore-element geochemical anomalies discussed above.

Additional observations of structures made by Freeman and others (1987) are noted here. In the Liberty Bell Mine area, broad, open, vertical, north-northwest-trending folds with asymmetrical, small-scale, brittle kink folds formed axial plane fractures that host tourmaline, sulfide, and gold vein mineralization. The axial plane fractures probably acted as conduits for hydrothermal fluids. In Moose Creek, tensional gashes oriented N75°W that also host gold-bearing quartz-sericite-arsenopyrite veins are associated with shear pairs trending N75°E. Freeman and others (1987) also noted isoclinal folds in metamorphosed rock outcrops with their axial planes subparallel to foliation, and a possible second isoclinal fold direction with fold axes rotated 90° horizontally from the first direction.

## MINERALIZATION AND CRETACEOUS INTRUSIONS

Lode mineralization in the study area is widespread along the broad east-west-trending ridge of Paleozoic metamorphic rocks that crosses the middle of the map area (Freeman and Shaefer, 2001; Athey and others, 2005; appendix G). Mineralization and (or) hornfels occur in all of the Paleozoic units except those in the area that corresponds with Wahrhaftig's (1970c) Keevy Peak Formation, quartz metawacke (unit Dqw) and graphitic quartzite (unit Dgq). In addition, some granite (unit Kg) and granodiorite (unit Kgd) bodies are altered and mineralized. The lode occurrences include arsenopyrite ± gold ± bismuth minerals ± stibnite ± tourmaline + quartz veins and replacements, and pyrrhotite ± gold ± arsenopyrite + actinolite + biotite skarn (this study; Yesilyurt, 1996). Skarn mineralization occurs in metasomatized carbonate-altered metabasite (unit Db) and possibly unrecognized calcareous sediments. Cu-, Sb-, Pb- and Zn-bearing ore minerals are associated with gold-arsenopyrite mineralization and (or) are present as distal

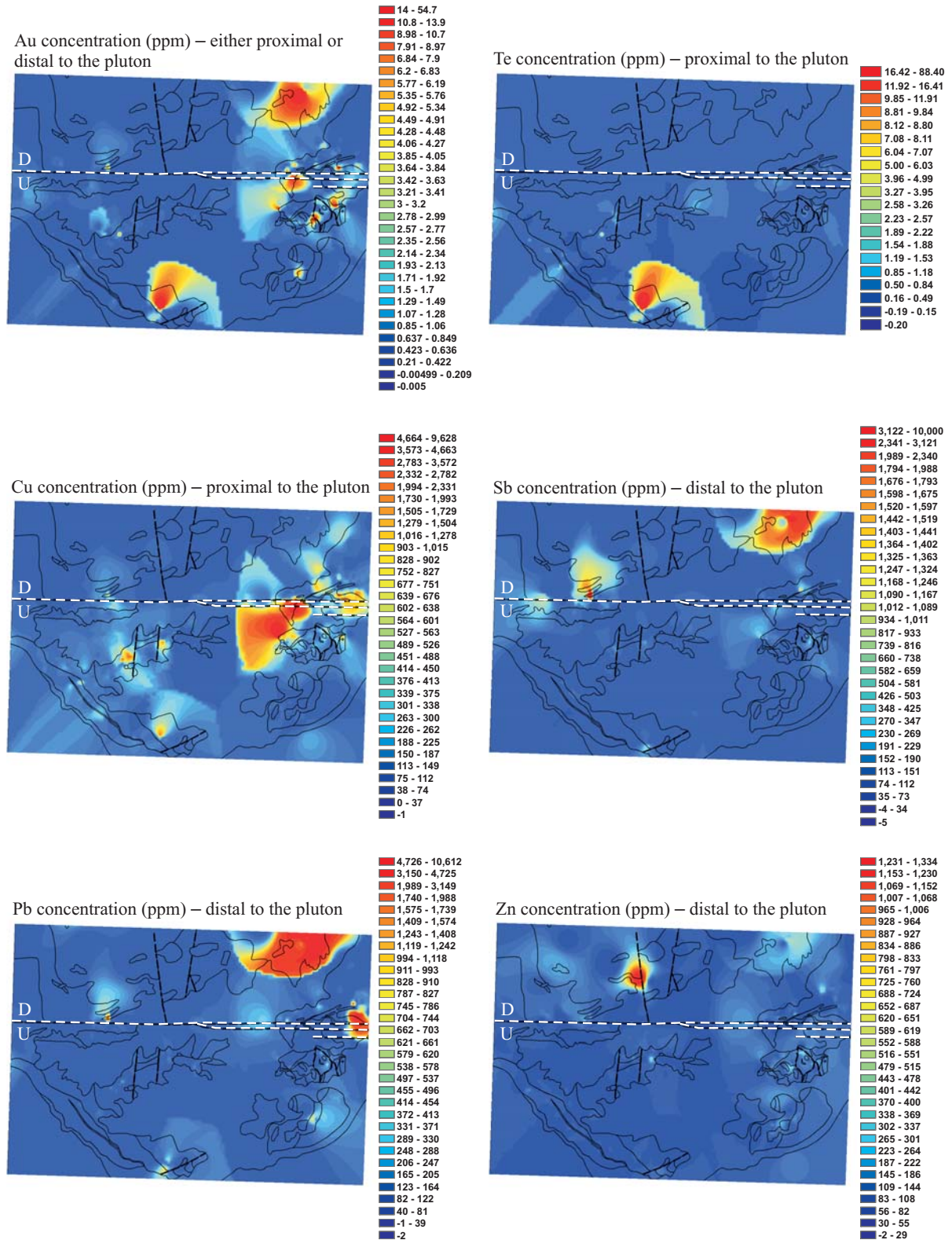


Figure 8. Gridded ore-element data from rock samples in the Liberty Bell Mine area. Grid method is Inverse Distance Weighted Interpolation with a power of 4. All elemental grids were plotted from ESRI ArcMap using Quantile classification with 32 classes, except Te, which had 20 classes, and Zn, which was plotted using Jenks Natural Breaks classification with 32 classes. Negative concentrations represent below-detection-limit data. Eva Creek fault is highlighted in white. Data from Galey and others, 1993; Bidwell, 1994; Yesilyurt, 1994, 1996; and Athey and others, 2005.

expressions of Au–As–Bi mineralization. Enriched gold values are associated with potassium silicate (alkali feldspar–biotite–tourmaline–quartz), chlorite–sericite–quartz, and widespread quartz–sericite alteration assemblages (Yesilyurt, 1996). Tourmaline is rarely found in Interior plutonic systems; three exceptions are Vinasale (Bundtzen, 1986), Democrat (McCoy and others, 1997), and possibly Nixon Fork (L.K. Freeman, oral commun., 2006).

Hydrothermal activity is not restricted to any one Paleozoic unit, and is texturally expressed as simple brittle veins, stockwork vein sets, breccias, and (or) replacement zones. Hydrothermal minerals include varying proportions of white- to gray-colored quartz, fine-grained, acicular, felted masses of medium brown (less commonly medium green) tourmaline, fine-grained white mica, arsenopyrite, and stibnite. Native gold in Moose Creek is associated with light green-gray, locally felted, tourmaline–monazite–quartz veins that cross-cut earlier dark brown massive biotite and quartz veins and breccia (Ray “Mudd” Lyle, oral commun., 2006; XRF data, this study). Timothy Ruppert (oral commun., 2005) reported native gold in crushed granodiorite in Little Moose Creek.

In the western half of the map area, an approximately 8 by 5.5 km magnetic high in airborne magnetic data (Burns and others, 2002) delineates a zone of hornfelsed metasedimentary and meta-igneous rocks (units Daw, Dq, Dgq, Dar, Dr, Dg, and Db), which suggests a large intrusion underlies the granite (unit Kg) and granodiorite (unit Kgd) dikes and stocks exposed at the surface. These granitic intrusions are interpreted to be genetically related to the hydrothermal event responsible for forming the Liberty Bell Mine gold deposit and other nearby gold occurrences. This interpretation is based on the close spatial association between these intrusions and gold-bearing veins and rocks, and comparison of the geochemical signature of gold-bearing rocks to other Interior Alaska gold deposits of this age (e.g., Fort Knox). Hydrothermal biotite and sericite are consistently 92–93 Ma. Secondary biotite from a quartz–orthoclase–biotite–tourmaline–sulfide vein that cross-cuts fine-grained phyllite yielded a K–Ar age of  $91.6 \pm 0.9$  Ma and sericite from a quartz–sericite–tourmaline–sulfide alteration zone associated with a cross-cutting felsic dike yielded a K–Ar age of  $93.0 \pm 1.0$  Ma (Yesilyurt, 1996). Biotite-altered arkosic metawacke yielded an  $^{40}\text{Ar}/^{39}\text{Ar}$  plateau age of  $92.0 \pm 0.5$  Ma (map location A3; table 5; this study). These ages match the age of the granodiorite intrusions ( $^{40}\text{Ar}/^{39}\text{Ar}$  biotite plateau age of  $91.6 \pm 0.5$  Ma, map location A2;  $^{40}\text{Ar}/^{39}\text{Ar}$  biotite plateau age of  $92.9 \pm 0.5$  Ma, map location A4; table 5), and by inference, the granite intrusions.

Several lines of evidence suggest that the Liberty Bell pluton is emplaced >300 m below the presently exposed mineralization. Placer gold from Little Moose Creek has a fineness of ~830, and contains ~6 percent Hg and <0.01 percent Cu (this study, table 6). The gold nuggets analyzed are subangular to subrounded, with dimensions of 1–3 mm x 1–3 mm x 0.3–0.6 mm, that is, with a length:width:height ratio of approximately 4:4:1. Surface roughness is readily apparent on most grains. Polishing revealed no obvious silver-depleted rim. The chemistry of the placer gold is similar to that of other typical lower-temperature, plutonic-related gold systems in Interior Alaska (fig. 9a). Figure 9b shows that gold of this composition is usually formed at temperatures of 300–400°C. The lack of high-temperature skarn mineralization is another indicator that the fluids were moderately cool at this distance (300–1,000 m) from the pluton, perhaps around temperatures of 300–350°C. By extrapolation, the size of the hornfelsed area indicates the maximum depth at which the pluton can be buried. Two examples of hornfelsing from Interior Alaskan plutons intruding low grade metamorphic rocks are Elephant Mountain (a 2–3-km-diameter pluton with a 300-m-thick hornfels rim) and Approach Hill (a 2-km-diameter pluton with a 200-m-thick hornfels rim; R.J. Newberry, oral commun., 2006). If the Liberty Bell pluton really is 2–4 times larger than the Elephant Mountain and Approach Hill plutons, as the aeromagnetic geophysical data suggest, one would expect a hornfels rim 400–1,200 m thick. Not accounting for variables such as topography, extent of hornfels already eroded, and surface irregularity of the pluton, gold chemistry and hornfels extent suggest the pluton lies at a depth between 300 and 1,200 m below the present-day surface.

Another potential source of mineralization may be present in the map area. The Tertiary Suntrana Formation (unit Tsn) forms a cap on one of the hills just west of California Creek. Although this unit typically consists of unconsolidated sand and gravel, at this location it forms massive, cliff-forming outcrops of silica-cemented sand and gravel. Along California Creek,

Table 6. *Placer gold composition from Little Moose Creek. Average of fifteen analyses. Composition by X-Ray fluorescence (XRF) at the University of Alaska Fairbanks.*

<b>Element</b>	<b>Average (Wt.%)</b>	<b>Std. Dev.</b>
Au	82.5	1.4
Ag	16.9	1.5
Hg	0.57	0.2
Cu	0.005	0.004
<b>Fineness</b>	830	+/- 15

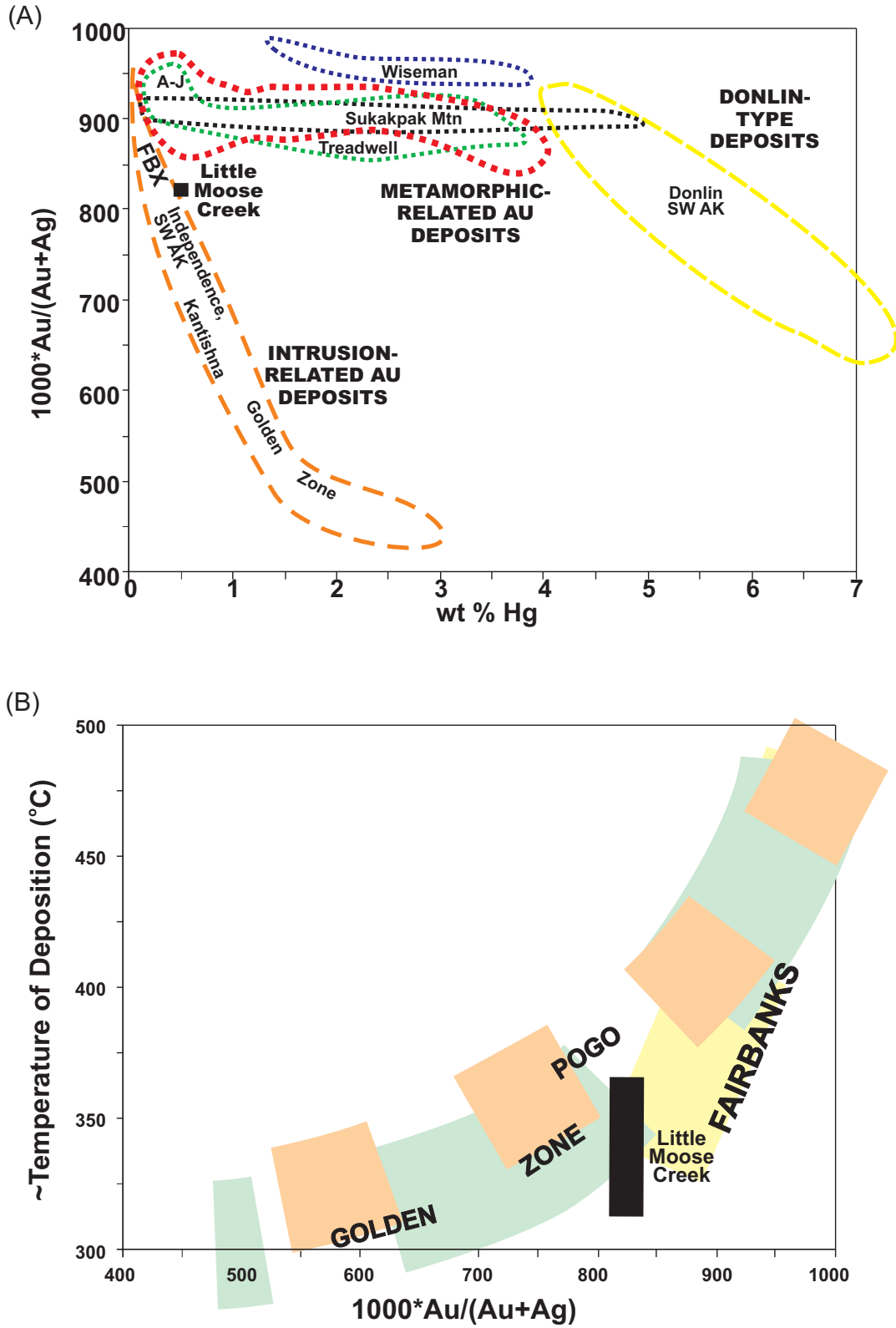


Figure 9. Typical(?) gold composition patterns for Interior Alaskan intrusion-related deposits. Unpublished data from R.J. Newberry, 2006. (A) Gold fineness versus mercury content. (B) Approximate temperature of gold deposition versus gold fineness.

at least one of the high-angle faults cutting the Paleozoic rocks is highly sheared, and the fault gouge and adjacent wall rocks are silicified. At other localities, the Paleozoic rocks are cut by shear veins containing quartz, arsenopyrite, and  $\pm$  pyrite. The presence of silica-rich pore fluids within the Tertiary Suntrana Formation, and potentially(?) some of the arsenic-bearing shears in California Creek, indicate the presence of a young (<15 Ma) hydrothermal system.

There are three obvious exploration targets for a plutonic-related gold system in the Liberty Bell area. The first is a Ft. Knox-type intrusion-hosted target, which would have a larger ore body with a lower grade. Because the Liberty Bell pluton is probably deeper than

300 m, this target is unattractive. The second type of target is replacement and skarn formed in calcareous units Db and any available calcareous sedimentary rocks. This type of ore body would have a smaller extent but higher grade. The third type of target is ore formed within structurally controlled veins or stockworks, again a smaller but high-grade ore body. Both replacement/skarn and structurally controlled mineralization are documented at Liberty Bell; however, more exploration is needed to delineate an economic deposit from the significant and widespread mineralization. The only significant hindrance to mineral exploration and possible future mine development is the Tertiary cover.

## UNIT DESCRIPTIONS

### TERTIARY SEDIMENTARY ROCKS

- Tn NENANA GRAVEL (Pliocene)—Light brown to orange-brown, poorly consolidated, clast-supported pebble conglomerate and sandstone. Conglomerate layers are commonly 1–60 cm thick but range up to 5 m thick. Gravel is well rounded to subrounded, averaging 5–30 mm in diameter with clasts up to 45 cm in diameter. Composition of gravel and larger clasts is 20–50 percent quartz and quartzite, 10–30 percent black and other chert, 10–80 percent plutonic (granite, gabbro, diorite), <20 percent volcanic (basalt, latite, diabase, andesite, porphyry), <20 percent metamorphic (phyllite, schist, orthogneiss), and <10 percent sedimentary (Cantwell Formation conglomerate, siltstone, mudstone, sandstone; not including chert). Gravel layers are commonly cemented with iron oxides forming ferricretes. Sites rich in gabbro cobbles and boulders, located in the northwest corner of the map area, possibly correlate with the upper 305 m of the Nenana Gravel section (Wahrhaftig, 1987) or the gabbro could be glacially transported (De Anne Stevens, oral commun., 2006). Gravel layers are interbedded with gray to pale brown to orange-brown, locally silty and clayey, very fine- to coarse-grained sand layers 5–20 cm thick, but up to 10 m thick. Sand is composed of quartz grains and sedimentary lithic fragments with significant but lesser amounts of feldspar grains and metamorphic, volcanic, and plutonic fragments (table 2). Clay fraction of the sand is composed of a small to moderate amount of kaolinite and montmorillonite, and possible zeolite and chlorite (table 3). Unit also contains thin, gray to orange clay layers, clay concretions up to 10 cm in diameter, and thin lignite layers with occasional plant remains (one log 10 cm in diameter). Magnetic susceptibility is low to moderate (0.00–1.34 averaging  $0.22 \times 10^{-3}$  SI [Système International]). Visual observations and measurements of cross-bedding generally indicate a northeastward paleocurrent direction (fig. 4). Possibly conformable on the Lignite Creek Formation in the southwestern corner of the map, but unconformable on a variety of units elsewhere in the map area. The intervening Grubstake Formation was not recognized in this map area. Wahrhaftig and others (1969) pinch the Grubstake Formation out along Elsie Creek, which crosses the southern boundary of the map area. Age from palynological and paleobotanical data (Wolfe and Tanai, 1980; Leopold and Liu, 1994). Maximum measured thickness is approximately 1,040 m in the headwaters of Suntrana Creek, located 15 km south of the map area (Wahrhaftig, 1987). Interpreted as coalescing alluvial fans shed during uplift of the Alaska Range (Wahrhaftig, 1987).
- Tlc LIGNITE CREEK FORMATION (Late Miocene)—Very fine- to medium-grained sandstone and gravel. Sandstone is white, light gray, cream, and orange, well sorted, well rounded, and rarely coarse-grained with <2 percent granules. The sand fraction is composed primarily of quartz grains and metamorphic lithic fragments, and lesser feldspar grains, sedimentary lithic fragments, and volcanic lithic fragments. Plutonic lithic fragments are rare (table 2). Beds are occasionally micaceous, contain clay concretions, and the silt content varies widely. The clay fraction of the sandstone is composed of low to moderate amounts of kaolinite, moderate to no amounts of montmorillonite (occasionally higher amounts), and possible zeolite and chlorite (table 3). Sandstone beds 3–4.5 m thick are commonly interbedded with light brown to

orange-brown, poorly sorted conglomerate layers 1–4 cm thick to less commonly 30.5–60 cm thick. Cross-bedding is infrequently observed in outcrop. Outcrops are generally composed of <5 percent, but up to 30 percent, conglomerate. Pebbles and cobbles in the conglomerate are well rounded to subangular and 0.5–8 cm in diameter (averaging 1 cm in diameter; rare cobbles up to 25 cm in diameter). Composition of clasts is 10–50 percent quartz, 35–50 percent metamorphic (black quartzite, other quartzite, quartz schist, slate, gneiss, greenstone), 20–50 percent chert (10–40 percent black chert, 0–5 percent red chert), 10–40 percent plutonic (gabbro, diorite, granite, clinopyroxenite?), 5–20 percent volcanic (basalt, rhyolite, hornblende andesite, dacite?), and 0–5 percent sedimentary (Cantwell Formation conglomerate, argillite, sandstone, limestone). Locally iron cemented, forming ferricrete and occasionally contains iron concretions 2–15 cm in diameter. Unit also contains platy- to blocky-parting, light gray to brown shale <57 cm thick and friable coal <0.7 m thick (apparent coal rank is Lignite A; table F1). Magnetic susceptibility is low to moderate (0.00–3.44, averaging  $0.22 \times 10^{-3}$  SI; one sandstone sample registered  $20.5 \times 10^{-3}$  SI). Visual observations and measurements of cross-bedding generally indicate a southward or westward paleocurrent direction (fig. 4). Conformably overlies the Suntrana Formation (Wahrhaftig and others, 1969). Age from paleobotanical data (Wolfe and Tanai, 1980). Thickest measured section is 244 m in the Wood River coal basin, located 45 km east of the map area (Wahrhaftig and others, 1969). Interpreted as point bar deposits, gravelly and sandy braided stream deposits, and lesser overbank deposits (Buffler and Triplehorn, 1976; Stanley and others, 1992).

- Tsn SUNTRANA FORMATION (Middle Miocene)—Fine- to medium-grained with minor very fine- to coarse-grained, “salt and pepper” sandstone and conglomerate. Sandstone has an overall gray to light yellow-brown color. Rarely beds are iron-oxide stained. Sandstone is well-sorted, rarely clayey (kaolinite > montmorillonite) or silty and is composed primarily of quartz, minor feldspar grains, and lesser sedimentary and metamorphic lithic fragments; volcanic and plutonic lithic fragments are rare (table 2). Conglomerate beds 10–70 cm thick occur in about 5–50 percent of the outcrops. Conglomerate is composed of 25–80 percent white quartz, 15–50 percent black chert, 20–25 percent white and black quartzite, 5–60 percent metamorphic clasts (schist, phyllite), <10 percent red and green chert, <5 percent granitic rocks and minor conglomerate, diabase, and porphyritic igneous rocks. Gravel averages 1–2 cm in diameter (ranges 3 mm to 10 cm). Outcrops contain fining-upward sequences and cross-bedding. Unit also contains glassy, conchoidally fracturing coal up to 6 m thick (apparent coal rank is Lignite A and B and High-volatile Subbituminous C; table F1) and gray to chocolate brown, platy, friable shale. Magnetic susceptibility is variable (0.0–13.0, averaging  $1.32 \times 10^{-3}$  SI; coal had magnetic susceptibilities up to  $43.4 \times 10^{-3}$  SI). Cross-bedding in the Suntrana Formation throughout the Nenana coal basin generally indicates a south- or westward paleoflow (Wahrhaftig and others, 1969; Ridgway and others, 1999). Unit is almost entirely burnt in the Rex Dome area, and local, small pockets of clinker occur south of hill VABM Coal. In the field area, Suntrana Formation may conformably overlie Healy Creek Formation without the intervening Sanctuary Formation. Sanctuary Formation as described by Wahrhaftig and others (1969) and Wahrhaftig (1987) was not recognized in the field area. Assigned stratigraphic age from paleobotanical data (Wolfe and Tanai, 1980). Thickest section of unit is 393 m on Coal Creek, tributary of Healy Creek, 13.5 km south of the map area (Wahrhaftig and others, 1969). Interpreted as high-energy fluvial channels filled by gravel and sand bars (Buffler and Triplehorn, 1976; Wahrhaftig, 1987; Stanley and others, 1992).
- Thc HEALY CREEK FORMATION (Early Miocene–Early Oligocene/Late Eocene?)—Interbedded, poorly sorted pebbly sandstone, siltstone, claystone, conglomerate, and coal. Sandstone is white to light gray, very fine- to fine-grained, with lesser medium- and coarse-grained sandstone; it contains about 60–80 percent sand, 5–40 percent pebbles, and 5 percent cobbles. Sand is composed of quartz grains, metamorphic rock fragments, feldspar grains, minor sedimentary rock fragments, and rare plutonic or volcanic rock fragments. Brown to gray, platy, micaceous siltstone and claystone (primarily kaolinite) weathers bright white, locally exhibits varves, and frequently contains subangular to angular, 2–3 mm quartz and chert granules. White to light brown conglomerate contains well rounded to subangular gravel 1–3 cm in diameter (up to 40 cm in diameter) in a sandy + silty + clayey matrix. Gravel is composed of 30–92 percent quartz, 20–45 percent locally derived metamorphic clasts, 5–45 percent chert, 5 percent red chert, and rare quartzite and granite. Platy, friable, locally resinous coal beds are 8 cm to 2.5 m thick (apparent coal rank is Lignite A and B and High-volatile Subbituminous C; table F1). On the northern edge of the map, one

outcrop contains at least 14 fining-upward sequences of pebbles to 8-cm-thick coal beds. Magnetic susceptibility is moderate (0.0–1.49, averaging  $0.43 \times 10^{-3}$  SI); coal exhibits magnetic susceptibilities up to  $11.5 \times 10^{-3}$  SI. Unit is commonly burnt north of hill VABM Coal. Cross-bedding in the Healy Creek Formation throughout the Nenana coal basin indicates a variety of paleocurrent directions (Wahrhaftig and others, 1969; Ridgway and others, 1999). Unit was deposited on an irregular surface, infilling valleys (Wahrhaftig and others, 1969); significant thickness changes over short distances and unit's composition was heavily influenced by surrounding bedrock. Assigned stratigraphic age from palynological and paleobotanical data (Wolfe and Tanai, 1987; Leopold and Liu, 1994). Thickness of unit in the map area is unknown; unit is 350 m thick at the eastern edge of the Healy Creek coal basin, 13 km south of the map area (Wahrhaftig and others, 1969). Interpreted as sand and gravel bars in shallow, low-sinuosity channels of high-energy, braided streams and fine-grained sediment deposited in abandoned, quiet-water stream channels (Buffler and Triplehorn, 1976; Wahrhaftig, 1987; Stanley and others, 1992).

### TERTIARY–CRETACEOUS IGNEOUS ROCKS

- Td** DACITE FLOWS (Tertiary)—Fine-grained, massive, jointed ( $\pm$  columnar?), porphyritic flows crop out in the southeastern map area. Unit is at least 200 m thick. Light- to dark-green colored, with varying proportions of hornblende, biotite, pyroxene, plagioclase, and (or) quartz phenocrysts up to 6 mm in length in an aphanitic groundmass. Modal composition is 62 percent plagioclase, 10 percent hornblende, 20 percent quartz, 3 percent pyroxene, 3 percent biotite, and 2 percent opaque minerals (both magnetite and ilmenite? based on shapes). Secondary chlorite partially to completely replaces mafic minerals. Major- and minor-oxide and trace-element analyses indicate the dacite flows are calc-alkalic and likely to be subduction related (fig. 7). Magnetic susceptibility is high (1.00–10.00, averaging  $3.78 \times 10^{-3}$  SI). Unit corresponds to a pronounced magnetic high in airborne geophysical data (Burns and others, 2002).  $^{40}\text{Ar}/^{39}\text{Ar}$  biotite plateau age of  $37.4 \pm 0.3$  Ma (map location A1; table 5). This unit is not related to the Jumbo Dome intrusive center, located 3 km south of the map border. Jumbo Dome is a much younger system ( $^{40}\text{Ar}/^{39}\text{Ar}$  hornblende weighted average age of  $1.026 \pm 0.057$  Ma) and compositionally an Adakite (Sr:Y ratio approximately 1,000:1; C.J. Nye, written commun., 2006), while the Sr:Y ratio of this unit is 7:1. The closest, dated, volcanic rock of that approximate age is from Sugar Loaf Mountain, a fossilized volcanic vent located 24 km to the south (K-Ar ages of  $32.4 \pm 1.0$  to  $35.2 \pm 1.0$  Ma; Albanese and Turner, 1980). Unit is offset by a late, north–northeast-trending, high-angle fault.
- Kg** GRANITE DIKES AND STOCKS (Cretaceous)—Fine- to very fine-grained, porphyritic-textured, lesser equigranular-textured, and rarely pegmatitic-textured, hypabyssal granite dikes (up to 10 m wide; average less than 3 m wide) and stocks (at least 1.2 km long and 0.3 km wide) are present throughout the map area. Orange to light yellow-brown weathering, white to light gray colored. Porphyritic intrusions contain widely varying proportions of quartz, feldspar, and  $\pm$  biotite phenocrysts (10–42 percent; average 21 percent) in an aphanitic to finely granular matrix. Modal composition ranges from 2–38 percent quartz (average 13 percent), 4–65 percent feldspar (average 16 percent), 0–7 percent biotite, 0–2 percent primary(?) tourmaline, and accessory sphene, zircon, rutile, and apatite. Freeman and others (1987) reported the presence of small, pink to red, clear, glassy euhedral garnets. Dikes that intrude graphitic phyllite (unit Dgq) north of Cody Creek in the western map area contain up to 3 percent graphite, and 70 percent perthite. Weight percent CIPW normative compositions were assigned to igneous rocks using the methodology of Irvine and Baragar (1971). The granite intrusions are locally intensely sericitized, silicified, and tourmalinized with occasional chlorite, epidote, and clinozoisite alteration. Associated mineralization includes arsenopyrite, scorodite, and stibiconite. Major- and minor-oxide and trace-element analyses indicate the granite intrusions are subduction-related and formed in an island-arc tectonic setting (fig. 7). Magnetic susceptibility is low (0.00–0.31, averaging  $0.05 \times 10^{-3}$  SI). Age estimated to be 93 Ma based on a  $93.0 \pm 0.95$  Ma K-Ar age of sericite from a quartz–sericite–tourmaline–sulfide alteration zone associated with a cross-cutting felsic dike in the Liberty Bell Mine area (Yesilyurt, 1996) and spatial association with, and trace-element-indicated tectonic setting similarity to, unit Kgd.
- Kgd** GRANODIORITE DIKES AND STOCK (Cretaceous)—Fine- to medium-grained, porphyritic to equigranular granodiorite dikes (average 3 m wide) and stocks (at least 1.2 km long and 80 m wide) are present along Moose Creek, Little Moose Creek, and on the southern flank of hill VABM Coal. Brown weathering;

white, light yellow-brown, and gray-green colored. Porphyritic intrusions contain highly variable proportions of quartz, feldspar,  $\pm$  biotite, and  $\pm$  hornblende phenocrysts (up to 65 percent; average 29 percent) in an aphanitic to finely granular matrix. Modal composition ranges from 0–15 percent quartz, 16–35 percent plagioclase, 16–30 percent K-feldspar, 0–30 percent hornblende, 0–28 percent biotite, and accessory apatite, zircon, rutile, and opaque minerals. Rock names were assigned from weight percent CIPW normative calculations; one sample from lower Moose Creek is a tonalite and may represent a more mafic phase of the pluton. Intrusions contain chlorite, epidote,  $\pm$  actinolite altered from hornblende and biotite, and are locally silicified and sericitized. Mineralization includes gold (panned from a crushed rock sample from Little Moose Creek; Timothy Ruppert, oral commun., 2005), pyrite, arsenopyrite, and scorodite. Major- and minor-oxide and trace-element analyses indicate the granite intrusions are subduction-related and formed in an island-arc tectonic setting (fig. 7). Magnetic susceptibility is low ( $0.00\text{--}0.31$ , averaging  $0.05 \times 10^{-3}$  SI).  $^{40}\text{Ar}/^{39}\text{Ar}$  ages of 92–93 Ma (hornblende plateau age of  $91.6 \pm 0.5$  Ma [map location A2]; biotite plateau age of  $92.9 \pm 0.5$  Ma [map location A4]; table 5). Unit Kgd is possibly a more mafic, marginal phase of a larger, subsurface granitic(?) pluton.

- Kb** GABBRO DIKES (Cretaceous)—Fine-grained, blocky to spheroidally weathering, equigranular to porphyritic gabbro dikes up to 3 m in width are present on hill VABM Coal in the eastern map area. Medium-brown weathering, dark-green colored, with rare quartz- and calcite-filled amygdules up to 5 mm in diameter. Porphyritic dikes contain plagioclase phenocrysts up to 1 cm in length. Modal composition ranges from 55 to 58 percent plagioclase, 0–38 percent hornblende, 3–25 percent biotite, 0–15 percent olivine, 0–5 percent opaque minerals, and accessory apatite. Secondary minerals include talc, chlorite, calcite, quartz, and (or) white mica. Major- and minor-oxide and trace-element analyses indicate the gabbro dikes are subduction-related and formed in an island-arc tectonic setting (fig. 7). Magnetic susceptibility is moderate to high ( $0.30\text{--}1.95$ , averaging  $2.57 \times 10^{-3}$  SI).  $^{40}\text{Ar}/^{39}\text{Ar}$  biotite plateau age of  $95.6 \pm 0.5$  Ma (map location A5; table 5). Unit Kb is about 3 million years older than unit Kgd; the two igneous units may not be genetically related.

#### PALEOZOIC UNITS

- Dg** METAGRANITE (Devonian)—Megacrystic to lesser fine-grained, equigranular to porphyritic metagranite. Orange weathered; white, light green, and light gray colored. Foliated outcrops break in semi-massive blocks to schistose sheets. Modal composition is 10–40 percent relict quartz phenocrysts (average 22 percent) and 10–65 relict feldspar phenocrysts (average 34 percent). Metagranite is defined as having relict quartz + feldspar phenocrysts  $> 60$  percent based on typical textures exhibited by extrusive volcanic and hypabyssal rocks (K.F. Bull, oral commun., 2006). Megacrystic samples from Rex Dome and other similar bodies in the northern map area, which contain relict feldspar phenocrysts 1.5–3.0 cm (average 1.6 cm) and relict quartz phenocrysts 1–10 mm (average 4.3 mm), artificially generate low modal compositions because not every small sample or thin section contains the correct ratio of megacryst to matrix. Megacrystic samples are assumed to be metagranite instead of metarhyolite. Porphyritic samples with high crystal contents may represent a continuous increase in relict phenocrysts from metarhyolite, unit Dr. Conversely, groundmass composed of white mica and very fine-grained quartz and feldspar may have been seriate-textured before metamorphic recrystallization. Relict phenocrysts are commonly euhedral and sub-euhedral to less commonly spindle-shaped and sheared along foliation. Also contains biotite, chlorite (from biotite), rutile, epidote, clinozoisite, zircon, sphene, and opaque minerals. Rarely contains inclusions of unit Dgq. Weight percent CIPW normative composition is granite. Both varieties typically have  $\text{Nb} + \text{Y} > 50$  ppm and  $\text{TiO}_2 < 0.3$  ppm. Metagranite is locally hornfelsed and mineralized by arsenopyrite, pyrite, and pyrrhotite as disseminated crystals and in cross-cutting quartz  $\pm$  tourmaline veins. Feldspars commonly, partially to wholly replaced by sericite and quartz. Magnetic susceptibility is low ( $0.0\text{--}0.6$ , averaging  $0.09 \times 10^{-3}$  SI); hornfelsed samples containing pyrrhotite have magnetic susceptibilities up to  $6.0 \times 10^{-3}$  SI. Major- and minor-oxide and trace-element analyses indicate the metagranite formed in a within-plate, extensional tectonic setting (fig. 7). Represents metamorphosed plugs, dikes, and (or) sills at least 3.4 km long and 0.6 km thick (probably stretched and thinned within foliation, respectively) emplaced within units Daw and Dgq. Where spatial extent is unknown, locations are marked with a symbol (see ‘Map Symbols,’ sheet RI 2006-2). Equivalent to augen gneiss in the California Creek Member of the Totatlanika Schist and comprises a portion of the area mapped as the Moose Creek Member of the

Totatlanika Schist on Wahrhaftig's map (1970c) of the Fairbanks A-4 Quadrangle. Zircons from California Creek Member augen gneiss located about 37.5 km southeast of the map area and dated by SHRIMP U-Pb exhibit an age of  $373 \pm 3$  Ma (fig. 5; Dusel-Bacon and others, 2004).

- Dr METARHYOLITE (Devonian)—Very fine- to medium-grained, porphyritic metarhyolite. Orange and brown weathered; white, gray, and light green colored and possibly flow banded. Forms massive, blocky outcrops with poorly formed foliation to well-foliated outcrops with strong cleavage. Modal composition is 1–40 percent relict feldspar phenocrysts (average 18 percent), 1–20 percent relict quartz phenocrysts (average 10 percent), and accessory apatite, zircon, and rutile. Feldspar crystals are 1–15 mm in diameter (average 2.3 mm) and quartz crystals are 0.5–4 mm in diameter (average 1.8 mm). Relict quartz (frequently embayed) and feldspar phenocrysts are euhedral to rarely subrounded, and frequently shattered and sheared in foliation. Groundmass is composed of very fine-grained (<0.02 mm), granular quartz, feldspar, and white mica. No tuffaceous textures are present. Metarhyolite is defined as having relict quartz + feldspar crystals < 60 percent based on typical textures in extrusive volcanic and hypabyssal rocks (K.F. Bull, oral commun., 2006). Weight percent CIPW normative composition is primarily granite (rhyolitic texture); a few samples from the mine area are dacitic ( $\text{SiO}_2 < 68$  percent). Metarhyolite typically has  $\text{Nb} + \text{Y} > 50$  ppm and  $\text{TiO}_2 < 0.3$  ppm. Where hornfelsed, metarhyolite contains biotite and (or) phlogopite, and is locally cross-cut and brecciated by quartz + sericite + tourmaline + arsenopyrite  $\pm$  pyrrhotite  $\pm$  pyrite(?) veins. Frequently samples have iron oxide pseudomorphs after pyrite(?) and feldspar is altered to sericite and quartz. Other alteration products include epidote, chlorite, and carbonate. Magnetic susceptibility is low (0–0.8, averaging  $0.12 \times 10^{-3}$  SI); hornfelsed samples have magnetic susceptibilities up to  $3.07 \times 10^{-3}$  SI. Major- and minor-oxide and trace-element analyses indicate the metarhyolite formed in a within-plate, extensional tectonic setting (fig. 7). Represents flows or hypabyssal intrusions at least 5 km long and 0.4 km wide (probably stretched and thinned within foliation, respectively) that intrude units Daw, Dgq, and Dqw. Where spatial extent is unknown, locations are marked with a symbol (see 'Map Symbols,' sheet RI 2006-2). Equivalent to "Dacite crystal tuff" in Liberty Bell Mine sequence (Freeman and others, 1987) and comprises most of the area mapped as the Moose Creek Member of the Totatlanika Schist on Wahrhaftig's map (1970c) of the Fairbanks A-4 Quadrangle. Zircons from "Moose Creek Member" metarhyolite located about 39 km southeast of the map area and dated by SHRIMP U-Pb exhibit an age of  $365 \pm 5$  Ma (fig. 5; Dusel-Bacon and others, 2004).
- Dar APHYRIC METARHYOLITE (Devonian)—Aphyric, finely laminated, metamorphosed rhyolite flow or sill located at the head of Cody and Spruce creeks and one metamorphosed dike(?) located between Spruce and California creeks. White- to light gray- to light yellow-brown-weathering, with pale gray to pale greenish-gray color laminations (possible flow banding). Typically forms rounded hills of loose, fissile chips, but near the head of Spruce Creek, forms prominent outcrops that exhibit isoclinal folding of laminations. In thin section, composed of an aphanitic to finely granular mixture of quartz and feldspar, some of which may exhibit relict spherulitic texture. Phenocrysts of quartz are very rare. Weight percent CIPW normative composition is granite (rhyolitic texture). Typically has  $\text{Nb} + \text{Y} > 50$  ppm and  $\text{TiO}_2 < 0.3$  ppm. Major- and minor-oxide and trace-element analyses indicate the aphyric metarhyolite formed in a within-plate, extensional tectonic setting (fig. 7). Also contains rare, blocky, laminated pieces of bright red- and white-colored, banded, hematite-bearing, granular quartzite (jasperoid). Magnetic susceptibility is low (0.00–0.11, averaging  $0.04 \times 10^{-3}$  SI). Topographically overlies units Daw and interfoliated Dgq. Age is based on a trace-element-indicated tectonic setting similar to, and loose spatial association with, units Dg and Dr.
- Db METABASITE (Devonian)—Carbonate-altered, metamorphosed mafic flows, sills, dikes, and (or) tuff. Primarily gray and green colored, but also brown and black. Metabasite is aphanitic to medium-grained (rarely coarse-grained), locally banded and laminated, and foliated. Outcrops are platy-breaking to massive. Primary igneous textures are erased by recrystallization and alteration. Mineral composition varies widely, but chemical composition suggests a mafic parent (high  $\text{TiO}_2$  and MgO). Where metamorphosed but not carbonate-altered, major element composition is clearly basaltic; mineralogy is 30–50 percent chlorite, 20–30 percent albite, 10–20 percent clinozoisite, <10 percent carbonate, <10 percent quartz, and 1–2 percent rutile + sphene + magnetite. Where carbonate-altered but not metasomatized, composition is 15–55 percent carbonate, <35 percent chlorite, <30 percent albite, <25 percent white mica, <15 percent

quartz, and accessory rutile, ilmenite, magnetite, and other opaque minerals. Due to its high carbonate content, metabasite is the preferred ore host at the Liberty Bell Mine. Where variably metasomatized and hornfelsed in the general mine area, composition is <95 percent tremolite, <70 percent biotite/phlogopite, <67 percent calcite, <60 percent black to dark green chlorite, <60 percent white mica, <60 percent pyrophyllite, <45 percent actinolite, <40 percent plagioclase, <40 percent quartz, <30 percent clinopyroxene (diopside?), <25 tourmaline (brown- and green-gray-zoned), lesser epidote, clinozoisite, and accessory rutile, sphene, zircon, monazite, magnetite, ilmenite, and other opaque minerals. Ore minerals include arsenopyrite, pyrite, chalcopyrite, and pyrrhotite. Locally contains pyrrhotite–arsenopyrite–actinolite–calcite veins that cross-cut and subparallel foliation. Unit is rarely carbonaceous; a portion of the calcareous material may originally have had a sedimentary, instead of a mafic igneous, protolith. Magnetic susceptibility is moderate to high (0.0–5.92, averaging  $0.63 \times 10^{-3}$  SI), primarily reflecting the pyrrhotite content. Major- and minor-oxide and trace-element analyses indicate the metabasite is alkalic and formed in a within-plate, extensional tectonic setting (fig. 7). Equivalent to the “Eva Creek phyllite” (Freeman and others, 1987) and possibly the chloritic schist of the Moose Creek Member of the Totatlanika Schist (Wahrhaftig, 1968). In the map area, the longest, continuous metabasite body is 2.5 km and the thickest is at least 300 m. Spatially associated and interfoliated with units Dgq, Dq, Dr, and Dg such that the group forms a laterally extensive E–W subunit, suggesting stratigraphic significance. This grouping is essentially the Liberty Bell Mine sequence (Freeman and others, 1987). Metabasite is found within these units and unit Daw, and is the mafic portion of the bimodal suite of alkalic, igneous rocks. Where spatial extent is unknown, locations are marked with a symbol (see ‘Map Symbols,’ sheet RI 2006-2). Age is based on a trace-element-indicated tectonic setting similar to, and spatial association with, units Dg and Dr.

**Daw** ARKOSIC METAWACKE (Devonian)—Fine- to medium-grained with minor very fine- and coarse-grained, metamorphosed arkosic wacke and lesser feldspathic wacke. Also contains rare metamorphosed quartz wacke and fine-grained quartzite. Forms light green, gray, and white colored, commonly iron-stained, well-foliated and schistose outcrops; less commonly forms massive outcrops. Modal composition is 5–85 percent feldspar porphyroclasts (average 32 percent; average 2.2 mm in diameter), <80 percent clear, white, and smoky quartz porphyroclasts (average 17 percent; average 2 mm in diameter), and <5 percent lithics in very fine-grained (<0.02 mm) sericite ± chlorite ± biotite + quartz + feldspar matrix. Matrix is interpreted to be recrystallized mud. Accessory minerals include zircon, apatite, sphene, opaque minerals, and monazite. Metamorphosed lithic fragments include carbonaceous slate (mud rip-up clasts?), polycrystalline quartz, chert, quartz–feldspar amalgams, and rare scheelite and garnet. Exhibits crystal sorting (bedding?). Although a large percentage of the porphyroclasts are rounded, shattered, and (or) sheared along foliation, occasional euhedral to sub-euhedral porphyroclasts, quartz embayments, and a homogeneous quartz + feldspar clast composition suggest the sediments are derived from felsic igneous rocks. Typically has Y + Nb < 50 ppm (fig. 6) and TiO<sub>2</sub> >0.3 ppm. Locally contains disseminated arsenopyrite and pyrite, scorodite and stibiconite staining, and quartz ± tourmaline veins up to 5 cm thick. Magnetic susceptibility is low (0.0–0.92, averaging  $0.10 \times 10^{-3}$  SI); higher values are from hornfelsed samples. Except for the megacrystic variety of Dg, interfoliated units Db, Dg, Dq, Dr, Dar, and Dgq decrease in abundance to the north toward the topographic top of the unit. Unit is at least 900 m thick in Last Chance Creek, located 18 km southeast of the map area (Wahrhaftig, 1968). Equivalent to the “Lower tuffite sequence” in the Liberty Bell Mine sequence (Freeman and others, 1987) and quartz–orthoclase–sericite schist from the California Creek Member of the Totatlanika Schist (Wahrhaftig, 1970c). Age is assumed to be Devonian; unit is intruded by Devonian-aged meta-igneous units Dg and Dr and stratigraphically(?) overlain by the Devonian Chute Creek Member of the Totatlanika Schist (fig. 5; Dusel-Bacon and others, 2004).

**Dq** QUARTZITE AND METAPELITE (Devonian)—Very fine- to fine-grained, sucrosic quartzite and metapelite. Orange-weathered, white-colored outcrops are either platy-breaking or hard and massive depending on the mica content of the rock. Modal composition is 50–97 percent quartz (grains up to 0.1 mm in diameter), 3–50 percent white mica, 5(?) percent feldspar, and 2 percent calcite. Commonly contains <2 percent disseminated pyrrhotite, <5 percent pyrite, and lesser tourmaline, arsenopyrite, and phlogopite/biotite in wispy bands and laminations. This unit only appears in the hornfelsed zone. Magnetic susceptibility is moderate to high (0.0–4.0, averaging  $0.45 \times 10^{-3}$  SI), and variable due to the

amount of unoxidized pyrrhotite in the rock. In Little Moose Creek, unit is at least 350 m thick. Equivalent to the “Hangingwall slaty phyllite” in the Liberty Bell Mine sequence (Freeman and others, 1987) and slate within the California Creek and Moose Creek(?) members of the Totatlanika Schist (Wahrhaftig, 1968). Quartzite and metapelite is found interfoliated with units Dgq, Daw, Dr, Dg, and Db. Age is based on spatial association with these Devonian units.

**Dgq** GRAPHITIC QUARTZITE (Devonian)—Very fine- to fine-grained, sucrosic, foliated graphitic quartzite. Gray- to black-colored outcrops are fissile to blocky-breaking. Composition is <90 percent quartz, <36 percent white mica, <10 percent graphite, with accessory apatite, zircon, and opaque minerals. Graphite occurs disseminated throughout the rock, in lenses, sooty partings, and rare nodules. Locally hornfelsed and bleached to light gray and white, and commonly iron-oxide stained. Hornfels contains up to 30 percent pyrrhotite and occasionally quartz–tourmaline–biotite/phlogopite veins. Intense mineralization is expressed as brecciated quartz veins with iron oxide, scorodite, and arsenopyrite cement. Magnetic susceptibility is generally low (0.0–1.0, averaging  $0.1 \times 10^{-3}$  SI); hornfelsed samples containing pyrrhotite have magnetic susceptibilities up to  $2.53 \times 10^{-3}$  SI. In the map area, unit ranges from 3-m-thick lenses to approximately 700-m-thick sections, and decreases in thickness topographically (and stratigraphically?) up-section. Unit found interfoliated with all of the Devonian units in the map area, and age of unit is also assumed to be Devonian. Equivalent to “Graphitic (Footwall) phyllite” of the mine sequence (Freeman and others, 1987) and graphitic quartzite and schist in the California Creek and Moose Creek Members of the Totatlanika Schist and the Keevy Peak Formation (Wahrhaftig, 1968).

**Dqw** QUARTZ METAWACKE AND META-ARENITE (Devonian)—Very fine- to medium-grained, rarely coarse-grained, metamorphosed quartz wacke and arenite, and minor feldspathic wacke. Light gray and light gray-green colored, hard and massive to platy-breaking, and foliated in outcrop. Modal composition is 14–80 percent quartz porphyroclasts (mono- and polycrystalline), 0–25 percent feldspar porphyroclasts (varying amounts of K-feldspar and plagioclase/albite), 0–10 percent chert or chalcedony grains, and a matrix of 5–50 percent white mica, 0–25 percent chlorite, and 20–35 percent very fine-grained quartz (<0.02 mm). Accessory minerals include tourmaline, rutile, ilmenite, graphite, pyrite, and zircon. Subangular to rounded, 0.2–3.0 mm grains are common. Magnetic susceptibility is low (0.0–0.5, averaging  $0.09 \times 10^{-3}$  SI). In the map area, unit is at least ~600 m thick. Topographically underlies California Creek Member and units Dg and Dr, mapped as the Moose Creek Member of the Totatlanika Schist (Wahrhaftig, 1970c). Equivalent to “arkosic gritlike schist” of Keevy Peak Formation (Wahrhaftig, 1970c). Age is presumed to be Devonian; unit is intruded by meta-igneous unit Dr, stratigraphically(?) overlain by unit Daw, and stratigraphically(?) underlain by Devonian(?) Healy Schist (Birch Creek Schist of former usage; Wahrhaftig, 1968; Newberry and others, 1997; Dusel-Bacon and others, 2004) (fig. 5).

## ACKNOWLEDGMENTS

This project is part of the Alaska Airborne Geophysical/Geological Mineral Inventory Program funded by the Alaska State Legislature and managed by State of Alaska, Department of Natural Resources (DNR), Division of Geological & Geophysical Surveys (DGGS). Partial funding for the geologic mapping was also provided by the U.S. Geological Survey, National Cooperative Geologic Mapping Program, under STATEMAP award number 05HQAG0025, and the State’s General Fund. Partial funding for the proximate and ultimate coal analyses presented in tables F1 and F2 (appendix F) was provided through a grant from the U.S. Geological Survey’s National Coal Resource Data System. The views and conclusions contained in this document are those of the authors and should not be interpreted as necessarily representing the official policies, either expressed or implied, of the U.S. Government.

The following people are recognized for their various contributions to this map.

**Quaternary:** De Anne S.P. Stevens (DGGS) for geologic discussions and sharing preliminary data from the surficial-geologic study.

**Tertiary:** Rocky R. Reifentuhl (DGGS) and Kenneth P. Helmold (Alaska Division of Oil & Gas) for discussions regarding grain mounts and point counting; Paul J. McCarthy (University of Alaska Fairbanks) for discussions about Tertiary sample processing; Robert L. Ravn (the IRF group, inc.) for assistance interpreting pollen data; Paul A. Metz (University of Alaska Fairbanks) for the use of his sedimentary lab; Paul W. Layer (University of Alaska Fairbanks) for providing an  $^{40}\text{Ar}/^{39}\text{Ar}$  analysis of a fused sedimentary rock sample; Alan Renshaw (Usibelli Coal Mine) for hosting a field trip through

the Tertiary section; James G. Clough (DGGS) for providing coal energy analyses; and Ronald H. Affolter (USGS–Denver), Gary D. Stricker (USGS–Denver), and Jamey D. McCord (USGS–Energy Lab) for providing geochemical analyses of coal ash.

**Pre-Tertiary and mineralization:** Katharine F. Bull (DGGS) for assistance distinguishing greenschist facies metavolcanic and volcanic textures; Erik W. Hansen for facilitating review of industry data and maps; John T. Galey, Jr. for providing industry data and thoughts about the mineralizing system; Richard R. Lessard (DGGS) for compilation of industry data and compiling geochemical data release RDF 2005-5; Christopher J. Nye (DGGS/Alaska Volcano Observatory) for providing an Ar-Ar age; the Ruppert family for donating a placer gold sample from Little Moose Creek; and Ray “Mudd” Lyle and Jim Roland for Moose Creek lode samples.

**Other:** David L. LePain (DGGS) and Richard W. Flanders for their thoughtful, technical reviews; Paula K. Davis (DGGS) for her editorial review; Wesley K. Wallace (University of Alaska Fairbanks) and Robert F. Swenson (DGGS) for structural geology discussions, Laurel E. Burns (DGGS) for assistance with interpretation of geophysical and statistical data; student interns William A. Smith, II, Benjamin D. Christian, and Brian A. McNulty for their assistance on various parts of this project; Robin L. Smith (DGGS) for help with point counting and final map preparation; Mike Franger (Alaska Mental Health Trust Land Office) for providing access to Mental Health lands; Jim Roland, Wallace O. Turner, II, and the Blair family for allowing us access to industry data from their property; and the Blair family (Boothill Gold, Inc.) for letting us stay at the Eva Creek camp.

This publication is dedicated to the memory of Boyd J. Blair, owner of the Liberty Bell Mine from 1964 until his death in 2004.

## REFERENCES CITED

- Albanese, M.D., and Turner, D.L., 1980,  $^{40}\text{K}$ - $^{40}\text{Ar}$  ages from rhyolite of Sugar Loaf Mountain, central Alaska Range: Implications for offset along the Hines Creek strand of the Denali Fault system, *in* DGGS Staff, Short Notes on Alaskan Geology, 1979–1980: Alaska Division of Geological & Geophysical Surveys Geologic Report 63B, p. 7–10.
- Athey, J.E., Weldon, M.B., Newberry, R.J., Szumigala, D.J., Freeman, L.K., and Lessard, R.R., 2005, Major-oxide, minor-oxide, and trace-element geochemical data from rocks collected in the Liberty Bell area, Fairbanks A-4 Quadrangle, Alaska in 2005: Alaska Division of Geological & Geophysical Surveys Raw Data File 2005-5, 29 p.
- Bemis, S.P., 2004, Neotectonic framework of the north-central Alaska Range foothills: Fairbanks, University of Alaska, Master of Science thesis, 142 p.
- Bidwell, Gerry, 1994, 1994 Exploration Program, Liberty Bell Property, Bonnifield Mining District, Fairbanks A-4 Quadrangle, T10S R6–7W, Alaska, USA: Noranda Exploration Company, 17 p., appendices I–III.
- Buffler, R.T., and Triplehorn, D.M., 1976, Depositional environments of the Tertiary coal-bearing group, central Alaska, in Miller, T.P., ed., Recent and ancient sedimentary environments *in* Alaska, Proceedings of Symposium, April 2–4, Anchorage: Anchorage, Alaska Geological Society, p. H1–H10.
- Bundtzen, T.K., 1986, Prospect examination of a gold-tungsten placer deposit at Alder Creek, Vinasale Mountain area, western Alaska: Alaska Division of Geological & Geophysical Surveys Public Data File 86-15, 10 p.
- Burns, L.E., Fugro Airborne Surveys, and Stevens Exploration Management Corp., 2002, Plot files of the airborne geophysical survey data of the Liberty Bell area, western Bonnifield mining district, central Alaska: Alaska Division of Geological & Geophysical Surveys, Geophysical Report (GPR) 2002-06, 1 CD-ROM.
- Capps, S.R., 1912, The Bonnifield region, Alaska: U.S. Geological Survey Bulletin 501, 64 p.
- Davis, J.C., 1986, Statistics and data analysis in geology, 2nd ed.: John Wiley and Sons, Inc., 646 p.
- Decker, J.E., 1985, Sandstone model analysis procedure: Alaska Division of Geological & Geophysical Surveys Public Data File 85-3, 38 p.
- DGGS, 1994, Unpublished geologic mapping of Liberty Bell Mine area (Reifenstuhel, R.R., Weldon, M.B., and Wiltse, M.A.).
- Dickinson, W.R., Beard, L.S., Brakenridge, G.R., Etjavec, J.L., Ferguson, R.C., Inman, K.F., Knepp, R.A., Lindberg, F.A., and Ryberg, P.T., 1983, Provenance of North American Phanerozoic sandstones in relation to tectonic setting: Geological Society of America Bulletin, v. 94, no. 2, p. 222–235.
- Dusel-Bacon, Cynthia, Wooden, J.L., and Hopkins, M.J., 2004, U-Pb zircon and geochemical evidence for bimodal mid-Paleozoic magmatism and syngenetic base-metal mineralization in the Yukon–Tanana terrane, Alaska: Geological Society of America Bulletin, v. 116, no. 7, p. 989–1,015.
- Ellis, William, Hawley, C.C., and Dashevsky, Samuel, 2004, Alaska Resource Data File, Mount Hayes Quadrangle, Alaska: U.S. Geological Survey Open-File Report 2004-1266.

- Freeman, C.J., and Schaefer, Janet, 2001, Alaska Resource Data File, Fairbanks Quadrangle: U.S. Geological Survey Open-File Report 01-0426, 355 p.
- Freeman, L.K., Hanneman, N.L., and Flanders, R.W., 1987, Liberty Bell Joint Venture Report of 1987 Exploration: Resource Associates of Alaska, Inc., v. I, II, and IV.
- Galey, J.T., Jr., Hahn, Raimundo, and Duncan, W.M., 1993, 1991 Exploration Program, Liberty Bell Project, Bonfield mining district, Nenana recording district, Alaska: AMAX Gold, Inc., 39 p., appendices A–E.
- Gilbert, W.G., and Bundtzen, T.K., 1979, Mid-Paleozoic tectonics, volcanism, and mineralization in the north-central Alaska Range: Geological Society of Alaska Symposium 1977, p. F1–F22.
- Ingersoll, R.V., Bullard, T.F., Ford, R.L., Grimm, J.P., Pickle, J.D., and Sares, S.W., 1984, The effect of grain size on detrital modes: A test of the Gazzi-Dickinson point-counting method: *Journal of Sedimentary Petrology*, v. 54, p. 103–116.
- Irvine, T.N., and Baragar, W.R.A., 1971, A guide to the chemical classification of the common volcanic rocks: *Canadian Journal of Earth Sciences*, v. 8, p. 523–548.
- Lanphere, M.A., and Dalrymple, G.B., 2000, First-principles calibration of  $^{38}\text{Ar}$  tracers: Implications for the ages of  $^{40}\text{Ar}/^{39}\text{Ar}$  fluence monitors: U.S. Geological Survey Professional Paper 1621, 10 p.
- Layer, P.W., 2000,  $^{40}\text{Ar}/^{39}\text{Ar}$  age of the El'gygytgyn impact event, Chukotka, Russia: *Meteoritics and Planetary Science*, v. 35, p. 591–599.
- Layer, P.W., Hall, C.M., and York, Derek, 1987, The derivation of  $^{40}\text{Ar}/^{39}\text{Ar}$  age spectra of single grains of hornblende and biotite by laser step heating: *Geophysical Research Letters*, v. 14, p. 757–760.
- Leopold, E.B., and Liu, Gengwu, 1994, A long pollen sequence of Neogene age, Alaska Range: *Quaternary International*, v. 22/23, p. 103–140.
- McCoy, D., Newberry, R.J., Layer, P.W., DiMarchi, J.J., Bakke, A., Masterman, J.S., and Minehanne, D.L., 1997, Plutonic-related gold deposits of Interior Alaska, in Goldfarb, R.J., and Miller, L.D., eds., *Mineral deposits of Alaska: Economic Geology Monograph 9*, p. 191–241.
- McDougall, Ian and Harrison, T.M., 1999, *Geochronology and Thermochronology by the  $^{40}\text{Ar}/^{39}\text{Ar}$  method*, 2nd ed., Oxford University Press: New York, 269 p.
- Meschede, Martin, 1986, A method of discriminating between different types of mid-ocean ridge basalts and continental tholeiites with the Nb–Zr–Y diagram: *Chemical Geology*, v. 56, p. 207–218.
- Newberry, R.J., Crafford, T.C., Newkirk, S.R., Young, L.E., Nelson, S.W., and Duke, N.A., 1997, Volcanogenic massive sulfide deposits of Alaska: *Economic Geology Monograph 9*, p. 120–150.
- Pearce, J.A., Harris, N.B.W., and Tindle, A.G., 1984, Trace element discrimination diagrams for the tectonic interpretation of granitic rocks: *Journal of Petrology*, v. 25, p. 956–983.
- Pettijohn, F.J., Potter, P.E., and Siever, Raymond, 1987, *Sand and sandstone*, 2nd ed.: New York, Springer-Verlag, 553 p.
- Plafker, George, Naeser, C.W., Zimmermann, R.A., Lull, J.S., and Hudson, Travis, 1992, Cenozoic uplift history of the Mount McKinley area in the central Alaska Range based on fission-track dating: U.S. Geological Survey Bulletin 2041, p. 202–212.
- Puchner, C.C., and Freeman, L.K., 1988, Summary of Liberty Bell area prospects and recommendations for future exploration: NERCO Exploration Company internal correspondence.
- Ridgway, K.D., Trop, J.M., and Jones, D.E., 1999, Petrology and provenance of the Neogene Usibelli Group and Nenana Gravel: Implications for the denudation history of the central Alaska Range: *Journal of Sedimentary Research*, v. 69, no. 6, p. 1,262–1,275.
- Ridgway, K.D., Trop, J.M., Nokleberg, W.J., Davidson, C.M., and Eastham, K.R., 2002, Mesozoic and Cenozoic tectonics of the eastern and central Alaska Range: Progressive basin development and deformation in a suture zone: *Geological Society of America Bulletin*, v. 114, no. 12, p. 1480–1504.
- Samson, S.D., and Alexander, E.C., 1987, Calibration of the interlaboratory  $^{40}\text{Ar}/^{39}\text{Ar}$  dating standard, MMhb1: *Chemical Geology*, v. 66, p. 27–34.
- Stanley, R.G., Flores, R.M., and Wiley, T.J., 1992, Fluvial facies architecture in the Tertiary Usibelli Group of Suntrana, central Alaska, in Bradley, D.C., and Ford, A.B., eds., *Geologic studies in Alaska by the U.S. Geological Survey, 1990: U.S. Geological Survey Bulletin 1999*, p. 204–211.
- Steiger, R.H., and Jaeger, Emilie, 1977, Subcommittee on geochronology: Convention on the use of decay constants in geo and cosmochronology: *Earth and Planet Science Letters*, v. 36, p. 359–362.
- Szumigala, D.J., and Hughes, R.A., 2005, Alaska's Mineral Industry 2004: Alaska Division of Geological & Geophysical Surveys, Special Report 59, 75 p.
- Thoms, E.E., 2000, Late Cenozoic unroofing sequence and foreland basin development of the central Alaska Range: Implications from the Nenana Gravel: Fairbanks, University of Alaska, Master of Science thesis, 215 p.
- Triplehorn, D.M., 1976, Clay mineralogy and petrology of the coal-bearing group near Healy: Alaska Division of Geological & Geophysical Surveys Geologic Report 52, 14 p.

- Van Der Plas, L., and Tobi, A.C., 1965, A chart for judging the reliability of point counting results: *American Journal of Science*, v. 263, p. 87–90.
- Wahrhaftig, Clyde, 1968, Schists of the central Alaska Range: U.S. Geological Survey Bulletin 1254-E, 22 p.
- Wahrhaftig, Clyde, 1970a, Geologic map of the Fairbanks A-2 quadrangle, Alaska: U.S. Geological Survey Geologic Quadrangle Map GQ-808, 1 sheet, scale 1:63,360.
- Wahrhaftig, Clyde, 1970b, Geologic map of the Fairbanks A-3 quadrangle, Alaska: U.S. Geological Survey Geologic Quadrangle Map GQ-809, 1 sheet, scale 1:63,360.
- Wahrhaftig, Clyde, 1970c, Geologic Map of the Fairbanks A-4 quadrangle, Alaska: U.S. Geological Survey Geologic Quadrangle Map GQ-810, 1 sheet, scale 1:63,360.
- Wahrhaftig, Clyde, 1970d, Geologic map of the Healy D-2 quadrangle, Alaska: U.S. Geological Survey Geologic Quadrangle Map GQ-804, 1 sheet, scale 1:63,360.
- Wahrhaftig, Clyde, 1970e, Geologic map of the Healy D-3 quadrangle, Alaska: U.S. Geological Survey Geologic Quadrangle Map GQ-805, 1 sheet, scale 1:63,360.
- Wahrhaftig, Clyde, 1970f, Geologic Map of the Healy D-4 quadrangle, Alaska: U.S. Geological Survey Geologic Quadrangle Map GQ-806, 1 sheet, scale 1:63,360.
- Wahrhaftig, Clyde, 1987, The Cenozoic section at Suntrana Creek, *in* Hill, M.L., ed., *Geological Society of America, Cordilleran Section, Centennial Field Guide*, v. 1, p. 445–450.
- Wahrhaftig, Clyde, Wolfe, J.A., Leopold, E.B., and Lanphere, M.A., 1969, The coal-bearing group in the Nenana Coal Field, Alaska: U.S. Geological Survey Bulletin 1274-D, p. D1–D30.
- Williams, Howel, Turner, F.J., and Gilbert, C.M., 1982, *Petrography, an introduction to rocks in thin section*, 2nd ed.: San Francisco, CA, W.H. Freeman and Company, 626 p.
- Wolfe, J.A., and Tanai, Toshimasa, 1980, The Miocene Seldovia Point flora from the Kenai Group, Alaska: U.S. Geological Survey Professional Paper 1105, 52 p.
- Wolfe, J.A., and Tanai, Toshimasa, 1987, Systematics, phylogeny, and distribution of *Acer* (Maples) in the Cenozoic of western North America: *Hokkaido University Faculty of Science Journal*, ser. 4, v. 22, p. 1–246.
- Wood, G.H., Kehn, T.M., Carter, M.D., and Culbertson, W.C., 1983, Coal resource classification system of the U.S. Geological Survey: U.S. Geological Survey Circular 891, 65 p.
- Yesilyurt, Suleyman, 1994, Geology, geochemistry, and mineralization of the Liberty Bell gold mine area, Alaska: Oregon State University, unpublished Master of Science thesis, 189 p., 1 plate.
- Yesilyurt, Suleyman, 1996, Geology, geochemistry, and mineralization of the Liberty Bell gold mine area, Alaska, *in* Coyner, A.R., and Fahey, P.L., eds., *Geology and Ore Deposits of the American Cordillera: Symposium Proceedings*, Reno/Sparks, Nevada, April 1995, p. 1,281–1,316.
- York, Derek, Hall, C.M., Yanase, Yotaro, Hanes, J.A., and Kenyon, W.J., 1981,  $^{40}\text{Ar}/^{39}\text{Ar}$  dating of terrestrial minerals with a continuous laser: *Geophysical Research Letters*, v. 8, p. 1,136–1,138.



## **Appendix A**

### **Geochemical analyses of Paleozoic samples**

Gold-bearing samples from Athey and others (2005) were re-analyzed in order to obtain concentrations of certain elements that exceeded the upper detection limits, were less than the lower detection limits, or were not analyzed by inductively coupled plasma–atomic emission spectroscopy (ICP–AES; table A1). Analyses were performed by ALS Chemex. Rock samples were already crushed and pulverized using the techniques described in Athey and others (2005). Trace-element analyses were performed on a 200-gram split. Most elements were analyzed by inductively coupled plasma with mass spectroscopy or atomic emission spectroscopy (ICP–MS/AES) after four-acid, near-total digestion. This method of digestion is possibly incomplete for some elements and may result in lower analytical results for certain elements. A complete listing of analytical methods, lower and upper detection limits, and the elements that may be affected by incomplete digestion are included in table A2.

Major- and minor-oxide and trace-element compositions in table A3 were performed by X-ray fluorescence at the University of Alaska Fairbanks on polished slabs and are necessarily approximations to the true compositions. Fine-grained rocks (maximum grain size <1 mm) were cut to fit in 27-mm-diameter sample holders; coarser grained rocks (maximum grain size <3 mm) were analyzed in 37-mm-diameter holders. Analyses were standardized using well-characterized natural fine-grained rock and pure mineral standards as well as conventional pressed pellets of international rock standards.

Because volatile components were not measured and rocks were of varying porosities, the analyses were normalized to 100 percent totals. In the vast majority of cases the original analyses yielded totals of approximately 95 to 102 weight percent. Comparison between these analyses and those produced on the same rocks by conventional pressed pellet (trace elements) and fused disk (major elements) techniques indicates that major-oxide concentrations are most likely within 10 percent of the ‘true’ concentrations; trace-element concentrations are typically within 20 percent of true concentrations.

This page has intentionally been left blank.

Table A1. Location, description, and concentration of trace elements for samples collected in the Liberty Bell area of the Fairbanks A-4 Quadrangle, Alaska. Rock names in ( ) are derived from geochemical data and rock textures in hand samples. Location coordinates were collected using a hand-held GPS unit (no differential correction was applied), and coordinates are presented in latitude and longitude (based on the NAD27 Alaska datum) and in UTM coordinates (based on the Clark 1866 spheroid, NAD27 datum, UTM zone 6 projection). Note: — = not analyzed.

Sample Number	Latitude	Longitude	UTM Easting	UTM Northing	Description	Ag ppm
05JEA49A	64.0732	-148.8636	409092	7106300	Phyllite; quartz veined and sericitized, with 1 percent arsenopyrite and scorodite staining. Prospect pits.	20.8
05LF53B	64.0689	-148.6453	419726	7105536	Quartz-tourmaline vein; 10 percent of regolith, 2-10 cm pieces in 10-m-wide zone, contains 5-40 percent red-brown/limonite coated boxwork, with no relict sulfides.	3.56
05LF61B	64.0707	-148.6042	421738	7105685	Granite; porphyritic, strongly altered, sericitized, relict fine grain textured quartz, and fractures with veinlets of green-yellow and gray boxwork quartz.	69.5
05LF231A	64.0585	-148.8577	409330	7104660	Skarn; (skarn), medium- to coarse-grained, random-oriented actinolite with interstitial plagioclase, 1-4 percent pyrrhotite, 2-3 percent chalcopyrite, 1 percent arsenopyrite. Industry map unit "Mesozoic meta-gabbro."	1.35
05MBW224A	64.0494	-148.5785	422929	7103278	Meta-ash(?); gray colored, yellow-, orange-, and gray-weathering, foliated, aphanitic to very finely granular, finely color laminated, with Fe-oxide and possibly stibiconite(?) coatings. Contains disseminated, empty vugs (up to 0.2 mm in diameter) that may have contained sulfides.	28.7
05MBW298A	64.0643	-148.7233	415908	7105119	Metarhyolite; brecciated, sheared, and ± quartz-veined. Quartz veins ± disseminated vugs, ± coated with scorodite.	0.7
05MBW374A	64.0528	-148.9624	404205	7104179	Hornfelsed meta-argillite; white, foliated, very finely granular, cut by veins (up to 1 inch wide) and veinlets containing various combinations of white crystalline quartz, sprays and mats of very tiny, acicular, brown- to forest green-colored tourmaline crystals, and disseminated Fe-oxides (after pyrite(?) cubes).	1.01
05JEA121B	64.0856	-148.6123	421384	7107352	Quartz vein; with green mineral (epidote?) and weathered pyrite.	---
05LF141B	64.0660	-148.5014	426738	7105041	Quartz breccia vein; angular blocks of quartz in matrix and with fractures filled with massive stibnite, with possible arsenopyrite and galena. Grab sample of 0.4-m-thick zone in larger quartz vein.	---
05LF77A	64.0792	-148.5820	422844	7106607	Quartz vein; 5-cm-thick, drusy quartz, with 30 percent arsenopyrite infill.	---
05LF78A	64.0798	-148.5817	422860	7106673	Quartz vein; 2- to 5-cm-wide, brecciated, with 75 percent gray-white quartz, 5-20 percent arsenopyrite infill, 5 percent green tourmaline, 5 percent boxwork, and 0-20 percent green-blue cryptocrystalline infill - unknown.	---
05LF79B	64.0832	-148.5802	422944	7107050	Fault breccia; bleached, with quartz-arsenopyrite-unknown-gray mineral vein, 0.6-m-wide chip sample.	---
05LF228A	64.0556	-148.8664	408900	7104351	Vein; 3- to 5-cm-wide, in white sericite altered felsic rock, with quartz, tourmaline, and arsenopyrite from push-pile in "northwest copper zone," Liberty Bell property.	---
05MBW50A	64.0475	-148.9273	405897	7103538	Intermediate composition dike; (granodiorite), grayish-green, brown weathering, porphyritic, with biotite and quartz phenocryst. Contains disseminated pyrite and arsenopyrite.	---
05MBW174A	64.0571	-148.5496	424362	7104098	Quartz vein; small prospecting pit containing light yellow-stained quartz vein material, dark-brown Fe-oxide and quartz-crystal breccias, and intergrown quartz and Fe-oxide. Scattered vein material composed of massive, dark-gray stibnite, and cubic pyrite. Mineralized fault zone trends approximately 155 degrees (azimuth).	---
05MBW292A	64.0564	-148.7276	415672	7104245	Fault gouge; 1- to 2-inch-wide fault zone that widens out to approximately 1 foot wide, cutting foliation in phyllite. Fault is filled with brecciated, angular wall rock fragments, rock flour, and quartz veins with finely disseminated arsenopyrite. Fault strikes 309 degrees (azimuth) and dips 30 degrees.	---
05MBW296B	64.0606	-148.7236	415883	7104714	Quartz vein; from shear zone up to 3 inches wide. Sample contains light gray to clear quartz with disseminated crystals (≤ 3 mm) of arsenopyrite up to 40 percent of vein but generally < 20 percent. Shear zone strikes 258 degrees (azimuth) and dips 38 degrees.	---
05MBW303A	64.0671	-148.7230	415930	7105437	Shear zone; varies from 1 to 3 feet wide, with peripheral quartz + iron oxide veins extending off of the main shear zone. Heavily Fe-oxide- and yellow-stained veins contain quartz, pyrite, and arsenopyrite, with dark brownish-green tourmaline sprays, chlorite(?), secondary Fe-oxide, and scorodite. Shear zones strike 310 degrees (azimuth) and dip 60 degrees.	---
05MBW363A	64.0566	-148.9543	404610	7104593	Quartz vein; Loose rubble of hornfelsed, carbonaceous metasedimentary rocks that have been intruded and hornfelsed by a fine-grained, equigranular, granite dike, which is cut by quartz veins. Sampled heavily Fe-oxide-coated, gray, massive, granular quartz vein material that is intergrown with very fine-grained arsenopyrite and stibnite. Locally, stibnite crystals are up to 2 inches long.	---
05MBW407A	64.0532	-148.7248	415799	7103886	Quartz vein; abundant Fe-oxide coating, yellow oxides (scorodite), and local ≤ 1 percent pyrite in hornfelsed phyllite.	---
05Z108B	64.0655	-148.6579	419103	7105167	Quartz-tourmaline-arsenopyrite-Fe-oxide vein; dark brown and orange, gossanous, Fe-oxide stained, with patches of pale yellow staining and clots of discontinuous patches of very fine grained arsenopyrite (2-3 percent up to 7 percent).	---



Table A1. Location, description, and concentration of trace elements for samples collected in the Liberty Bell area of the Fairbanks A-4 Quadrangle, Alaska. Rock names in ( ) are derived from geochemical data and rock textures in hand samples. Location coordinates were collected using a hand-held GPS unit (no differential correction was applied), and coordinates are presented in latitude and longitude (based on the NAD27 Alaska datum) and in UTM coordinates (based on the Clark 1866 spheroid, NAD27 datum, UTM zone 6 projection). Note: — = not analyzed—continued.

Sample Number	Li ppm	Mg %	Mn ppm	Mo ppm	Na %	Nb ppm	Ni ppm	P ppm	Pb ppm	Rb ppm	Re ppm	S %	Sb ppm	Sb %	Se ppm	Sn ppm	Sn ppm	Sr ppm	Ta ppm	Te ppm	Th ppm
05JEA49A	13.6	0.11	429	0.62	0.03	2.8	1.9	200	1315	62.1	<0.002	0.18	244	---	2	29.3	---	25.6	0.17	<0.05	9.1
05LF53B	6.1	0.71	2020	1.18	0.3	3.2	12.7	920	424	41.7	<0.002	0.02	57.3	---	2	68.1	---	80.7	0.22	0.08	11.3
05LF61B	9.3	0.17	103	2.55	0.08	16.3	1.6	990	5190	253	<0.002	0.71	72.2	---	2	34.4	---	63.8	2.28	<0.05	23.3
05LF231A	13.8	8.55	1855	4.77	0.25	10.4	47.4	230	10.1	6	0.022	1.92	10.9	---	16	29.2	---	215	0.66	0.48	6.9
05MBW224A	1.5	0.03	28	0.94	0.01	0.4	0.7	470	206	30	<0.002	0.2	18.2	---	2	0.7	---	10.9	<0.05	<0.05	0.6
05MBW298A	22.9	0.45	197	0.43	0.13	5.5	2.4	810	26.5	217	<0.002	0.73	50.3	---	1	19.3	---	19	0.43	<0.05	11.8
05MBW374A	4.2	0.35	59	2.16	0.1	2.3	3.2	80	51.5	10.9	<0.002	0.01	55.3	---	1	6.7	---	30.2	0.16	0.11	2.2
05JEA121B	---	---	---	---	---	---	---	---	---	---	---	---	---	---	---	---	---	114	---	---	---
05LF141B	---	---	---	---	---	---	---	---	---	---	---	---	---	6.51	---	---	---	359	---	---	---
05LF77A	---	---	---	---	---	---	---	---	---	---	---	---	---	---	---	---	---	20	---	---	---
05LF78A	---	---	---	---	---	---	---	---	---	---	---	---	---	---	---	---	---	<5	---	---	---
05LF79B	---	---	---	---	---	---	---	---	---	---	---	---	---	---	---	---	---	31	---	---	---
05LF228A	---	---	---	---	---	---	---	---	---	---	---	---	---	---	---	---	---	5	---	---	---
05MBW50A	---	---	---	---	---	---	---	---	---	---	---	---	---	---	---	---	---	17	---	---	---
05MBW174A	---	---	---	---	---	---	---	---	---	---	---	---	---	6.3	---	---	---	155	---	---	---
05MBW292A	---	---	---	---	---	---	---	---	---	---	---	---	---	---	---	---	---	24	---	---	---
05MBW296B	---	---	---	---	---	---	---	---	---	---	---	---	---	---	---	---	---	18	---	---	---
05MBW303A	---	---	---	---	---	---	---	---	---	---	---	---	---	---	---	---	---	14	---	---	---
05MBW363A	---	---	---	---	---	---	---	---	---	---	---	---	---	8.86	---	---	---	192	---	---	---
05MBW407A	---	---	---	---	---	---	---	---	---	---	---	---	---	---	---	---	---	12	---	---	---
05Z108B	---	---	---	---	---	---	---	---	---	---	---	---	---	---	---	---	---	30	---	---	---



Table A2. Detection limits for trace-element geochemical analyses. Analytical methods include: ICP-MS/AES = Inductively Coupled Plasma with Mass Spectroscopy or Atomic Emission Spectroscopy, ICP-AES = Inductively Coupled Plasma with Atomic Emission Spectroscopy, PP-XRF = X-Ray Fluorescence on pressed pellet, AAS = Atomic Absorption Spectroscopy. Four acid digestion = HF-HNO<sub>3</sub>-HClO<sub>4</sub> and HCl leach. NOTE: \* = possibly incomplete digestion dependent on mineralogy.

Element	Units	Lower Detection Limit	Upper Detection Limit	Digestion	Analytical Method
Ag	ppm	0.01	100	four acid	ICP-MS/AES
Ag(+)	ppm	1	1,000	four acid	AAS
Al	percent	0.01	25	four acid	ICP-MS/AES
As	ppm	0.2	10,000	four acid	ICP-MS/AES
As(+)	percent	0.01	30	four acid	AAS
Ba*	ppm	10	10,000	four acid	ICP-MS/AES
Be	ppm	0.05	1,000	four acid	ICP-MS/AES
Bi	ppm	0.01	10,000	four acid	ICP-MS/AES
Ca	percent	0.01	25	four acid	ICP-MS/AES
Cd	ppm	0.02	500	four acid	ICP-MS/AES
Ce	ppm	0.01	500	four acid	ICP-MS/AES
Co	ppm	0.1	10,000	four acid	ICP-MS/AES
Cr*	ppm	1	10,000	four acid	ICP-MS/AES
Cs	ppm	0.05	500	four acid	ICP-MS/AES
Cu	ppm	0.2	10,000	four acid	ICP-MS/AES
Fe	percent	0.01	25	four acid	ICP-MS/AES
Ga	ppm	0.05	500	four acid	ICP-MS/AES
Ge	ppm	0.05	500	four acid	ICP-MS/AES
Hf	ppm	0.1	500	four acid	ICP-MS/AES
In	ppm	0.005	500	four acid	ICP-MS/AES
K	percent	0.01	10	four acid	ICP-MS/AES
La	ppm	0.5	500	four acid	ICP-MS/AES
Li	ppm	0.2	500	four acid	ICP-MS/AES
Mg	percent	0.01	15	four acid	ICP-MS/AES
Mn	ppm	5	10,000	four acid	ICP-MS/AES
Mo	ppm	0.05	10,000	four acid	ICP-MS/AES
Na	percent	0.01	10	four acid	ICP-MS/AES
Nb	ppm	0.1	500	four acid	ICP-MS/AES
Ni	ppm	0.2	10,000	four acid	ICP-MS/AES
P	ppm	10	10,000	four acid	ICP-MS/AES
Pb	ppm	0.5	10,000	four acid	ICP-MS/AES
Rb	ppm	0.1	500	four acid	ICP-MS/AES
Re	ppm	0.002	50	four acid	ICP-MS/AES
S	percent	0.01	10	four acid	ICP-MS/AES
Sb	ppm	0.05	1,000	four acid	ICP-MS/AES
Sb(+)	percent	0.01	100	KClO <sub>3</sub> /HCl	ICP-AES or AAS
Se	ppm	1	1,000	four acid	ICP-MS/AES
Sn*	ppm	0.2	500	four acid	ICP-MS/AES
Sn(+)	ppm	5	10,000	—	PP-XRF
Sr	ppm	0.2	10,000	four acid	ICP-MS/AES
Ta*	ppm	0.05	100	four acid	ICP-MS/AES
Te	ppm	0.05	500	four acid	ICP-MS/AES
Th	ppm	0.2	500	four acid	ICP-MS/AES
Ti*	percent	0.005	10	four acid	ICP-MS/AES
Tl	ppm	0.02	500	four acid	ICP-MS/AES
U	ppm	0.1	500	four acid	ICP-MS/AES
V	ppm	1	10,000	four acid	ICP-MS/AES
W*	ppm	0.1	10,000	four acid	ICP-MS/AES
Y	ppm	0.1	500	four acid	ICP-MS/AES
Zn	ppm	2	10,000	four acid	ICP-MS/AES
Zr*	ppm	0.5	500	four acid	ICP-MS/AES

This page intentionally left blank.

Table A3. Location, description, and concentration of major oxides, minor oxides, and trace elements for samples collected in the Liberty Bell area of the Fairbanks A-4 Quadrangle, Alaska. Root names are derived from geochemical data and rock textures in hand samples. Location coordinates were collected using a hand-held GPS unit (no differential correction was applied), and coordinates are presented in latitude and longitude (based on the NAD27 Alaska datum) and in UTM coordinates (based on the Clark 1866 spheroid, NAD27 datum, UTM zone 6 projection). Note: — = not analyzed.

Sample Number	Latitude	Longitude	UTM Easting	UTM Northing	Root Name	SiO <sub>2</sub>	Al <sub>2</sub> O <sub>3</sub>	BaO	CaO	FeO	K <sub>2</sub> O	MgO	MnO	Na <sub>2</sub> O	P <sub>2</sub> O <sub>5</sub>	TiO <sub>2</sub>	F	Nb	Rb	Sr	Th	U	Y	Zr	As	Cl	Cr	Cu	Ga	Ni	Pb	S	Sb	Sn	V	Zn	Se	Te	Bi	Co	Mo	
						%	%	%	%	%	%	%	%	%	%	%	%	ppm	ppm	ppm	ppm	ppm	ppm	ppm	ppm	ppm	ppm	ppm	ppm	ppm	ppm	ppm	ppm	ppm	ppm	ppm	ppm	ppm	ppm	ppm	ppm	ppm
2005JEA106A	64.073619	-148.607249	421596	7106011	arkosic metawacke	82	13	<0.05	0.12	0.8	2.4	0.4	0.005	0.05	0.2	0.38	0.06	13	50	228	22	1	22	165	---	68	---	29	12	---	11	---	---	---	---	9	---	---	---	---	---	69
2005JEA10A	64.068863	-148.804677	411952	7105739	feldspathic metawacke	78.4	13	0.25	0.1	1.3	5.1	0.3	0.013	0.8	0.03	0.20	0.1	12	248	44	11	2	24	100	37	149	---	71	13	---	39	52	---	34	---	---	---	---	---	---	---	---
2005JEA114A	64.079585	-148.618913	421044	7106690	metarhyolite	79	12	0.2	0.03	0.9	7.2	0.2	0.01	0.1	0.02	0.14	---	40	169	39	24	3	39	177	38	119	---	38	18	---	31	66	---	8	---	23	---	---	---	---	---	---
2005JEA117B	64.081468	-148.615864	421198	7106896	altered metabasite	37	22	0.1	0.06	2.8	1.1	12	0.3	0.1	0.02	0.05	---	6	28	21	---	---	6	6	40	296	25	---	63	93	75	290	---	46	222	670.5	---	---	---	---	117	---
2005JEA13A	64.065167	-148.79794	412269	7105318	arkosic metawacke	78	12	0.09	0.15	0.5	6	0.6	0.008	2.1	0.1	0.24	0.2	16	344	68	10	3	30	139	11	93	---	29	9	---	36	48	13	9	---	11	---	---	---	---	---	---
2005JEA14A	64.061315	-148.795827	412360	7104886	arkosic metawacke	76	14	0.14	0.14	2.1	4.4	1.1	0.015	1.3	0.18	0.33	0.1	11	141	36	12	3	23	141	16	137	6	18	11	8	18	670	1	3	31	38	---	---	---	9	---	
2005JEA16B	64.060483	-148.790486	412618	7104786	arkosic metawacke	77	14	0.18	0.03	1.5	6	0.8	0.009	0.2	0.09	0.25	0.07	16	199	62	11	4	37	125	27	133	---	34	16	---	39	59	---	13	---	---	---	---	---	---	---	---
2005JEA176A	64.110475	-148.515083	426189	7110007	metarhyolite	77	13	0.2	0.04	1.2	5.8	0.2	0.009	2.5	0.026	0.13	0.12	37	141	46	25	4	29	184	17	264	---	29	18	---	35	95	---	---	---	---	---	---	---	---	---	---
2005JEA17A	64.061679	-148.783061	412984	7104909	arkosic metawacke	74	14	0.17	0.2	2.5	4.6	1.3	0.032	2.1	0.158	0.28	0.07	14	160	53	11	2	25	136	36	416	---	27	21	---	50	217	---	16	---	---	---	---	---	---	---	---
2005JEA198A	64.120088	-148.807814	411961	7111450	metarhyolite	70	14	0.34	0.11	0.2	14	0.03	0.005	0.3	0.1	0.94	<0.05	43	235	44	13	5	83	1450	<3	<50	8	27	---	8	<5	356	<2	<4	24	16	---	---	---	<2	---	
2005JEA20A	64.061467	-148.769521	413644	7104867	arkosic metawacke	78	13	0.09	0.2	1.5	4.5	0.8	0.018	1.2	0.176	0.17	0.10	15	222	35	9	5	31	113	17	301	---	71	19	---	128	3900	---	---	---	---	---	---	---	---	---	---
2005JEA212A	64.102745	-148.843675	410159	7109568	arkosic metawacke	72	16	0.2	0.07	2.7	4.5	1.6	0.019	2.3	0.03	0.4	0.38	15	140	46	23	2	15	194	---	141	---	20	10	19	26	127	---	11	---	---	---	---	---	---	---	---
2005JEA254A	64.094502	-148.822507	411164	7108620	arkosic metawacke	78	13	0.17	0.05	1.3	5.7	0.3	0.008	1.1	0.024	0.25	0.12	16	251	20	14	3	24	178	32	102	---	32	13	---	36	111	---	---	---	---	---	---	---	---	---	---
2005JEA28A	64.055255	-148.747284	414710	7104145	arkosic metawacke	74.4	14	0.15	0.13	2.3	5.6	1.5	0.011	0.6	0.22	0.43	0.07	13	179	72	12.3	---	18	158	45	629	---	19	18	---	34	7890	---	12	---	44	---	---	---	---	---	---
2005JEA29A	64.054122	-148.747439	414699	7104019	metarhyolite	77.5	13	0.13	0.05	0.7	4.6	0.2	0.019	2.3	0.03	0.13	1.3	48	119	62	25	6	52	185	17	293	---	10	15	---	18	282	---	10	---	41	---	---	---	---	---	---
2005JEA31A	64.06654	-148.820352	411180	7105502	metagranite	75	15	0.2	0.02	1.7	6.2	0.7	0.01	0.2	0.06	0.4	0.09	15	278	63	13	1	49	141	28	387	---	46	20	---	59	94	24	18	---	27	---	---	---	---	---	---
2005JEA32A	64.070728	-148.816361	411388	7105963	feldspathic metawacke	81	12	0.12	0.03	0.7	5.1	0.2	0.007	0.36	0.036	0.25	0.09	11	171	43	10	3	24	108	16	200	---	39	17	---	54	77	---	20	---	47	---	---	---	---	---	---
2005JEA34A	64.073624	-148.823091	411069	7106295	arkosic metawacke	75	12	0.37	0.08	3.4	7.4	0.8	0.053	0.4	0.09	0.31	0.06	13	199	49	10	2	15	110	29	576	---	31	16	20	48	65	---	16	---	461	---	---	---	---	---	---
2005JEA35A	64.07544	-148.825711	410947	7106501	arkosic metawacke	76	14	0.14	0.46	1.6	4.4	0.7	0.017	1.9	0.21	0.28	0.1	36	169	42	13	1	19	135	13	343	---	21	13	---	42	59	---	10	---	59	---	---	---	---	---	
2005JEA36A	64.07651	-148.822705	411097	7106616	arkosic metawacke	78	13	0.11	0.19	1.4	5.1	0.4	0.019	0.9	0.128	0.15	0.1	13	241	44	10	4	30	89	24	808	---	38	---	---	43	183	---	19	---	196	---	---	---	---	---	---
2005JEA38A	64.078913	-148.822924	411094	7106884	arkosic metawacke	75	14	0.2	0.23	1.5	6.9	0.5	0.019	0.4	0.3	0.44	0.1	19	253	75	15	2	34	173	53	183	---	39	19	---	77	343	---	---	---	92	---	---	---	---	---	---
2005JEA44A	64.07468	-148.853705	409580	7106478	metarhyolite	73	15	0.1	0.25	1.1	3	1.2	0.008	4.9	0.22	0.22	0.8	37	98	47	38.2	---	45	78	11	125	---	11	---	21	69	---	---	---	---	---	---	---	---	---	---	---
2005JEA48A	64.07185	-148.862505	409141	7106153	feldspathic metawacke	79.5	13	0.09	0.05	1.5	3.7	0.7	0.008	1.1	0.12	0.13	0.13	13	164	35	11	6	25	82	32	49	---	48	13	---	38	207	---	---	---	---	---	---	---	---	---	---
2005JEA52A	64.069801	-148.869687	408784	7105935	quartz metawacke	82	11	0.2	0.05	0.6	5.6	0.3	0.007	0.31	0.046	0.19	0.05	14	197	72	4	1	20	82	57	98	---	57	16	---	248	310	---	157	---	---	---	---	---	---	---	---
2005JEA55A	64.070993	-148.876143	408473	7106077	greenstone	52	17	0.05	1.5	12	1.9	13	0.16	0.3	0.31	1.9	---	36	151	44	---	---	26	189	30	110	60	122	35	45	32	180	---	---	---	---	---	---	---	---	---	---
2005JEA56A	64.071828	-148.873329	408613	7106166	calcareous metabasite	37	15	0.06	20	13	2.7	8.4	0.19	0.5	0.33	2.4	---	39	120	356	---	---	28	219	---	143	89	118	24	40	---	181	---	---	---	---	---	---	---	---	---	---
2005JEA57A	64.07232	-148.871353	408711	7106218	arkosic metawacke	78	13	0.09	0.12	1.5	3.5	0.8	0.007	2.5	0.07	0.21	0.08	15	109	67	15	4	18	123	28	99	---	13	---	34	853	---	---	---	---	---	---	---	---	---	---	
2005JEA66A	64.060236	-148.844042	410004	7104833	metarhyolite	78	11	0.16	0.32	1.6	2.0	5.4	0.008	0.6	0.04	0.12	0.19	35	81	47	34	11	48	108	26	109	<3	11	14	7	17	1380	<1	24	14	114	---	---	---	---	<2	---
2005JEA67A	64.06047	-148.84043	410181	7104854	altered granite	86	7.5	0.02	0.12	0.71	0.41	0.2	0.01	4.3	0.08	0.13	0.02	9	28	50	11	<1	8	59	2226	291	<3	22	10	5	3	840	13	<2	10	12	---	1	4	<2	12	---
2005JEA67B	64.06047	-148.84043	410181	7104854	metarhyolite	74	16	0.16	0.09	0.7	3.4	2	0.005	2.8	0.05	0.41	0.13	35	196	43	16	---	46	283	145	183	---	33	29	---	20	660	---	24								

Table A3. Location, description, and concentration of major oxides, minor oxides, and trace elements for samples collected in the Liberty Bell area of the Fairbanks A-4 Quadrangle, Alaska. Root names are derived from geochemical data and rock textures in hand samples. Location coordinates were collected using a hand-held GPS unit (no differential correction was applied), and coordinates are presented in latitude and longitude (based on the NAD27 Alaska datum) and in UTM coordinates (based on the Clark 1866 spheroid, NAD27 datum, UTM zone 6 projection). Note: — = not analyzed—continued.

Sample Number	Latitude	Longitude	UTM Easting	UTM Northing	Root Name	SiO <sub>2</sub>	Al <sub>2</sub> O <sub>3</sub>	BaO	CaO	FeO	K <sub>2</sub> O	MgO	MnO	Na <sub>2</sub> O	P <sub>2</sub> O <sub>5</sub>	TiO <sub>2</sub>	F	Nb	Rb	Sr	Th	U	Y	Zr	As	Cl	Cr	Cu	Ga	Ni	Pb	S	Sb	Sn	V	Zn	Se	Te	Bi	Co	Mo	
						%	%	%	%	%	%	%	%	%	%	%	%	ppm	ppm	ppm	ppm	ppm	ppm	ppm	ppm	ppm	ppm	ppm	ppm	ppm	ppm	ppm	ppm	ppm	ppm	ppm	ppm	ppm	ppm	ppm	ppm	
2005LF49A	64.052714	-148.738356	415138	7103850	metagranite	77	15	0.25	0.14	0.9	5.3	0.5	0.004	0.2	0.209	0.21	0.08	6	206	47	10	2	174	145	49	68	—	46	15	—	34	85	—	15	—	39	—	—	—	—	—	
2005LF50A	64.070441	-148.656923	419164	7105719	arkosic metawacke	75	12	0.2	<0.01	2.7	6.0	0.8	0.03	2.3	0.08	0.38	—	11	119	88	—	—	20	93	—	—	5	<30	—	8	<2	<20	—	—	31	40	—	—	—	—	1	—
2005LF56A	64.065118	-148.632318	420349	7105095	arkosic metawacke	77	13	0.2	0.11	1.8	4.9	0.7	0.024	2	0.14	0.3	0.05	15	128	58	15	3	13	128	24	98	—	42	14	—	24	30	—	21	—	50	—	—	—	—	—	
2005LF59A	64.067777	-148.615235	421190	7105370	arkosic metawacke	78	13	0.12	0.17	1.3	4.9	0.6	0.017	1.5	0.18	0.23	0.11	16	155	36	14	4	25	119	23	103	—	42	17	—	30	111	—	13	—	26	—	—	—	—	—	
2005LF5A	64.048503	-148.857505	409309	7103545	hornfelsed metabasite	50.5	19	0.03	8.9	4.6	0.2	6.7	0.08	7.2	0.7	1.6	—	29	12	282	—	—	68	146	20	403	90.6	29	14	146	18	3870	13	8	168	61	—	—	—	—	25	—
2005LF71A	64.072275	-148.584968	422679	7105834	metarhyolite	77	13	0.19	0.03	1.3	6	0.7	0.007	1.3	0.09	0.13	0.10	47	190	32	44	7	46	160	—	101	—	20	32	—	21	86	—	—	—	33	—	—	—	—	—	
2005LF74A	64.075571	-148.581547	422855	7106197	feldspathic metawacke	74	14	0.16	0.07	2.8	4.8	1.0	0.023	2.6	0.19	0.60	—	17	115	63	—	—	22	193	—	—	11	<30	—	8	9	<20	—	—	38	60	—	—	—	<1	—	
2005LF75A	64.078485	-148.580933	422893	7106521	altered granite	78	16	0.09	0.06	1.3	4.1	0.6	0.12	0.1	0.07	0.14	0.16	27	275	27	35	—	33	79	6	106	—	21	25	—	60	183	91	—	—	96	—	—	—	—	—	
2005LF90A	64.063617	-148.635715	420179	7104932	altered granodiorite	68	17	0.27	0.23	2.9	3.1	2.4	0.03	5	0.2	0.32	—	8	87	267	10.2	—	17	143	25	103	—	15	13	—	42	198	—	—	—	39	—	—	—	7	—	
2005LF93A	64.062127	-148.626159	420641	7104754	arkosic metawacke	84	8.9	0.13	<0.01	1.0	4.6	0.4	0.012	0.09	0.04	0.26	—	12	123	46	—	—	43	80	—	—	<5	<30	—	6	19	<20	—	—	11	47	—	—	—	<1	—	
2005LF94B	64.060429	-148.626224	420633	7104565	very altered granodiorite	64.4	14	0.19	0.62	6.5	3.5	6.5	0.14	2.5	0.31	0.67	0.08	8	125	670	28	9	29	188	9	40	238	89	23	112	17	324	14	20	158	189	—	2	<1	17	5	
2005LF99A	64.051379	-148.636903	420086	7103570	arkosic metawacke	77	11	0.13	0.63	2.6	4.4	0.7	0.032	2.1	0.1	0.34	—	13	133	100	—	—	21	115	—	—	<5	<30	—	7	2	96	—	—	21	54	—	—	<1	—		
2005MBW100A	64.074303	-148.897712	407432	7106477	arkosic metawacke	83	9.6	0.04	0.02	1.2	2.8	0.7	0.009	2.3	0.11	0.25	—	13	84	58	—	—	28	64	—	—	<10	<30	—	7	3	20	—	—	12	44	—	—	<1	—		
2005MBW105B	64.07627	-148.883163	408148	7106675	arkosic metawacke	85	8.2	0.07	<0.01	0.4	2.3	0.2	0.004	3.3	0.01	0.10	—	5	52	72	—	—	5	19	—	—	<10	<30	—	3	52	1938	—	—	11	31	—	—	<1	—		
2005MBW124A	64.100417	-148.846703	410004	7109313	arkosic metawacke	75	13	0.17	0.07	2.3	6.3	0.6	0.014	2.2	0.14	0.34	—	11	164	94	—	—	26	126	—	—	4	<30	—	7	16	<20	—	—	25	54	—	—	<1	—		
2005MBW130A	64.074205	-148.91208	406731	7106487	aphyric metarhyolite	78	14	0.08	0.13	1.5	0.4	1.2	0.01	4	0.0386	0.123	—	32	33	80	24	5	39	186	11	102	—	5	11	—	35	35	—	—	75	—	—	—	—			
2005MBW136A	64.073448	-148.92595	406052	7106423	arkosic metawacke	77	13	0.1	0.01	1.3	4.1	0.9	0.008	3.0	0.12	0.31	—	12	139	61	—	—	26	99	—	—	<5	<30	—	6	17	19	—	—	22	45	—	—	<1	—		
2005MBW201B	64.066711	-148.55329	424209	7105176	gabbro	59	12	0.16	9.6	5.9	4.0	6.0	0.11	2.4	0.25	0.64	—	7	167	660	—	—	27	250	—	—	676	<30	—	146	6	62	—	—	151	82	—	—	32	—		
2005MBW228A	64.0463	-148.579949	422852	7102934	arkosic metawacke	77	12	0.17	0.04	1.5	8.5	0.5	0.027	0.18	0.13	0.20	—	10	206	54	—	—	33	63	—	—	<10	<30	—	6	397	<20	—	—	13	218	—	—	<1	—		
2005MBW248A	64.027821	-148.651591	419301	7100964	hematite sandstone	31.4	6.7	0.0664	1.2	56.1	0.723	0.8	1.4	0.959	0.359	0.249	—	—	262	79.4	—	—	37	142	—	953	66.9	—	—	—	—	178	—	—	117	121	—	—	—	—		
2005MBW305A	64.068167	-148.728946	415644	7105559	quartzite	87	8.5	0.12	<0.01	0.1	4.2	0.04	0.004	0.1	0.02	0.15	—	8	88	49	—	—	16	44	—	—	<10	<30	—	4	2	131	—	—	7	31	—	—	<1	—		
2005MBW308A	64.062723	-148.917565	406425	7105216	aphyric metarhyolite	70	18	0.17	0.05	0.26	6.4	0.2	<0.005	4.7	0.12	0.141	0.60	66	282	42	35	5	75	301	11	210	—	18	19	19	17	119	—	9	—	—	11	—	—	—	—	
2005MBW316A	64.065663	-148.919263	406352	7105546	aphyric metarhyolite	75	14	0.17	0.05	0.54	7.5	0.0786	<0.005	2.4	0.0146	0.17	0.06	51	193	41	31	3	34	262	13	85	—	24	28	—	29	47	—	—	12	—	—	35	—	—	—	—
2005MBW320B	64.062892	-148.921799	406219	7105241	aphyric metarhyolite	70	17	0.15	<0.01	0.2	7.6	<0.03	0.003	5.0	0.01	0.16	—	36	121	48	—	—	18	69	—	—	<10	<30	—	4	<2	<20	—	—	3	37	—	—	<1	—		
2005MBW339A	64.064832	-148.943292	405177	7105489	graphitic quartzite	97	1.3	0.04	<0.01	0.2	0.7	0.2	0.004	0.07	0.01	0.10	—	4	46	9	—	—	2	<5	—	—	70	<30	—	8	<2	26	—	—	120	30	—	—	<1	—		
2005MBW348A	64.061195	-148.942116	405222	7105082	quartzite	89	6.3	0.02	<0.01	0.6	0.09	0.07	0.004	4.0	0.02	0.09	—	46	8	49	—	—	53	103	—	—	<10	<30	—	5	<2	28	—	—	3	34	—	—	<1	—		
2005MBW40B	64.048526	-148.924702	406029	7103645	metarhyolite	83	10	0.08	<0.01	1.5	3.1	1.6	0.005	0.15	0.01	0.08	—	32	216	17	—	—	43	68	—	—	<10	<31	—	10	6	2191	—	—	4	60	—	—	<1	—		
2005MBW49A	64.047927	-148.927283	405901	7103582	metarhyolite	67	19	0.15	0.04	3.0	7.2	1.5	0.01	2.3	0.02	0.15	—	39	336	79	—	—	61	141	—	—	<10	<30	—	8	21	18	—	—	8	59	—	—	<1	—		
2005MBW51A	64.050214	-148.920855	405871	7103838	granite	92	7.4	0.02	<0.01	0.2	0.5	0.05	0.004	0.0	0.01	0.08	—	28	33	15	—	—	31	55	—	—	<10	<30	—	4	12	823	—	—	2	32	—	—	<1	—		
2005MBW58A	64.048326	-148.929687	405785	7103630	metarhyolite	73	18	0.14	<0.01	1.3	5.3	1.5	0.005	0.2	0.02	0.26	—	64	210	19	—	—	69	286	—	—	<10	<10	—	7	<2	88										

Table A3. Location, description, and concentration of major oxides, minor oxides, and trace elements for samples collected in the Liberty Bell area of the Fairbanks A-4 Quadrangle, Alaska. Root names are derived from geochemical data and rock textures in hand samples. Location coordinates were collected using a hand-held GPS unit (no differential correction was applied), and coordinates are presented in latitude and longitude (based on the NAD27 Alaska datum) and in UTM coordinates (based on the Clark 1866 spheroid, NAD27 datum, UTM zone 6 projection). Note: — = not analyzed—continued.

Sample Number	Latitude	Longitude	UTM Easting	UTM Northing	Root Name	SiO <sub>2</sub>	Al <sub>2</sub> O <sub>3</sub>	BaO	CaO	FeO	K <sub>2</sub> O	MgO	MnO	Na <sub>2</sub> O	P <sub>2</sub> O <sub>5</sub>	TiO <sub>2</sub>	F	Nb	Rb	Sr	Th	U	Y	Zr	As	Cl	Cr	Cu	Ga	Ni	Pb	S	Sb	Sn	V	Zn	Se	Te	Bi	Co	Mo		
						%	%	%	%	%	%	%	%	%	%	%	%	ppm	ppm	ppm	ppm	ppm	ppm	ppm	ppm	ppm	ppm	ppm	ppm	ppm	ppm	ppm	ppm	ppm	ppm	ppm	ppm	ppm	ppm	ppm	ppm	ppm	
2005RN304C	64.010311	-148.539479	424731	7098876	metarhyolite	72	14	0.09	1.5	4.4	3.4	1.2	0.043	2.1	0.2	0.62	0.1	39	134	29	14	6	29	187	22	160	---	24	22	---	31	216	---	---	---	52	---	---	---	---	---	---	
2005RN307A1	64.015347	-148.535991	424915	7099433	calcareous metabasite	38	17	0.44	20	11	4.4	5.8	0.23	0.2	0.24	2	---	18	242	624	---	---	28	105	133	185	---	24	27	48	55	734	---	---	---	---	64	---	---	---	---	---	
2005RN307A2	64.015347	-148.535991	424915	7099433	calcareous metabasite	46	16	0.3	13	13	3.7	5.5	0.18	0.16	0.149	1.8	---	12	134	283	2	---	12	94	116	181	492	112	20	92	16	191	---	---	437	138	---	---	---	112	---	---	
2005RN313C	64.02394	-148.550851	424212	7100408	graphitic quartzite	96	2.0	0.04	0.04	0.3	0.5	0.3	0.004	0.04	0.06	0.04	0.06	6	25	<10	---	---	14	14	22	126	24	35	4	29	268	142	---	---	---	225	14	---	---	---	---		
2005RN313D	64.02394	-148.550851	424212	7100408	metapelite	75	16	0.08	0.09	1.5	5.4	1.6	0.032	0.05	0.04	0.12	0.20	17	220	6	12	6	32	117	35	280	---	32	19	---	89	343	---	325	---	---	47	---	---	---	---	---	
2005RN317A1	64.010337	-148.497504	426783	7098830	metapelite	80	11	0.12	0.25	1.4	5.5	0.5	0.006	0.40	0.29	0.14	0.22	17	346	31	11	16	29.8	95	40	153	---	34	19	---	32	402	---	---	---	48	---	---	---	---	---	---	
2005RN317A2	64.010337	-148.497504	426783	7098830	metapelite	83	9.6	0.1	0.23	1.3	5.1	0.4	0.005	0.20	0.21	0.12	0.13	17.3	344	26	8	15	28.5	90	33	160	---	25	21	35	38	364	---	17	---	---	39	---	---	---	---	---	
2005RN317B	64.010337	-148.497504	426783	7098830	quartz metawacke	80	13	0.07	0.03	0.9	4.4	0.4	0.004	0.1	0.04	0.17	0.4	17	311	26	6	6	25	107	21	71	---	15	12	---	11	48	---	---	---	29	---	---	---	---	---		
2005RN318B	64.011422	-148.498422	426741	7098952	quartz metawacke	83	10	0.10	<0.1	1.7	3.6	0.8	0.008	0.06	0.09	0.19	---	15	126	32	---	---	34	111	---	<10	<30	---	14	19	879	---	---	48	148	---	---	---	<1	---	---	---	
2005RN325A	64.013517	-148.521365	425625	7099212	greenstone	52	17	0.07	7.5	9.1	0.6	7.1	0.13	4.9	0.3	1.3	---	17	27	406	---	---	30	259	25	130	242	24	15	81	24	66	---	---	---	77	---	---	---	111	---	---	
2005RN326A	64.013662	-148.524647	425465	7099232	greenstone	53	18	0.33	4.8	10	2.8	6.1	0.17	3.4	0.39	1.4	---	22	107	270	---	---	<10	336	13	131	304	37	26	50	2	129	---	---	37	187	---	---	61	---	---	---	
2005RN327A	64.013382	-148.524877	425453	7099201	graphitic quartzite	94	3.6	0.05	0.07	0.2	1.2	0.6	0.001	0.03	0.03	0.12	0.06	8	49	<10	---	---	14	62	2	118	156	---	63	29	1260	22	---	2380	13	1100	---	---	---	---	---	---	
2005RN327B	64.013382	-148.524877	425453	7099201	feldspathic metawacke	81	12	0.22	0.22	1.0	3.3	1.3	0.00174	0.423	0.1535	0.30	0.15	18	98	11	8	6	16	94	28	145	---	35	17	---	34	791	---	---	34	---	---	---	---	---	---		
2005RN328A	64.013341	-148.526225	425387	7099198	greenstone	46	17	0.07	9.0	14	1.2	6.2	0.16	3.3	0.42	2.3	---	28	62	166	---	---	46	234	55	148	448	117	31	72	28	116	---	---	---	213	---	---	---	55	---	---	
2005RN329A	64.014125	-148.528436	425281	7099288	greenstone	49	18	0.06	5.8	11	0.17	10	0.11	4.4	0.11	1.1	---	11	216	---	---	25	78	64	168	460	23	22	183	17	118	---	---	---	115	---	---	---	49	---	---		
2005RN349B	64.016033	-148.536479	424893	7099510	arkosic metawacke	80	12	0.2	0.04	0.2	4.8	0.5	0.003	1.6	0.01	0.07	---	4	95	27	---	---	6	47	---	92	---	17	13	21	30	87	---	---	23	8	---	---	---	---	---	---	
2005RN350B	64.016923	-148.537183	424861	7099610	graphitic arkosic metawacke	82	12	0.13	0.04	0.09	3	0.5	0.002	2.7	0.01	0.06	---	6	57	14	---	---	4	19	16	124	---	16	10	20	21	348	---	---	---	9	---	---	---	---	---		
2005RN350C	64.016923	-148.537183	424861	7099610	arkosic metawacke	80	13	0.15	0.06	0.2	5.2	0.6	0.001	0.07	0.02	0.08	0.14	10	143	22	5	---	10	46	12	127	---	16	12	17	23	560	---	---	---	7	---	---	---	---	---		
2005RN350D	64.016923	-148.537183	424861	7099610	feldspathic metawacke	79	13	0.2	0.24	0.6	5.9	0.9	0.004	0.1	0.045	0.18	0.10	16	146	26	8	4	22	132	27	104	---	30	13	39.9	46	3580	---	---	---	15	---	---	---	---	---		
2005RN369A	64.018775	-148.620362	420801	7099917	quartz metawacke	84	10	0.07	0.01	0.76	3.6	0.4	0.002	0.02	0.023	0.18	0.08	16	190	22	8	4	25	90	29	54	---	27	18	24	66	66	---	---	---	40	---	---	---	---	---		
2005RN420A	64.020189	-148.535582	424948	7099972	altered diabase	58	19	0.3	4.2	9.5	4.2	1.5	0.57	0.3	0.36	1.1	0.11	11	183	185	16	---	66	261	52	395	239	41	23	14	51	2220	---	---	---	385	---	---	---	40	---	---	
2005RN424A	64.022686	-148.537111	424880	7100252	arkosic metawacke with pyrite vein	69	8.5	0.51	<0.1	6.1	5.7	0.2	0.001	1.1	0.01	0.17	---	11	151	47	---	---	23	79	---	<10	<30	---	5	31	84585	---	---	13	41	---	---	<1	---	---	---		
2005RN430A	64.025326	-148.551399	424189	7100563	quartzite	99	0.42	0.02	0.02	0.07	0.15	0.07	0.004	0.01	0.01	0.02	---	6	13	7	---	---	6	8	17	95	---	31	6	26	50	99	---	---	36	13	---	---	---	---	49	---	---
2005RN441B	64.049239	-148.852617	409550	7103620	hornfelsed metabasite	45	16	0.28	2.6	12	5.8	10	0.07	0.5	0.33	1.2	1.7	16	321	91	---	---	25	74	126	85	342	101	14	57	---	40200	28	31	246	70	13	27	---	33	---	---	
2005Z125A	64.124237	-148.8883	408056	7112026	metagranite	77	13	0.13	0.24	1.6	5.3	0.6	0.016	2.2	0.16	0.24	0.1	21	213	55	21	6	33	125	3	235	<3	20	20	7	28	168	2	2	18	39	---	---	---	<1	---	---	---
2005Z143A	64.001623	-148.656057	419007	7098051	quartz metawacke	66	23	0.2	0.64	3.4	4.8	0.8	0.003	0.2	0.02	1	0.04	24	221	27	16	5	23	181	---	215	---	22	32.2	---	27	96	---	12	---	58	---	---	---	---	---	---	
2005Z149A	64.00906	-148.657949	418936	7098882	quartz metawacke	76	15	0.1	0.12	3.5	2.9	0.4	0.001	1.2	0.04	0.6	---	14	103	76.7	17	2	19	298	---	251	---	17	13.6	---	35	44	---	---	77	---	---	---	---	---	---		
2005Z153A	64.009729	-148.66073	418802	7098960	quartz arenite	96	2.5	0.1	0.01	0.09	0.6	0.09	0.00197	0.05	0.01	0.05	---	6	31	6	---	---	6	62	---	346	---	22	---	28.5	33	75	---	10	7	---	---	---	---	---	---		
2005Z173A	64.069173	-148.930145	405833	7105953	aphytic metarhyolite	77	13	0.3	0.03	0.03	3.3	0.1	0.01	5.4	0.02	0.14	---	46	44	40	29	1	61	285	---	402	---	27	15	---	27	90	---	---	---	13	---	---	---	2	---	---	
2005Z173B	64.069173	-148.930145	405833	7105953	metapelite(?)	52	27	0.16	0.03	5.4	11	3.1	0.01	0.03	0.1	0.3	0.34	72	340	9	53	7	38	379	<3	<50	<3	19	---	18.3	19	284	11	14	32	136	---	---	11	---	---		
2005Z175																																											

This page intentionally left blank.

## Appendix B

### $^{40}\text{Ar}/^{39}\text{Ar}$ analyses

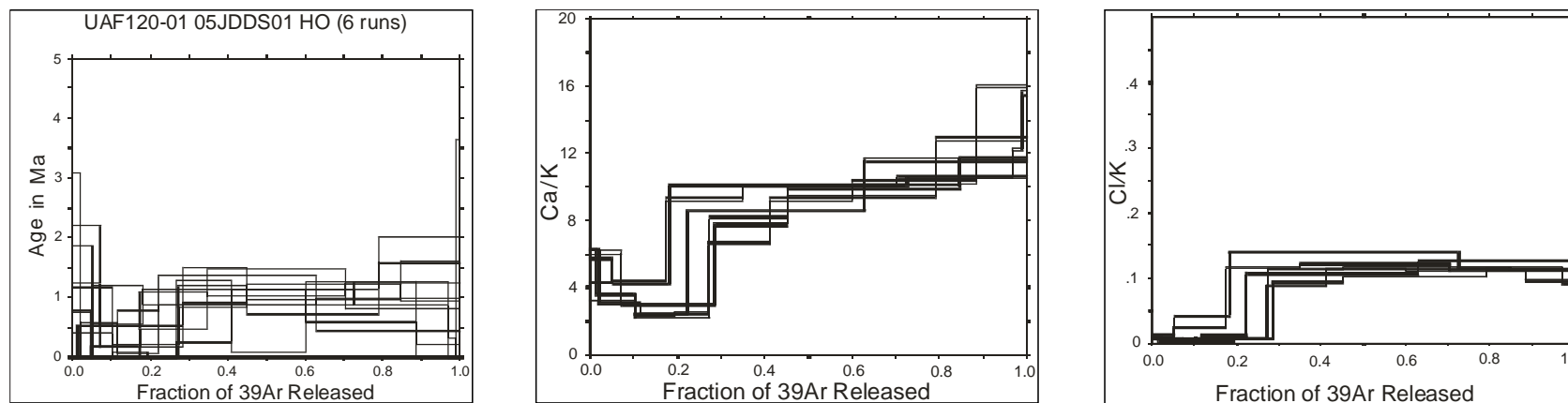
For  $^{40}\text{Ar}/^{39}\text{Ar}$  analysis, six samples were submitted to the Geochronology Laboratory at UAF. The samples were crushed, washed, and sieved to either 100–250 or 250–500 micron size fractions, and hand picked for datable mineral phases (one per sample). The monitor mineral MMhb-1 (Samson and Alexander, 1987) with an age of 513.9 Ma (Lanphere and Dalrymple, 2000) was used to monitor neutron flux (and calculate the irradiation parameter,  $J$ ). The samples and standards were wrapped in aluminum foil and loaded into aluminum cans of 2.5 cm diameter and 6 cm height. The samples were irradiated in position 5c of the uranium-enriched research reactor of McMaster University in Hamilton, Ontario, Canada, for 20 megawatt-hours.

Upon their return from the reactor, the samples and monitors were loaded into 2-mm-diameter holes in a copper tray that was then loaded in an ultra-high vacuum extraction line. The monitors were fused, and samples heated, using a 6-watt argon-ion laser following the technique described in York and others (1981), Layer and others (1987), and Layer (2000). Argon purification was achieved using a liquid nitrogen cold trap and an SAES Zr-Al getter at 400°C. The samples were analyzed in a VG-3600 mass spectrometer at the Geophysical Institute, University of Alaska Fairbanks. The argon isotopes measured were corrected for system blank and mass discrimination, as well as calcium, potassium, and chlorine interference reactions following procedures outlined in McDougall and Harrison (1999). System blanks generally were  $2 \times 10^{-16}$  mol  $^{40}\text{Ar}$  and  $2 \times 10^{-18}$  mol  $^{36}\text{Ar}$ , which are 10 to 50 times smaller than fraction volumes. Mass discrimination was monitored by running both calibrated air shots and a zero-age glass sample. These measurements were made on a weekly to monthly basis to check for changes in mass discrimination.

Sample information and a summary of all the  $^{40}\text{Ar}/^{39}\text{Ar}$  results are given in table 5, with all ages quoted to the  $\pm 1$  sigma level and calculated using the constants of Steiger and Jaeger (1977). (Sample 2005LF197B [table 5] does not have associated data in this appendix. The sample was too young to be dated by this method.) The integrated age is the age given by the total gas measured and is equivalent to a potassium-argon (K-Ar) age. The spectrum provides a plateau age if three or more consecutive gas fractions represent at least 50 percent of the total gas release and are within two standard deviations of each other (Mean Square Weighted Deviation less than  $\sim 2.5$ ). If a sample has experienced a partial thermal reset and (or) has cooled very slowly, argon is lost from the margins of the sample mineral. This argon loss is reflected in lower apparent-ages for the lower-temperature fraction. In this case, the lowest temperature fraction shows the approximate age of reheating (reset age). The age, Ca/K, and Cl/K spectra plots and detailed analyses are given in tables B1–B7.

This page has intentionally been left blank.

Table B1.  $^{40}\text{Ar}/^{39}\text{Ar}$  spectra and step-heating data for sample 2005JDDS01. Plateau age of  $1.026 \pm 0.057$  Ma.



UAF120-01 05JDDS01 HO#2													Weighted average of J from standards = 0.002351 +/- 0.000011			
Laser (mW)	Cum. $^{39}\text{Ar}$	$^{40}\text{Ar}/^{39}\text{Ar}$ measured	$\pm$	$^{37}\text{Ar}/^{39}\text{Ar}$ measured	$\pm$	$^{36}\text{Ar}/^{39}\text{Ar}$ measured	$\pm$	% Atm. $^{40}\text{Ar}$	Ca/K	$\pm$	Cl/K	$\pm$	$^{40}\text{Ar}^*/^{39}\text{Ar}_K$	$\pm$	Age (Ma)	$\pm$ (Ma)
500	0.0134	12.949	0.151	3.3954	0.0407	0.0545	0.0097	122.7	6.2439	0.0750	0.00744	0.00081	-2.9396	2.8721	-12.51	12.26
1000	0.1009	1.357	0.023	1.9643	0.0125	0.0052	0.0006	104.0	3.6088	0.0230	0.00350	0.00013	-0.0528	0.1773	-0.22	0.75
1500	0.1950	0.733	0.010	1.2980	0.0063	0.0031	0.0004	114.5	2.3837	0.0116	0.00367	0.00010	-0.1021	0.1235	-0.43	0.52
2000	0.2698	1.038	0.009	1.3410	0.0088	0.0044	0.0006	119.1	2.4627	0.0161	0.00816	0.00020	-0.1929	0.1713	-0.82	0.73
3000	0.4105	2.652	0.016	3.6045	0.0246	0.0092	0.0004	93.2	6.6293	0.0453	0.08805	0.00062	0.1797	0.1226	0.76	0.52
4000	0.5990	4.027	0.070	5.0282	0.0358	0.0143	0.0004	96.4	9.2564	0.0662	0.11384	0.00089	0.1445	0.1218	0.61	0.52
6000	0.8841	5.805	0.039	5.5798	0.0406	0.0202	0.0003	96.2	10.2754	0.0750	0.11166	0.00074	0.2190	0.0804	0.93	0.34
9000	1.0000	14.159	0.097	8.6744	0.0635	0.0504	0.0006	100.8	16.0068	0.1178	0.09527	0.00083	-0.1197	0.1708	-0.51	0.72
Integrated		4.873	0.019	4.4941	0.0145	0.0174	0.0002	99.3	8.2703	0.0267	0.07808	0.00026	0.0330	0.0614	0.14	0.26

UAF120-01 05JDDS01 HO#3													Weighted average of J from standards = 0.002351 +/- 0.000011			
Laser (mW)	Cum. $^{39}\text{Ar}$	$^{40}\text{Ar}/^{39}\text{Ar}$ measured	$\pm$	$^{37}\text{Ar}/^{39}\text{Ar}$ measured	$\pm$	$^{36}\text{Ar}/^{39}\text{Ar}$ measured	$\pm$	% Atm. $^{40}\text{Ar}$	Ca/K	$\pm$	Cl/K	$\pm$	$^{40}\text{Ar}^*/^{39}\text{Ar}_K$	$\pm$	Age (Ma)	$\pm$ (Ma)
1000	0.0519	6.194	0.036	2.3346	0.0139	0.0204	0.0004	95.0	4.2902	0.0256	0.01189	0.00016	0.3065	0.1305	1.30	0.55
2000	0.1803	2.100	0.013	2.2719	0.0158	0.0069	0.0003	90.2	4.1749	0.0290	0.04117	0.00032	0.2037	0.0763	0.86	0.32
3000	0.7254	3.898	0.025	5.4861	0.0369	0.0137	0.0001	93.8	10.1022	0.0682	0.14016	0.00095	0.2393	0.0312	1.01	0.13
4000	0.9694	4.530	0.027	5.7159	0.0407	0.0158	0.0002	94.4	10.5270	0.0752	0.11637	0.00071	0.2515	0.0461	1.07	0.20
6000	0.9891	6.919	0.044	6.6340	0.0422	0.0256	0.0008	102.5	12.2254	0.0782	0.09165	0.00070	-0.1722	0.2498	-0.73	1.06
9000	1.0000	10.648	0.084	8.4400	0.0639	0.0378	0.0027	99.3	15.5719	0.1186	0.09668	0.00136	0.0742	0.7869	0.31	3.34
Integrated		4.074	0.016	5.0220	0.0218	0.0142	0.0001	94.3	9.2449	0.0403	0.11356	0.00051	0.2313	0.0256	0.98	0.11

Table B1.  $^{40}\text{Ar}/^{39}\text{Ar}$  spectra and step-heating data for sample 2005JDDS01. Plateau age of  $1.026 \pm 0.057$  Ma—continued.

UAF120-01 05JDDS01 HO#4														Weighted average of J from standards = 0.002351 +/- 0.000011			
Laser (mW)	Cum. $^{39}\text{Ar}$	$^{40}\text{Ar}/^{39}\text{Ar}$ measured	$\pm$	$^{37}\text{Ar}/^{39}\text{Ar}$ measured	$\pm$	$^{36}\text{Ar}/^{39}\text{Ar}$ measured	$\pm$	% Atm. $^{40}\text{Ar}$	Ca/K	$\pm$	Cl/K	$\pm$	$^{40}\text{Ar}/^{39}\text{Ar}_K$	$\pm$	Age (Ma)	$\pm$ (Ma)	
1000	0.1039	2.747	0.018	1.7644	0.0129	0.0090	0.0003	93.2	3.2411	0.0237	0.00464	0.00007	0.1843	0.0919	0.78	0.39	
2000	0.2731	1.406	0.008	1.1884	0.0072	0.0049	0.0001	98.8	2.1822	0.0132	0.00875	0.00009	0.0169	0.0316	0.07	0.13	
3000	0.4511	4.825	0.028	4.4266	0.0263	0.0166	0.0001	95.1	8.1457	0.0486	0.11424	0.00074	0.2374	0.0405	1.01	0.17	
5000	0.8463	4.504	0.029	5.4193	0.0366	0.0157	0.0001	94.3	9.9789	0.0677	0.11704	0.00091	0.2556	0.0292	1.08	0.12	
9000	1.0000	5.439	0.035	6.3476	0.0421	0.0189	0.0003	94.5	11.6952	0.0779	0.11226	0.00076	0.2978	0.0797	1.26	0.34	
Integrated		4.000	0.013	4.2921	0.0155	0.0138	0.0001	94.7	7.8974	0.0286	0.08581	0.00037	0.2111	0.0213	0.89	0.09	

UAF120-01 05JDDS01 HO#5														Weighted average of J from standards = 0.002351 +/- 0.000011			
Laser (mW)	Cum. $^{39}\text{Ar}$	$^{40}\text{Ar}/^{39}\text{Ar}$ measured	$\pm$	$^{37}\text{Ar}/^{39}\text{Ar}$ measured	$\pm$	$^{36}\text{Ar}/^{39}\text{Ar}$ measured	$\pm$	% Atm. $^{40}\text{Ar}$	Ca/K	$\pm$	Cl/K	$\pm$	$^{40}\text{Ar}/^{39}\text{Ar}_K$	$\pm$	Age (Ma)	$\pm$ (Ma)	
1000	0.0181	10.447	0.077	3.4102	0.0302	0.0352	0.0015	97.2	6.2711	0.0557	0.01020	0.00037	0.2878	0.4385	1.22	1.86	
2000	0.1145	1.734	0.012	1.6866	0.0124	0.0060	0.0003	96.6	3.0981	0.0227	0.00406	0.00009	0.0580	0.0778	0.25	0.33	
3000	0.2224	1.623	0.014	1.3064	0.0114	0.0054	0.0003	93.8	2.3991	0.0210	0.01143	0.00015	0.0989	0.0821	0.42	0.35	
5000	0.6288	3.853	0.026	4.6597	0.0318	0.0132	0.0002	93.1	8.5760	0.0587	0.10679	0.00080	0.2639	0.0570	1.12	0.24	
9000	1.0000	5.899	0.037	6.2972	0.0396	0.0209	0.0002	97.2	11.6020	0.0733	0.12568	0.00082	0.1658	0.0637	0.70	0.27	
Integrated		4.289	0.017	4.5984	0.0187	0.0149	0.0001	95.5	8.4628	0.0346	0.09186	0.00041	0.1903	0.0360	0.81	0.15	

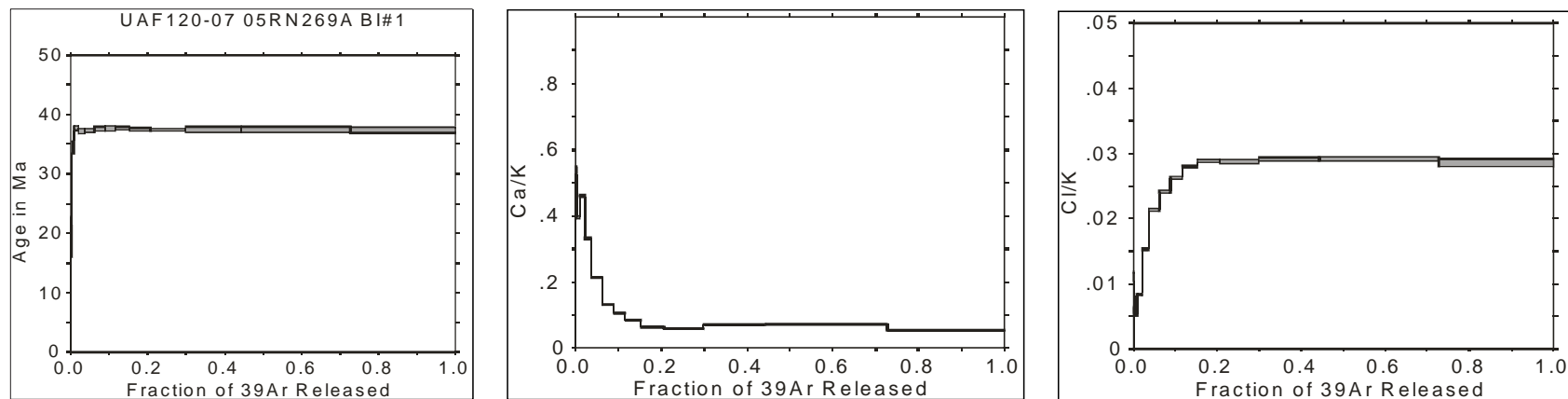
  

UAF120-01 05JDDS01 HO#6														Weighted average of J from standards = 0.002351 +/- 0.000011			
Laser (mW)	Cum. $^{39}\text{Ar}$	$^{40}\text{Ar}/^{39}\text{Ar}$ measured	$\pm$	$^{37}\text{Ar}/^{39}\text{Ar}$ measured	$\pm$	$^{36}\text{Ar}/^{39}\text{Ar}$ measured	$\pm$	% Atm. $^{40}\text{Ar}$	Ca/K	$\pm$	Cl/K	$\pm$	$^{40}\text{Ar}/^{39}\text{Ar}_K$	$\pm$	Age (Ma)	$\pm$ (Ma)	
1000	0.0490	6.329	0.046	3.1433	0.0237	0.0220	0.0005	99.4	5.7794	0.0436	0.00945	0.00016	0.0377	0.1474	0.16	0.63	
2000	0.1733	2.234	0.012	2.4110	0.0131	0.0081	0.0002	100.6	4.4308	0.0240	0.02463	0.00022	-0.0140	0.0558	-0.06	0.24	
3000	0.3489	4.043	0.024	5.0261	0.0459	0.0143	0.0002	95.5	9.2525	0.0847	0.11598	0.00114	0.1830	0.0715	0.78	0.30	
5000	0.7048	4.347	0.029	5.4448	0.0391	0.0150	0.0002	93.2	10.0261	0.0723	0.12233	0.00095	0.2939	0.0523	1.25	0.22	
9000	1.0000	4.458	0.028	5.7404	0.0391	0.0156	0.0002	94.6	10.5723	0.0722	0.10980	0.00078	0.2401	0.0518	1.02	0.22	
Integrated		4.161	0.014	4.9694	0.0192	0.0146	0.0001	95.0	9.1478	0.0355	0.09984	0.00043	0.2077	0.0290	0.88	0.12	

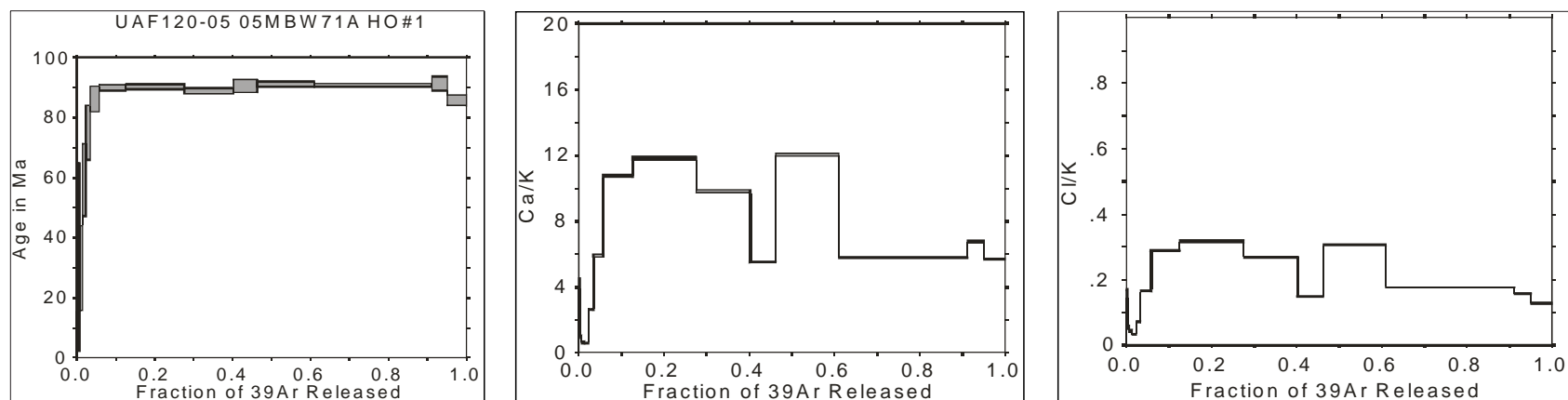
UAF120-01 05JDDS01 HO#7														Weighted average of J from standards = 0.002351 +/- 0.000011			
Laser (mW)	Cum. $^{39}\text{Ar}$	$^{40}\text{Ar}/^{39}\text{Ar}$ measured	$\pm$	$^{37}\text{Ar}/^{39}\text{Ar}$ measured	$\pm$	$^{36}\text{Ar}/^{39}\text{Ar}$ measured	$\pm$	% Atm. $^{40}\text{Ar}$	Ca/K	$\pm$	Cl/K	$\pm$	$^{40}\text{Ar}/^{39}\text{Ar}_K$	$\pm$	Age (Ma)	$\pm$ (Ma)	
1000	0.0725	5.610	0.063	3.3186	0.0368	0.0184	0.0004	92.7	6.1024	0.0678	0.00657	0.00017	0.4063	0.1146	1.72	0.49	
2000	0.2855	1.463	0.009	1.6196	0.0106	0.0050	0.0002	94.3	2.9749	0.0195	0.00632	0.00008	0.0811	0.0431	0.34	0.18	
3000	0.4509	4.621	0.028	4.2000	0.0280	0.0157	0.0002	93.8	7.7276	0.0517	0.09333	0.00058	0.2853	0.0692	1.21	0.29	
5000	0.7891	4.465	0.027	5.1024	0.0331	0.0156	0.0002	95.1	9.3935	0.0612	0.10199	0.00070	0.2194	0.0508	0.93	0.22	
9000	1.0000	6.384	0.040	6.9573	0.0463	0.0219	0.0002	93.4	12.8237	0.0856	0.11304	0.00085	0.4217	0.0493	1.79	0.21	
Integrated		4.341	0.014	4.4755	0.0154	0.0149	0.0001	94.1	8.2360	0.0284	0.07560	0.00030	0.2571	0.0262	1.09	0.11	

Table B2.  $^{40}\text{Ar}/^{39}\text{Ar}$  spectra and step-heating data for sample 2005RN269A. Map location "A1," sheet RI 2006-2. Plateau age of  $37.4 \pm 0.3$  Ma.



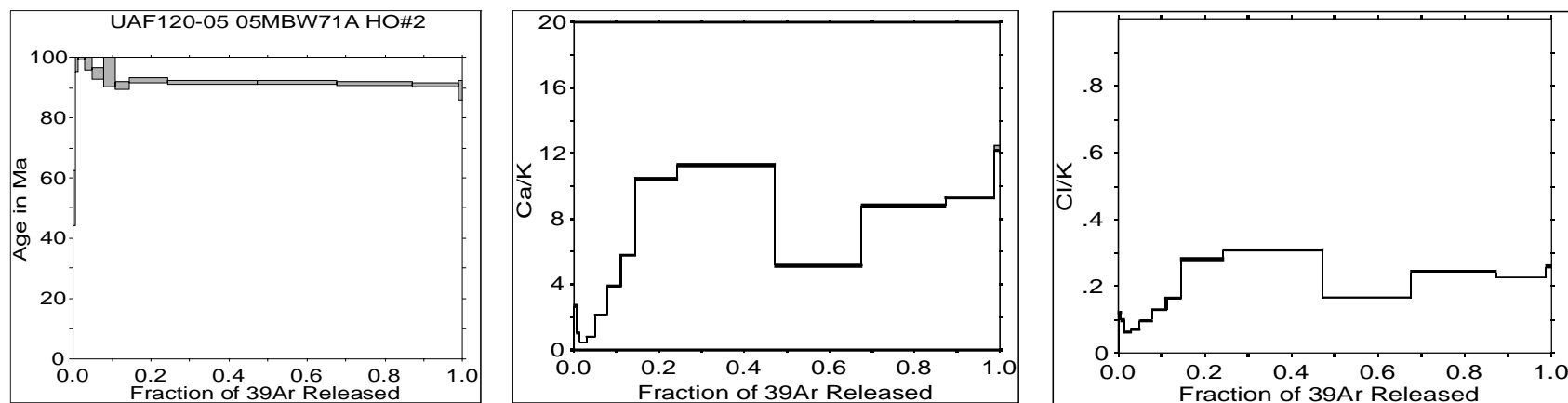
UAF120-07 05RN269A BI#1												Weighted average of J from standards = $0.002351 \pm 0.000011$				
Laser (mW)	Cum. $^{39}\text{Ar}$	$^{40}\text{Ar}/^{39}\text{Ar}$ measured	$\pm$	$^{37}\text{Ar}/^{39}\text{Ar}$ measured	$\pm$	$^{36}\text{Ar}/^{39}\text{Ar}$ measured	$\pm$	% Atm. $^{40}\text{Ar}$	Ca/K	$\pm$	Cl/K	$\pm$	$^{40}\text{Ar}^*/^{39}\text{Ar}_K$	$\pm$	Age (Ma)	$\pm$ (Ma)
300	0.0012	52.709	0.648	0.2735	0.0077	0.1647	0.0049	92.3	0.5019	0.0141	0.01113	0.00068	4.0354	1.3465	17.0	5.7
500	0.0030	25.981	0.208	0.2934	0.0057	0.0730	0.0022	83.0	0.5385	0.0104	0.00597	0.00047	4.4150	0.6368	18.6	2.7
700	0.0090	13.037	0.089	0.2153	0.0020	0.0163	0.0008	36.9	0.3952	0.0037	0.00522	0.00015	8.2134	0.2494	34.5	1.0
900	0.0211	10.674	0.051	0.2504	0.0018	0.0057	0.0003	15.6	0.4595	0.0034	0.00837	0.00015	8.9845	0.1028	37.7	0.4
1100	0.0367	10.026	0.057	0.1810	0.0014	0.0039	0.0003	11.3	0.3321	0.0026	0.01527	0.00016	8.8637	0.1147	37.2	0.5
1400	0.0619	9.492	0.061	0.1174	0.0008	0.0020	0.0002	6.0	0.2155	0.0015	0.02132	0.00019	8.8924	0.0871	37.3	0.4
1700	0.0888	9.320	0.056	0.0709	0.0007	0.0012	0.0002	3.6	0.1301	0.0013	0.02413	0.00022	8.9575	0.0788	37.6	0.3
2000	0.1157	9.257	0.055	0.0577	0.0006	0.0009	0.0003	2.8	0.1059	0.0010	0.02631	0.00020	8.9688	0.1137	37.6	0.5
2500	0.1527	9.158	0.058	0.0459	0.0005	0.0005	0.0001	1.6	0.0842	0.0009	0.02790	0.00018	8.9818	0.0713	37.7	0.3
3000	0.2068	9.085	0.056	0.0353	0.0004	0.0005	0.0001	1.5	0.0648	0.0007	0.02886	0.00022	8.9238	0.0641	37.5	0.3
3500	0.2988	9.013	0.057	0.0325	0.0003	0.0003	0.0001	0.8	0.0597	0.0005	0.02875	0.00032	8.9148	0.0595	37.4	0.3
4000	0.4430	9.036	0.115	0.0386	0.0003	0.0003	0.0000	0.9	0.0708	0.0005	0.02914	0.00025	8.9253	0.1146	37.5	0.5
6000	0.7268	9.013	0.121	0.0398	0.0004	0.0002	0.0000	0.6	0.0730	0.0007	0.02920	0.00028	8.9289	0.1209	37.5	0.5
9000	1.0000	9.005	0.124	0.0295	0.0006	0.0003	0.0000	0.8	0.0541	0.0011	0.02858	0.00062	8.9020	0.1245	37.4	0.5
Integrated		9.193	0.052	0.0459	0.0002	0.0009	0.0000	2.8	0.0843	0.0004	0.02783	0.00019	8.9037	0.0518	37.4	0.3

Table B3.  $^{40}\text{Ar}/^{39}\text{Ar}$  spectra and step-heating data for sample 2005MBW71A. Map location "A2," sheet RI 2006-2. (a) Plateau age of  $90.4 \pm 0.5$  Ma.



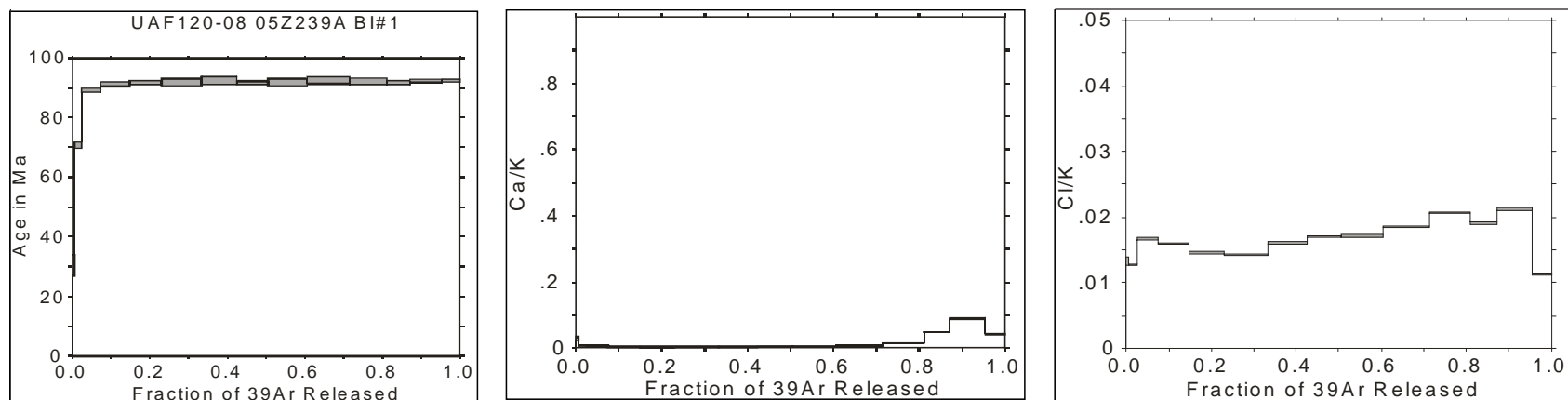
UAF120-05 05MBW71A HO#1											Weighted average of J from standards = $0.002351 \pm 0.000011$					
Laser (mW)	Cum. $^{39}\text{Ar}$	$^{40}\text{Ar}/^{39}\text{Ar}$ measured	$\pm$	$^{37}\text{Ar}/^{39}\text{Ar}$ measured	$\pm$	$^{38}\text{Ar}/^{39}\text{Ar}$ measured	$\pm$	% Atm. $^{40}\text{Ar}$	Ca/K	$\pm$	Cl/K	$\pm$	$^{40}\text{Ar}^*/^{39}\text{Ar}_K$	$\pm$	Age (Ma)	$\pm$ (Ma)
300	0.0019	277.139	14.935	2.2942	0.1636	0.9840	0.0775	104.9	4.2158	0.3010	0.15751	0.01312	-13.5122	16.7828	-58.2	73.5
500	0.0061	71.244	2.194	0.5362	0.0500	0.2141	0.0262	88.8	0.9841	0.0918	0.05534	0.00517	7.9943	7.5258	33.6	31.3
700	0.0138	27.926	0.561	0.3353	0.0303	0.0704	0.0115	74.5	0.6153	0.0556	0.04364	0.00293	7.1207	3.3918	30.0	14.2
900	0.0223	26.692	0.419	0.3209	0.0259	0.0423	0.0099	46.8	0.5889	0.0475	0.03333	0.00204	14.2006	2.9370	59.2	12.1
1100	0.0340	28.398	0.387	1.4267	0.0304	0.0353	0.0075	36.4	2.6201	0.0558	0.07231	0.00226	18.0489	2.2148	75.0	9.0
1400	0.0571	26.937	0.268	3.2144	0.0349	0.0215	0.0034	22.8	5.9104	0.0644	0.16680	0.00239	20.8288	1.0285	86.2	4.2
1700	0.1257	23.740	0.119	5.8310	0.0396	0.0084	0.0008	8.6	10.7399	0.0732	0.28955	0.00173	21.7550	0.2559	90.0	1.0
2000	0.2762	22.628	0.159	6.4207	0.0475	0.0046	0.0004	3.9	11.8306	0.0880	0.31790	0.00238	21.8175	0.1983	90.2	0.8
2500	0.4017	22.823	0.175	5.3346	0.0444	0.0060	0.0005	6.1	9.8224	0.0820	0.26967	0.00208	21.4845	0.2246	88.9	0.9
3000	0.4631	24.576	0.176	3.0021	0.0244	0.0099	0.0018	11.0	5.5193	0.0449	0.14982	0.00152	21.8885	0.5443	90.5	2.2
3500	0.6099	23.045	0.161	6.5434	0.0500	0.0053	0.0005	4.7	12.0577	0.0924	0.30671	0.00220	22.0363	0.2136	91.1	0.9
4000	0.9125	22.303	0.104	3.1604	0.0153	0.0021	0.0003	1.7	5.8109	0.0282	0.17774	0.00113	21.9396	0.1304	90.7	0.5
6000	0.9501	22.461	0.152	3.6828	0.0261	0.0023	0.0019	1.8	6.7736	0.0482	0.15771	0.00154	22.0808	0.5828	91.3	2.4
9000	1.0000	22.094	0.163	3.1037	0.0261	0.0055	0.0013	6.3	5.7065	0.0481	0.12992	0.00128	20.7130	0.4242	85.8	1.7
Integrated		23.703	0.056	4.5349	0.0124	0.0090	0.0003	9.7	8.3456	0.0229	0.22782	0.00064	21.4303	0.1054	88.7	0.6

Table B3.  $^{40}\text{Ar}/^{39}\text{Ar}$  spectra and step-heating data for sample 2005MBW71A. Map location "A2," sheet RI 2006-2. (a) Plateau age of  $90.4 \pm 0.5 \text{ Ma}$ —continued.



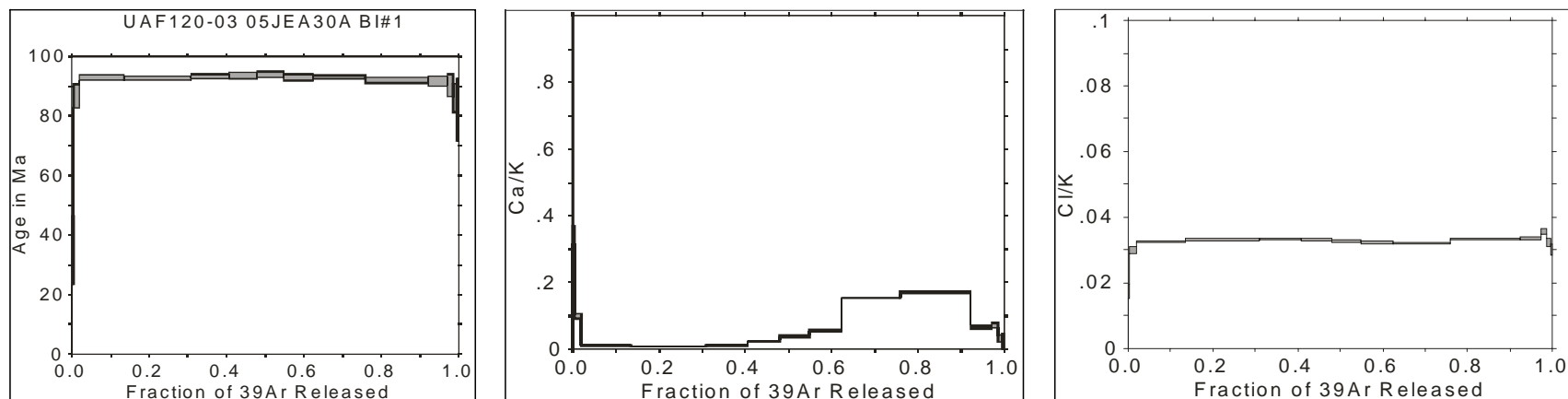
UAF120-05 05MBW71A HO#2												Weighted average of J from standards = $0.002351 \pm 0.000011$				
Laser (mW)	Cum. $^{39}\text{Ar}$	$^{40}\text{Ar}/^{39}\text{Ar}$ measured	$\pm$	$^{37}\text{Ar}/^{39}\text{Ar}$ measured	$\pm$	$^{36}\text{Ar}/^{39}\text{Ar}$ measured	$\pm$	% Atm. $^{40}\text{Ar}$	Ca/K	$\pm$	Cl/K	$\pm$	$^{40}\text{Ar}^*/^{39}\text{Ar}_K$	$\pm$	Age (Ma)	$\pm$ (Ma)
500	0.0065	92.388	1.728	1.4536	0.0298	0.2696	0.0089	86.2	2.6697	0.0549	0.12293	0.00257	12.8011	2.2442	53.5	9.2
750	0.0135	7.611	0.255	0.5595	0.0150	-0.0613	0.0091	-239.6	1.0270	0.0275	0.09877	0.00235	25.7613	2.7245	106.1	10.9
1000	0.0285	12.790	0.168	0.2520	0.0041	-0.0406	0.0024	-94.2	0.4624	0.0075	0.06370	0.00080	24.7890	0.7352	102.2	3.0
1250	0.0493	14.228	0.149	0.4434	0.0062	-0.0324	0.0021	-67.7	0.8139	0.0114	0.07211	0.00091	23.8228	0.6384	98.3	2.6
1500	0.0780	15.959	0.132	1.1791	0.0097	-0.0233	0.0014	-43.8	2.1651	0.0178	0.09880	0.00097	22.9264	0.4373	94.7	1.8
1750	0.1093	16.222	0.130	2.1134	0.0180	-0.0230	0.0046	-42.9	3.8831	0.0331	0.13094	0.00115	23.1678	1.3796	95.7	5.6
2000	0.1439	24.885	0.180	3.1346	0.0242	0.0108	0.0010	11.9	5.7634	0.0447	0.16468	0.00148	21.9420	0.3277	90.7	1.3
2500	0.2417	24.061	0.164	5.6763	0.0430	0.0075	0.0005	7.4	10.4538	0.0796	0.28205	0.00211	22.3370	0.2165	92.3	0.9
3000	0.4721	22.841	0.137	6.1060	0.0401	0.0039	0.0002	3.0	11.2483	0.0742	0.31072	0.00204	22.2059	0.1476	91.8	0.6
3500	0.6765	23.546	0.144	2.8029	0.0185	0.0054	0.0002	5.9	5.1524	0.0340	0.16700	0.00106	22.1796	0.1534	91.7	0.6
4000	0.8716	22.928	0.129	4.7757	0.0275	0.0041	0.0003	3.7	8.7900	0.0507	0.24458	0.00151	22.1102	0.1601	91.4	0.7
6000	0.9882	23.107	0.122	5.0403	0.0283	0.0051	0.0003	4.9	9.2786	0.0523	0.22674	0.00119	22.0182	0.1485	91.0	0.6
9000	1.0000	23.629	0.261	6.6855	0.0738	0.0090	0.0026	9.1	12.3206	0.1365	0.26117	0.00322	21.5444	0.8054	89.1	3.3
Integrated		22.844	0.055	4.3699	0.0120	0.0033	0.0002	2.8	8.0411	0.0221	0.22713	0.00062	22.2429	0.0836	91.9	0.5

Table B4.  $^{40}\text{Ar}/^{39}\text{Ar}$  spectra and step-heating data for sample 2005Z239A. Map location "A3," sheet RI 2006-2. Plateau age of  $92.0 \pm 0.5$  Ma.



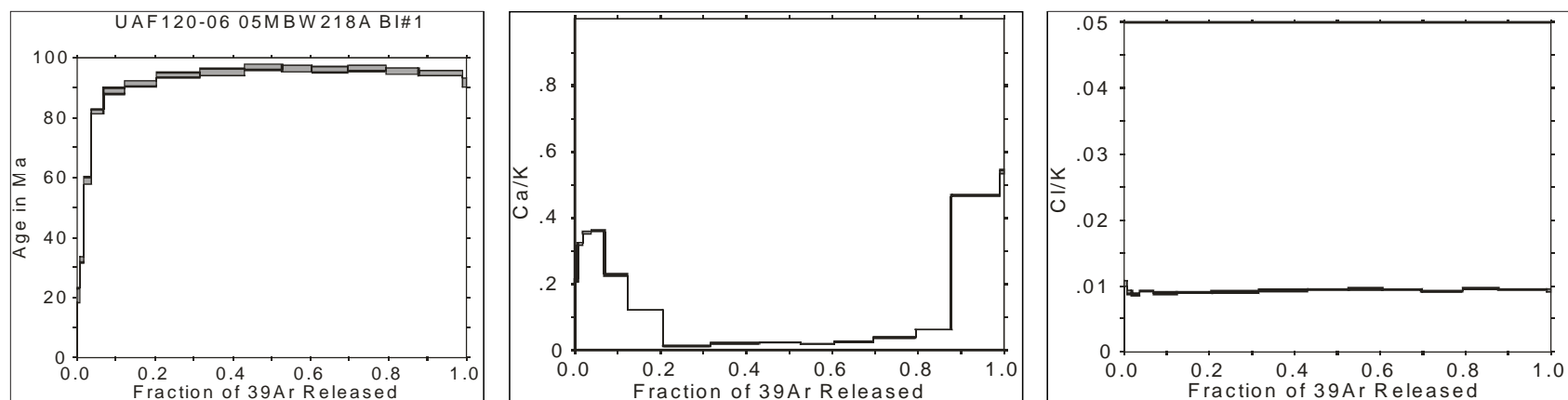
UAF120-08 05Z239A BI#1												Weighted average of J from standards = 0.002351 ± 0.000011				
Laser (mW)	Cum. $^{39}\text{Ar}$	$^{40}\text{Ar}/^{39}\text{Ar}$ measured	±	$^{37}\text{Ar}/^{39}\text{Ar}$ measured	±	$^{36}\text{Ar}/^{39}\text{Ar}$ measured	±	% Atm. $^{40}\text{Ar}$	Ca/K	±	Cl/K	±	$^{40}\text{Ar}^*/^{39}\text{Ar}_K$	±	Age (Ma)	± (Ma)
300	0.0060	29.847	0.401	0.0157	0.0028	0.0763	0.0029	75.6	0.0288	0.0052	0.01320	0.00064	7.2764	0.8596	30.6	3.6
500	0.0247	25.136	0.210	0.0045	0.0011	0.0274	0.0007	32.2	0.0083	0.0020	0.01275	0.00018	17.0211	0.2539	70.8	1.0
700	0.0739	22.947	0.130	0.0037	0.0003	0.0046	0.0003	6.0	0.0067	0.0006	0.01669	0.00019	21.5497	0.1450	89.1	0.6
900	0.1480	22.598	0.185	0.0023	0.0002	0.0017	0.0002	2.2	0.0042	0.0004	0.01601	0.00016	22.0727	0.1931	91.3	0.8
1100	0.2309	22.682	0.146	0.0018	0.0002	0.0016	0.0002	2.0	0.0034	0.0004	0.01457	0.00016	22.1923	0.1524	91.7	0.6
1400	0.3328	22.916	0.283	0.0021	0.0002	0.0022	0.0001	2.9	0.0038	0.0004	0.01419	0.00013	22.2310	0.2838	91.9	1.1
1700	0.4243	23.297	0.307	0.0024	0.0002	0.0030	0.0001	3.8	0.0043	0.0003	0.01610	0.00015	22.3857	0.3062	92.5	1.2
2000	0.5048	22.955	0.126	0.0030	0.0002	0.0025	0.0002	3.3	0.0056	0.0004	0.01704	0.00012	22.1774	0.1373	91.7	0.6
2500	0.6056	22.918	0.286	0.0033	0.0002	0.0022	0.0001	2.9	0.0060	0.0004	0.01709	0.00018	22.2343	0.2866	91.9	1.2
3000	0.7145	22.838	0.291	0.0043	0.0002	0.0015	0.0001	1.9	0.0078	0.0004	0.01855	0.00014	22.3808	0.2922	92.5	1.2
3500	0.8109	22.749	0.274	0.0081	0.0002	0.0015	0.0001	1.9	0.0149	0.0003	0.02073	0.00015	22.2902	0.2753	92.1	1.1
4000	0.8714	22.584	0.153	0.0265	0.0005	0.0012	0.0002	1.6	0.0486	0.0009	0.01911	0.00019	22.1971	0.1589	91.8	0.6
6000	0.9539	22.680	0.128	0.0479	0.0003	0.0011	0.0001	1.4	0.0880	0.0006	0.02120	0.00015	22.3360	0.1324	92.3	0.5
9000	1.0000	23.056	0.110	0.0229	0.0004	0.0022	0.0002	2.9	0.0421	0.0008	0.01119	0.00014	22.3681	0.1262	92.4	0.5
Integrated		22.938	0.070	0.0095	0.0001	0.0029	0.0001	3.8	0.0175	0.0001	0.01699	0.00004	22.0405	0.0706	91.1	0.5

Table B5.  $^{40}\text{Ar}/^{39}\text{Ar}$  spectra and step-heating data for sample 2005JEA30A. Map location "A4," sheet RI 2006-2. Plateau age of  $92.9 \pm 0.5$  Ma.



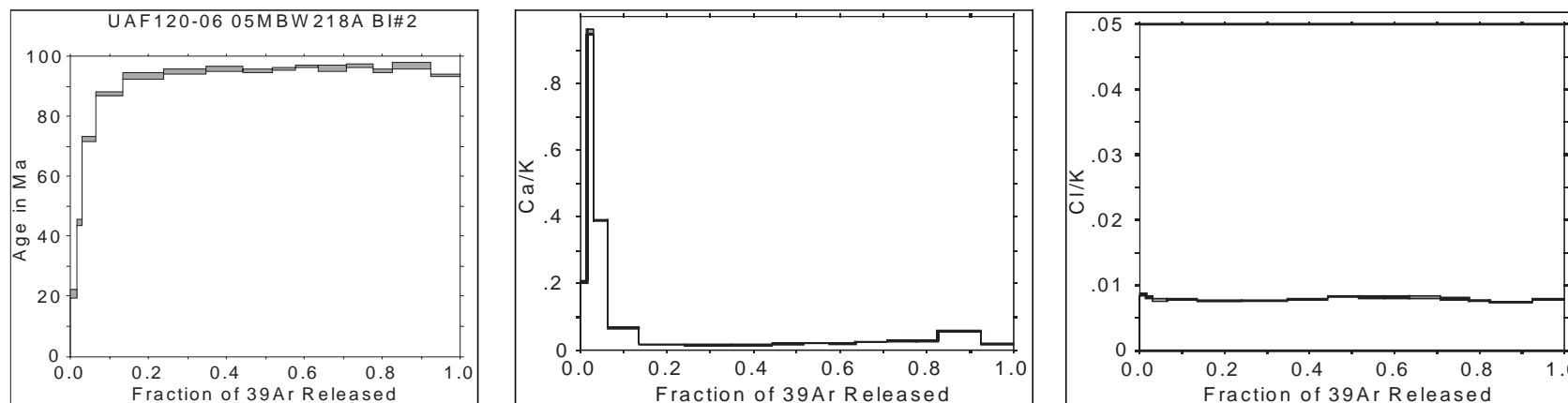
UAF120-03 05JEA30A BI#1													Weighted average of J from standards = $0.002351 \pm 0.000011$			
Laser (mW)	Cum. $^{39}\text{Ar}$	$^{40}\text{Ar}/^{39}\text{Ar}$ measured	$\pm$	$^{37}\text{Ar}/^{39}\text{Ar}$ measured	$\pm$	$^{36}\text{Ar}/^{39}\text{Ar}$ measured	$\pm$	% Atm. $^{40}\text{Ar}$	Ca/K	$\pm$	Cl/K	$\pm$	$^{40}\text{Ar}^*/^{39}\text{Ar}_K$	$\pm$	Age (Ma)	$\pm$ (Ma)
300	0.0045	28.917	0.696	0.1872	0.0153	0.0697	0.0094	71.2	0.3436	0.0281	0.01731	0.00203	8.3145	2.7460	34.9	11.4
500	0.0196	30.559	0.317	0.0541	0.0041	0.0324	0.0032	31.3	0.0992	0.0075	0.02982	0.00097	20.9677	0.9688	86.8	3.9
700	0.1345	24.193	0.174	0.0065	0.0007	0.0057	0.0004	7.0	0.0119	0.0012	0.03256	0.00029	22.4832	0.2006	92.9	0.8
900	0.3082	23.042	0.155	0.0049	0.0005	0.0020	0.0003	2.5	0.0090	0.0008	0.03322	0.00037	22.4341	0.1722	92.7	0.7
1100	0.4065	23.358	0.143	0.0071	0.0006	0.0025	0.0004	3.1	0.0129	0.0012	0.03320	0.00025	22.5970	0.1842	93.4	0.7
1400	0.4792	23.821	0.156	0.0131	0.0011	0.0038	0.0008	4.7	0.0240	0.0020	0.03325	0.00041	22.6667	0.2677	93.7	1.1
1700	0.5482	23.876	0.138	0.0213	0.0012	0.0038	0.0007	4.7	0.0392	0.0022	0.03263	0.00036	22.7264	0.2481	93.9	1.0
2000	0.6234	23.420	0.176	0.0303	0.0013	0.0030	0.0007	3.8	0.0557	0.0023	0.03217	0.00037	22.5133	0.2699	93.0	1.1
2500	0.7586	23.046	0.125	0.0838	0.0007	0.0017	0.0003	2.2	0.1538	0.0013	0.03206	0.00022	22.5222	0.1546	93.1	0.6
3000	0.9220	22.621	0.130	0.0924	0.0017	0.0012	0.0006	1.5	0.1696	0.0031	0.03336	0.00031	22.2542	0.2287	92.0	0.9
3500	0.9712	22.568	0.190	0.0362	0.0022	0.0012	0.0012	1.5	0.0665	0.0040	0.03350	0.00041	22.1933	0.4058	91.7	1.6
4000	0.9851	22.575	0.282	0.0396	0.0039	0.0024	0.0030	3.2	0.0726	0.0072	0.03556	0.00080	21.8332	0.9316	90.3	3.8
6000	0.9955	22.122	0.246	0.0177	0.0053	0.0044	0.0040	5.8	0.0325	0.0098	0.03216	0.00124	20.8076	1.2031	86.2	4.9
9000	1.0000	21.877	0.442	0.0109	0.0135	0.0069	0.0087	9.3	0.0201	0.0249	0.03025	0.00177	19.8226	2.6055	82.2	10.6
Integrated		23.375	0.051	0.0377	0.0004	0.0034	0.0002	4.3	0.0691	0.0007	0.03279	0.00011	22.3470	0.0768	92.4	0.5

Table B6.  $^{40}\text{Ar}/^{39}\text{Ar}$  spectra and step-heating data for sample 2005MBW218A. Map location "A5," sheet RI 2006-2. (a) Plateau age of  $95.5 \pm 0.5$  Ma.



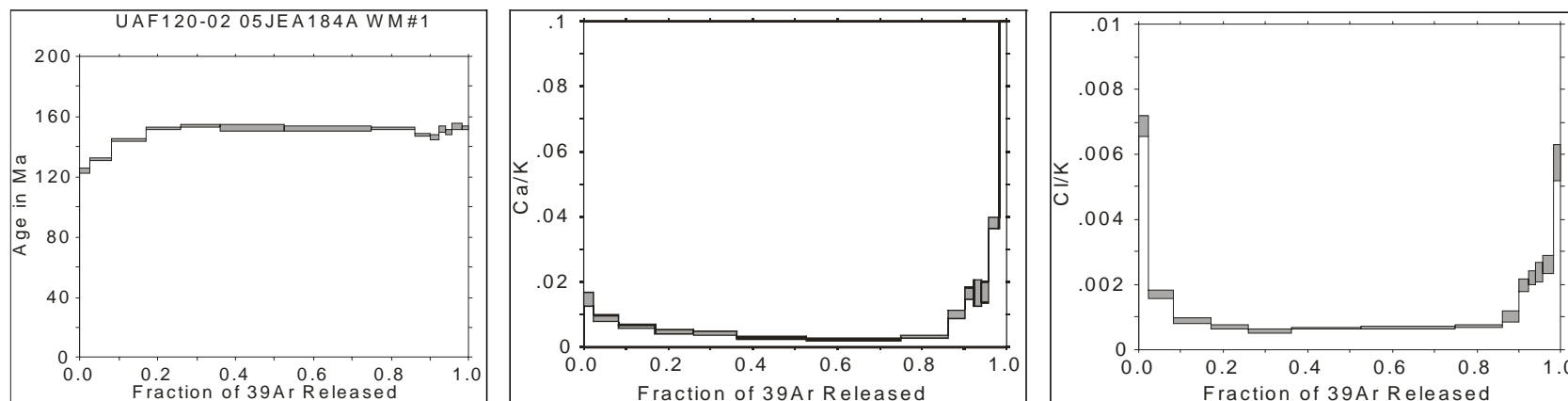
UAF120-06 05MBW218A BI#1														
Weighted average of J from standards = 0.002351 ± 0.000011														
Laser (mW)	Cum. $^{39}\text{Ar}$	$^{40}\text{Ar}/^{39}\text{Ar}$ measured ±	$^{37}\text{Ar}/^{39}\text{Ar}$ measured ±	$^{36}\text{Ar}/^{39}\text{Ar}$ measured ±	% Atm. $^{40}\text{Ar}$	Ca/K ±	Cl/K ±	$^{40}\text{Ar}/^{39}\text{Ar}_K$ ±	Age (Ma) ± (Ma)					
300	0.0065	36.166 0.320	0.1147 0.0028	0.1057 0.0020	86.4	0.2104 0.0052	0.01038 0.00045	4.9116 0.5714	20.7 2.4					
500	0.0178	16.500 0.127	0.1751 0.0016	0.0296 0.0008	53.0	0.3213 0.0030	0.00904 0.00028	7.7473 0.2360	32.6 1.0					
750	0.0366	19.486 0.244	0.1939 0.0020	0.0181 0.0007	27.4	0.3559 0.0037	0.00875 0.00020	14.1183 0.3008	58.9 1.2					
1000	0.0681	22.313 0.134	0.1970 0.0013	0.0085 0.0004	11.3	0.3615 0.0023	0.00920 0.00014	19.7775 0.1740	82.0 0.7					
1250	0.1227	22.881 0.257	0.1236 0.0015	0.0048 0.0002	6.1	0.2267 0.0027	0.00884 0.00013	21.4593 0.2548	88.8 1.0					
1500	0.2047	22.911 0.253	0.0666 0.0004	0.0027 0.0002	3.5	0.1222 0.0008	0.00895 0.00010	22.0815 0.2550	91.3 1.0					
1750	0.3159	23.176 0.205	0.0068 0.0002	0.0012 0.0001	1.6	0.0124 0.0004	0.00907 0.00010	22.7869 0.2067	94.1 0.8					
2000	0.4302	23.406 0.293	0.0116 0.0002	0.0012 0.0001	1.5	0.0213 0.0004	0.00932 0.00010	23.0154 0.2944	95.1 1.2					
2250	0.5266	23.883 0.240	0.0126 0.0002	0.0014 0.0001	1.7	0.0230 0.0003	0.00948 0.00008	23.4414 0.2429	96.8 1.0					
2500	0.6048	23.829 0.257	0.0104 0.0003	0.0016 0.0002	2.0	0.0191 0.0005	0.00955 0.00011	23.3266 0.2604	96.3 1.1					
3000	0.6966	23.835 0.254	0.0139 0.0002	0.0019 0.0001	2.4	0.0254 0.0003	0.00945 0.00009	23.2441 0.2544	96.0 1.0					
3500	0.7936	23.932 0.252	0.0207 0.0002	0.0019 0.0001	2.3	0.0380 0.0004	0.00915 0.00006	23.3481 0.2540	96.4 1.0					
4000	0.8775	23.824 0.254	0.0338 0.0003	0.0023 0.0001	2.8	0.0621 0.0005	0.00956 0.00008	23.1273 0.2544	95.5 1.0					
6000	0.9901	23.367 0.219	0.2548 0.0016	0.0015 0.0001	1.8	0.4676 0.0029	0.00949 0.00008	22.9204 0.2198	94.7 0.9					
9000	1.0000	22.970 0.107	0.2936 0.0034	0.0028 0.0013	3.5	0.5388 0.0062	0.00932 0.00024	22.1356 0.3872	91.5 1.6					
Integrated		23.404 0.074	0.0666 0.0002	0.0034 0.0001	4.3	0.1222 0.0003	0.00929 0.00003	22.3774 0.0744	92.5 0.5					

Table B6.  $^{40}\text{Ar}/^{39}\text{Ar}$  spectra and step-heating data for sample 2005MBW218A. Map location "A5," sheet RI 2006-2. (a) Plateau age of  $95.5 \pm 0.5$  Ma—continued.



UAF120-06 05MBW218A BI#2												Weighted average of J from standards = 0.002351 ± 0.000011				
Laser (mW)	Cum. $^{39}\text{Ar}$	$^{40}\text{Ar}/^{39}\text{Ar}$ measured	±	$^{37}\text{Ar}/^{39}\text{Ar}$ measured	±	$^{38}\text{Ar}/^{39}\text{Ar}$ measured	±	% Atm. $^{40}\text{Ar}$	Ca/K	±	Cl/K	±	$^{40}\text{Ar}/^{39}\text{Ar}_K$	±	Age (Ma)	± (Ma)
300	0.0153	30.352	0.167	0.1121	0.0014	0.0859	0.0011	83.7	0.2056	0.0025	0.00873	0.00017	4.9437	0.3153	20.8	1.3
500	0.0300	19.684	0.111	0.5208	0.0039	0.0307	0.0009	46.0	0.9558	0.0072	0.00826	0.00017	10.6209	0.2648	44.5	1.1
750	0.0641	20.964	0.146	0.2127	0.0018	0.0119	0.0003	16.7	0.3904	0.0033	0.00776	0.00018	17.4358	0.1642	72.5	0.7
1000	0.1356	22.462	0.139	0.0364	0.0005	0.0044	0.0002	5.7	0.0668	0.0008	0.00789	0.00010	21.1501	0.1460	87.5	0.6
1250	0.2396	23.367	0.236	0.0095	0.0002	0.0024	0.0001	3.0	0.0174	0.0004	0.00766	0.00010	22.6389	0.2363	93.5	1.0
1500	0.3472	23.773	0.228	0.0086	0.0002	0.0026	0.0001	3.2	0.0157	0.0003	0.00769	0.00009	22.9818	0.2283	94.9	0.9
1750	0.4429	24.118	0.250	0.0090	0.0002	0.0030	0.0001	3.7	0.0166	0.0004	0.00786	0.00011	23.2071	0.2508	95.8	1.0
2000	0.5159	24.017	0.157	0.0107	0.0002	0.0031	0.0002	3.8	0.0196	0.0004	0.00831	0.00009	23.0786	0.1603	95.3	0.6
2250	0.5763	24.193	0.134	0.0117	0.0002	0.0032	0.0002	3.9	0.0215	0.0005	0.00825	0.00012	23.2170	0.1491	95.9	0.6
2500	0.6346	24.360	0.126	0.0110	0.0003	0.0031	0.0003	3.8	0.0201	0.0006	0.00824	0.00011	23.4166	0.1491	96.7	0.6
3000	0.7086	24.178	0.249	0.0144	0.0003	0.0030	0.0003	3.7	0.0264	0.0006	0.00822	0.00021	23.2523	0.2542	96.0	1.0
3500	0.7758	24.312	0.160	0.0156	0.0004	0.0028	0.0002	3.4	0.0286	0.0007	0.00800	0.00012	23.4560	0.1650	96.8	0.7
4000	0.8253	23.850	0.148	0.0157	0.0004	0.0026	0.0002	3.3	0.0288	0.0007	0.00769	0.00014	23.0463	0.1599	95.2	0.6
6000	0.9240	24.606	0.254	0.0316	0.0003	0.0039	0.0001	4.6	0.0580	0.0006	0.00748	0.00007	23.4355	0.2534	96.7	1.0
9000	1.0000	23.064	0.137	0.0103	0.0002	0.0012	0.0001	1.6	0.0189	0.0004	0.00783	0.00009	22.6695	0.1417	93.7	0.6
Integrated		23.791	0.058	0.0309	0.0001	0.0049	0.0001	6.1	0.0567	0.0002	0.00791	0.00003	22.3124	0.0590	92.2	0.5

Table B7.  $^{40}\text{Ar}/^{39}\text{Ar}$  spectra and step-heating data for sample 2005JEA184A. Map location "A6," sheet RI 2006-2. Plateau age of  $152.8 \pm 1.0$  Ma.



UAF120-02 05JEA184A WM#1													Weighted average of J from standards = 0.002351 ± 0.000011			
Laser (mW)	Cum. $^{39}\text{Ar}$	$^{40}\text{Ar}/^{39}\text{Ar}$ measured	±	$^{37}\text{Ar}/^{39}\text{Ar}$ measured	±	$^{36}\text{Ar}/^{39}\text{Ar}$ measured	±	% Atm. $^{40}\text{Ar}$	Ca/K	±	Cl/K	±	$^{40}\text{Ar}^*/^{39}\text{Ar}_K$	±	Age (Ma)	± (Ma)
300	0.0237	40.254	0.328	0.0080	0.0011	0.0337	0.0008	24.7	0.0146	0.0021	0.00688	0.00033	30.2770	0.3660	124.0	1.5
500	0.0811	33.186	0.198	0.0048	0.0006	0.0030	0.0004	2.7	0.0088	0.0010	0.00168	0.00013	32.2730	0.2289	131.9	0.9
700	0.1696	35.898	0.210	0.0034	0.0003	0.0010	0.0003	0.8	0.0062	0.0005	0.00089	0.00008	35.5643	0.2216	144.8	0.9
900	0.2600	37.893	0.208	0.0026	0.0003	0.0010	0.0003	0.8	0.0047	0.0006	0.00069	0.00008	37.5761	0.2229	152.7	0.9
1100	0.3609	38.213	0.226	0.0023	0.0004	0.0011	0.0003	0.8	0.0043	0.0007	0.00056	0.00007	37.8717	0.2373	153.9	0.9
1400	0.5265	37.896	0.484	0.0016	0.0002	0.0009	0.0001	0.7	0.0028	0.0003	0.00065	0.00004	37.6150	0.4854	152.9	1.9
1700	0.7494	37.791	0.412	0.0012	0.0002	0.0007	0.0001	0.6	0.0022	0.0004	0.00067	0.00003	37.5493	0.4130	152.6	1.6
2000	0.8611	37.659	0.198	0.0017	0.0002	0.0005	0.0003	0.4	0.0031	0.0004	0.00072	0.00004	37.4949	0.2125	152.4	0.8
2500	0.9010	36.877	0.183	0.0055	0.0007	0.0017	0.0006	1.4	0.0100	0.0012	0.00101	0.00017	36.3369	0.2622	147.9	1.0
3000	0.9234	36.790	0.266	0.0090	0.0010	0.0026	0.0012	2.1	0.0165	0.0018	0.00197	0.00020	35.9828	0.4331	146.5	1.7
3500	0.9408	36.961	0.239	0.0090	0.0022	-0.0012	0.0016	-0.9	0.0166	0.0041	0.00221	0.00021	37.2815	0.5264	151.6	2.1
4000	0.9568	37.028	0.316	0.0091	0.0017	0.0006	0.0012	0.5	0.0168	0.0032	0.00238	0.00029	36.8207	0.4823	149.8	1.9
6000	0.9819	38.392	0.426	0.0207	0.0009	0.0020	0.0006	1.5	0.0379	0.0017	0.00262	0.00028	37.7907	0.4548	153.5	1.8
9000	1.0000	37.851	0.180	0.1112	0.0030	0.0010	0.0010	0.7	0.2040	0.0055	0.00574	0.00054	37.5448	0.3542	152.6	1.4
Integrated		37.402	0.130	0.0052	0.0001	0.0018	0.0001	1.4	0.0095	0.0002	0.00113	0.00002	36.8445	0.1325	149.8	0.8

## **Appendix C**

### **Grain-mount petrology of Tertiary samples**

Grain mounts were point-counted to determine sand composition using the methodology of Decker (1985) and the “traditional” methodology of Ingersoll and others (1984). Thin sections were made from rectangular billets of sandy sample mixed with epoxy. A minimum of 250 grains were counted on each thin section on a counting grid with grid points 0.5 mm apart by J.E. Athey and R.L. Smith. Matrix and cement were not counted, however the composition of grains >2 mm was noted. Feldspar was recognized by twinning, zoning, increased alteration, and cleavage; thin sections were not stained to determine feldspar composition. Athey and Smith communicated frequently in order to identify grain types consistently, and eight thin sections were point-counted by both geologists for comparative purposes. Consistent but acceptable differences occurred in the counts of coarse polycrystalline quartz, feldspar, and felsic volcanic rock fragments. Interpretations are based on 52 thin sections point-counted by Athey and eight thin sections point-counted by Smith (table C1). Sample locations, grain size, and a brief description of the matrix and cement are included in table C2.

This page has intentionally been left blank.

















Table C2. Supporting information including sample locations for sandstone samples collected in the Liberty Bell area, Fairbanks A-4 Quadrangle, Alaska. Location coordinates were collected using a hand-held GPS unit (no differential correction was applied), and coordinates are presented in latitude and longitude (based on the NAD27 Alaska datum) and in UTM coordinates (based on the Clark 1866 spheroid, NAD27 datum, UTM zone 6 projection).

Sample Number	Latitude	Longitude	UTM Easting	UTM Northing	Average Grain Size (mm)	Range (mm)	Cement and matrix comments	Other comments
2005JEA133A	64.093564	-148.577705	423092	7108197	0.3	0.15-1.2	silty matrix	5 large oversize grains
2005JEA157A	64.003297	-148.777907	413054	7098398	0.03	0.02-2.0	silty matrix with iron oxide and clay	1 large oversize grain
2005JEA160A	64.006314	-148.761612	413860	7098712	0.4	0.2-0.75		
2005JEA164A	64.012388	-148.732002	415326	7099349	0.25	0.05-0.75		2 oversize grains
2005JEA170A	64.047766	-148.733295	415370	7103292	0.5	0.02-1.65		
2005JEA173A	64.0442	-148.728199	415608	7102888	0.375	0.15-1.6	sparse clay matrix	
2005JEA178A	64.115652	-148.514441	426234	7110583	0.2	0.1-0.3		
2005JEA180A	64.119489	-148.522556	425849	7111020	0.25	0.02-1.75	discrete grains coated with iron oxide	4 large oversize grains
2005JEA209A	64.10764	-148.827083	410983	7110090	0.1	0.02-2.0	silty matrix	10 oversize grains
2005JEA213A	64.105797	-148.635565	420307	7109631	0.35	0.6-2.0		2 oversize grains; abundant chert
2005JEA219A	64.104799	-148.661061	419062	7109552	0.2	0.02-1.1	sparse silty matrix	3 large oversize grains
2005JEA229A	64.123932	-148.670831	418642	7111696	0.25	0.02-1.5	iron oxide coating, clay matrix	3 large oversize grains
2005JEA231A	64.007224	-148.970197	403666	7099112	0.25	0.02-2.0	silty matrix	
2005JEA232A	64.01224	-148.896199	407300	7099561	0.5	0.02-1.75	some grains have iron-oxide coating	
2005JEA235A	64.016303	-148.773537	413308	7099841	0.25	0.02-2.0	iron-oxide-coated grains, clayey and silty matrix	2 oversize grains
2005JEA236A	64.032161	-148.726861	415637	7101545	0.15	0.02-0.85		
2005JEA237C	64.029431	-148.7783	413116	7101310	0.15	0.02-0.5		
2005JEA238C	64.038074	-148.761445	413966	7102250	0.45	0.1-1.5		abundant oversize grains
2005JEA243A	64.128475	-148.630324	420627	7112151	0.5	0.35-1.5	iron-oxide-coated grains	4 oversize grains
2005JEA249A	64.074833	-148.744287	414916	7106322	0.875	0.125-2.0	silica cement	
2005JEA46C	64.075174	-148.840417	410229	7106492	0.25	0.05-2.0	most small grains coated with iron oxide, silty clayey matrix	8 large oversize grains
2005JEA501A	63.920759	-148.903578	406635	7089381	0.2	0.02-0.5		
2005JEA502A	63.925423	-148.754555	413957	7089691	0.35	0.2-1.0		
2005JEA503A	63.925255	-148.758052	413785	7089677	0.3	0.02-2.0		
2005JEA70C	64.063966	-148.82371	411008	7105220	0.25	0.02-1.0		2 oversize grains
2005JEA72A	64.066865	-148.816642	411362	7105533	0.4	0.02-2.0		6 large oversize grains
2005LF106A	64.040469	-148.64595	419613	7102366	0.1	0.02-1.75		
2005LF118A	64.048635	-148.664335	418739	7103299	0.2	0.03-1.0		
2005LF151A	64.091762	-148.547404	424564	7107960	0.25	0.02-1.8	iron-oxide cement	2 oversize quartz grains
2005LF173B	64.090168	-148.79346	412566	7108097	0.04	0.02-0.1	iron-oxide cement	
2005LF178B	64.094737	-148.799951	412264	7108615	0.02	<0.05	iron-oxide cement, fused	
2005LF203A	64.1063	-148.75876	414307	7109847	0.35	0.02-1.75	clayey matrix	
2005LF218B	64.036905	-148.544569	424554	7101845	0.25	0.20-1.75		
2005LF221A	64.040146	-148.550481	424274	7102213	0.2	0.02-0.5		
2005LF28A	64.052315	-148.791211	412557	7103877	0.25	0.2-0.0625		abundant chert
2005LF84A	64.087429	-148.562322	423825	7107495	0.2	0.02-0.5	silty matrix	6 large oversize grains
2005MBW128A	64.072141	-148.90997	406827	7106254	0.5	0.35-2.0		
2005MBW150A	64.095974	-148.95199	404859	7108971	0.5	0.1-1	iron-oxide coatings around most grains	
2005MBW231A	64.043246	-148.583402	422675	7102598	0.125	0.02-1.0	clayey and silty matrix	
2005MBW236A	64.038264	-148.587604	422456	7102048	0.2	0.02-2.0	clayey and silty matrix	
2005MBW248A	64.027821	-148.651591	419301	7100964	0.02	<0.075	silty matrix, iron-oxide cement	
2005MBW283A	64.102915	-148.590221	422508	7109254	0.3	0.03-1.0	sparse clayey matrix	
2005MBW284A	64.109604	-148.575165	423260	7109981	0.25	0.1-2.0	some iron-oxide-coated grains and ferricreted clay	4 large oversize grains
2005MBW384A	64.051249	-148.978693	403403	7104029	0.4	0.2-1.5	iron-oxide cement between sparse grains	abundant oversize grains
2005MBW81A	64.057201	-148.888229	407838	7104558	0.25	0.1-0.75	clayey silty matrix	
2005RN203A	64.048644	-148.837192	410301	7103532	0.25	0.02-0.065		
2005RN245A	64.044883	-148.995838	402544	7103346	0.2	0.05-1.0		
2005RN257A	64.022737	-148.913039	406512	7100755	0.2	0.15-1.5		

Table C2. Supporting information including sample locations for sandstone samples collected in the Liberty Bell area, Fairbanks A-4 Quadrangle, Alaska. Location coordinates were collected using a hand-held GPS unit (no differential correction was applied), and coordinates are presented in latitude and longitude (based on the NAD27 Alaska datum) and in UTM coordinates (based on the Clark 1866 spheroid, NAD27 datum, UTM zone 6 projection)—continued.

Sample Number	Latitude	Longitude	UTM Easting	UTM Northing	Average Grain) Size (mm)	Range (mm)	Cement and matrix comments	Other comments
2005RN265A	64.040954	-148.883279	408026	7102741	0.5	0.02-1.0		
2005RN367A	64.008057	-148.604236	421559	7098703	0.25	0.01-0.55	abundant clayey matrix	
2005Z160A	64.018709	-148.67524	418119	7099979	0.45	0.02-2.0		bimodal, very fine- and medium-grained
2005Z163A	64.011075	-148.677953	417964	7099132	0.25	0.02-1.0	clayey matrix	
2005Z191A	64.027039	-148.696065	417126	7100934	0.15	0.02-1.625	clayey matrix	
2005Z193A	64.028761	-148.683048	417767	7101109	0.175	0.02-2	sparse clayey, silty matrix	
2005Z216A	64.082108	-148.982238	403337	7107472	0.4	0.02-2.0	clayey matrix	
2005Z233A	64.009175	-148.673769	418163	7098915	0.3	0.15-0.5	iron-oxide cement	
2005Z255A	64.074286	-148.773144	414229	7106465	0.3	0.125-2.0	clay matrix	
2005Z38A	64.124866	-148.743541	415105	7111895	0.625	0.075-1.625		
2005Z75A	64.084901	-148.745266	414899	7107445	0.3	0.02-1.5	silty matrix	4 large oversize grains
2005Z96A	64.080278	-148.688271	417664	7106855	0.2	0.02-1.75	clayey matrix	

## **Appendix D**

### **Clay compositions of Tertiary samples**

Clay mineralogy was determined for 65 fine-grained, poorly consolidated, sedimentary rock samples (table D1). Compacted samples were gently broken apart with a rubber-topped pestle and ceramic mortar. A clay fraction with low silt content was prepared by dry sieving and retaining the -325 or -400 mesh fraction. After adding acetone to a representative portion, the suspended solids were transferred to a glass slide and allowed to dry. Diffractometer traces were obtained by scanning 5–13° at 0.5° per minute using Ni-filtered Cu radiation on a Rigaku XRD. Relative heights of the 12.5° (kaolinite and/or chlorite), 8.5–9° (illite/muscovite), and 6.2–6.9° (montmorillonite and/or chlorite) peaks were then recorded. Samples were also tested with Benzidine for the presence of montmorillonite; positive if the sample turned bright blue. If the sample turned greenish blue, montmorillonite was considered present if it also displayed a broad peak in the 6.2–6.9° range. (Chlorite displays a sharp peak in this region.) Nine of 15 samples with questionable Benzidine reactions had such peaks. Chlorite was unambiguously identified if the sample displayed both 6.2–6.9° and 12.5° peaks and also failed the Benzidine test. Kaolinite was unambiguously identified if the sample displayed a 12.5° peak but no 6.2–6.9° peak. Samples with an additional peak in the vicinity of 10° were noted as possibly containing a zeolite.

This page has intentionally been left blank.

Table D1. Qualitative clay compositions of Tertiary samples from the Liberty Bell area, Fairbanks, A-4 Quadrangle, Alaska determined by X-ray diffraction and benzidine application. Location coordinates were collected using a hand-held GPS unit (no differential correction was applied), and coordinates are presented in latitude and longitude (based on the NAD27 Alaska datum) and in UTM coordinates (based on the Clark 1866 spheroid, NAD27 datum, UTM zone 6 projection). Key: xxxxx = very large peak, xxx = large peak, xx = moderate peak, x = small peak, x = very small peak, and blank = no peak.

Sample Number	Latitude	Longitude	UTM Easting	UTM Northing	Kaolinite	Montorillonite	Other minerals
2005JEA133A	64.093564	-148.577705	423092	7108197	x	x	
2005JEA155A	63.997823	-148.795226	412190	7097812	xx	x	
2005JEA155B	63.997823	-148.795226	412190	7097812	x	xxx	
2005JEA157A	64.003297	-148.777907	413054	7098398	xxx	xx	
2005JEA160A	64.006314	-148.761612	413860	7098712	x		Possible zeolite
2005JEA164A	64.012388	-148.732002	415326	7099349	x	x	
2005JEA171A	64.045254	-148.730149	415516	7103008	xx	x	
2005JEA173A	64.0442	-148.728199	415608	7102888	xxxx	xxx	Chlorite?
2005JEA209A	64.10764	-148.827083	410983	7110090	xxx		
2005JEA213A	64.105797	-148.635565	420307	7109631	x	x	
2005JEA213A (duplicate)	64.105797	-148.635565	420307	7109631	x	xxx	Chlorite?
2005JEA219A	64.10479	-148.661061	419062	7109552	xxxx		
2005JEA229A	64.123932	-148.670831	418642	7111696		xxx	Chlorite?
2005JEA232A	64.01224	-148.896199	407300	7099561	x	x	
2005JEA234A	64.00725	-148.790779	412437	7098856	x	x	
2005JEA237C	64.029431	-148.7783	413116	7101310	xx		
2005JEA238C	64.038074	-148.761445	413966	7102250	xx	x	Possible zeolite
2005JEA266A	64.097881	-148.701281	417082	7108833	xxx		
2005JEA502A	63.925423	-148.754555	413957	7089691	xxx	x	Chlorite?
2005JEA503A	63.925255	-148.758052	413785	7089677	xxx	x	
2005JEA58A	64.04759	-148.882396	408091	7103479	x	x	
2005JEA59A	64.050125	-148.884226	408010	7103764	x		
2005JEA64A	64.062592	-148.850757	409684	7105105	xxx	xxxx	
2005JEA70C	64.063966	-148.82371	411008	7105220	x		
2005JEA72A	64.066865	-148.816642	411362	7105533	x		
2005LF103A	64.042218	-148.641363	419842	7102555	xxx	x	
2005LF106A	64.040469	-148.64595	419613	7102366	xxxx		
2005LF107A	64.039087	-148.648346	419492	7102215	xxxx	x	Chlorite?
2005LF108E	64.03838	-148.649758	419421	7102138	xxxxx		
2005LF110A	64.037474	-148.654435	419190	7102043	xxxx	x	
2005LF111A	64.03683	-148.656526	419086	7101974	xxxx	x	
2005LF118A	64.048635	-148.664335	418739	7103299	xxxx	xxx	
2005LF119A	64.046805	-148.665783	418663	7103097	xxxxx	xx	

Table D1. Qualitative clay compositions of Tertiary samples from the Liberty Bell area, Fairbanks, A-4 Quadrangle, Alaska determined by X-ray diffraction and benzidine application. Location coordinates were collected using a hand-held GPS unit (no differential correction was applied), and coordinates are presented in latitude and longitude (based on the NAD27 Alaska datum) and in UTM coordinates (based on the Clark 1866 spheroid, NAD27 datum, UTM zone 6 projection). Key: xxxxx = very large peak, xxx = large peak, xxx = moderate peak, xx = small peak, x = very small peak, and blank = no peak—continued.

Sample Number	Latitude	Longitude	UTM Easting	UTM Northing	Kaolinite	Montorillonite	Other minerals
2005LF120A	64.046054	-148.66709	418597	7103015	xxxx	xx	
2005LF186A	64.086335	-148.756658	414348	7107620	xxxx		
2005LF186A (duplicate)	64.086335	-148.756658	414348	7107620	xxxx		
2005LF203A	64.1063	-148.75876	414307	7109847	xxxxx		
2005LF217B	64.036322	-148.543758	424592	7101779	xxxxx		
2005LF218A	64.036905	-148.544569	424554	7101845	xxxxx	x	
2005LF218B	64.036905	-148.544569	424554	7101845	xxxxx	xx	Chlorite?
2005LF221A	64.040146	-148.550481	424274	7102213	xxxx		Chlorite?
2005LF27A	64.051843	-148.798926	412179	7103835			Chlorite?
2005LF31B	64.050347	-148.762752	413940	7103619	xx	x	Possible Zeolite
2005LF84A	64.087429	-148.562322	423825	7107495			All chlorite and mica
2005LF86A	64.089843	-148.554005	424237	7107754	xxx		Possible Zeolite
2005MBW128A	64.072141	-148.90997	406827	7106254	x	xx	
2005MBW150A	64.095974	-148.95199	404859	7108971	x	xxx	
2005MBW231A	64.043246	-148.583402	422675	7102598	xxxx	x	
2005MBW236A	64.038264	-148.587604	422456	7102048	xxx	x	
2005MBW283A	64.102915	-148.590221	422508	7109254	xx		
2005MBW81A	64.057201	-148.888229	407838	7104558	x		
2005RN203A	64.048644	-148.837192	410301	7103532	xx	x	
2005RN245A	64.044883	-148.995838	402544	7103346	x		
2005RN251A	64.03335	-148.981848	403187	7102040	x	x	
2005RN257A	64.022737	-148.913039	406512	7100755	xx	xxx	
2005RN265A	64.040954	-148.883279	408026	7102741	xx		
2005RN367A	64.008057	-148.604236	421559	7098703	xxxxx	xxxx	
2005RN371A	64.019655	-148.627514	420454	7100024	xxx		Chlorite?
2005RN372A	64.020129	-148.636505	420016	7100088	xxx		Chlorite?
2005RN373A	64.022734	-148.633915	420150	7100375	xxxx	xx	
2005RN374A	64.022589	-148.628401	420419	7100352	xxx		Chlorite?
2005RN398A	64.017414	-148.639211	419876	7099789	xxxx		
2005Z191A	64.027039	-148.696065	417126	7100934	xxxx	xx	Chlorite?
2005Z193A	64.028761	-148.683048	417767	7101109	x		Mostly chlorite
2005Z255A	64.075946	-148.758444	413507	7106300	xxxxx		
2005Z38A	64.124866	-148.743541	415105	7111895	xxx		
2005Z75A	64.084901	-148.745266	414899	7107445	xxxx		

## **Appendix E**

### **Palynology**

Fifteen fine-grained sedimentary rock and coal samples were selected for palynology (table E1). Samples were processed by Russ Harms of Global Geolab Ltd. and analyzed by R.L. Ravn of the IRF Group, Inc. See table 4 for assigned Tertiary units and indicated environmental conditions during deposition.

This page has intentionally been left blank.

Table E1. Raw pollen count data. Location coordinates were collected using a hand-held GPS unit (no differential correction was applied), and coordinates are presented in latitude and longitude (based on the NAD 27 Alaska datum) and in UTM coordinates (based on the Clark 1866 spheroid, NAD 27 datum, UTM zone 6 projection). Note: n = pollen grain was noted in the sample but not included in the total counted grains of the sample.

						Climate	warm	warm	warm	warm	warm
						Moisture					
						Common Name	basswood or linden	basswood or linden	cyprus	elm	fern
						Age	Miocene	Miocene	Miocene	Miocene	Miocene
Map Location	Sample Number	Latitude	Longitude	UTM Easting	UTM Northing	Sample Type	Tilia - microrugulate/reticulate	Tilia - nearly smooth	Taxodium	Ulmus	Deltoidospora spp. - indet.
P1	2005JEA160C	64.006314	-148.761612	413860	7098712	shale		n	n	4	
P2	2005JEA237B	64.029431	-148.7783	413116	7101310	siltstone	1	6		16	4
P3	2005MBW415A	64.046366	-148.729501	415551	7103131	coal		1		3	1
P4	2005Z235A	64.003595	-148.725669	415609	7098361	coal					
P5	2005Z165B	64.013015	-148.684044	417672	7099356	silty sandstone		1		n	3
P6	2005Z171B	64.021726	-148.697523	417039	7100344	siltstone		2			5
P7	2005LF124A	64.035824	-148.678539	418008	7101890	coal				1	5
P8	2005Z47B	64.102325	-148.734638	415470	7109372	siltstone			n	n	2
P9	2005MBW232A	64.042121	-148.582048	422738	7102471	coal				1	
P10	2005MBW144A	64.086613	-148.939087	405456	7107909	coal		1	1	1	
P11	2005JEA210C	64.106886	-148.828512	410911	7110008	siltstone		n	3	10	1
P12	2005LF105A	64.040906	-148.639873	419911	7102407	coal				12	2
P13	2005Z36C	64.125307	-148.752381	414676	7111956	siltstone		n	2	4	16
P14	2005LF217D	64.036322	-148.543758	424592	7101779	coal					1
P15	2005Z229A	64.00186	-148.67057	418298	7098096	coal					





Table E1. Raw pollen count data. Location coordinates were collected using a hand-held GPS unit (no differential correction was applied), and coordinates are presented in latitude and longitude (based on the NAD 27 Alaska datum) and in UTM coordinates (based on the Clark 1866 spheroid, NAD 27 datum, UTM zone 6 projection). Note: n = pollen grain was noted in the sample but not included in the total counted grains of the sample—continued.

		?	?	?	?	?	?	?	?	?	?	?	?
		angio-sperm	angio-sperm	angio-sperm	angio-sperm	angio-sperm	angio-sperm	angio-sperm	angio-sperm	angio-sperm	angio-sperm	angio-sperm	angio-sperm
		Miocene	Miocene	Miocene	Miocene	Miocene	Miocene	Miocene	Miocene	Miocene	Miocene	Miocene	Miocene
Map Location	Sample Number	trisyncolporate indet., oblate	tricolporate indet., spherical, large	Foveotricolporites sp. - rhombohedral	Tricolporites sp. - indet., large, triangular, thin	Ericaceae	tetraatriate pollen - indet., oblate, square	tricolporoidate pollen - indet., oblate, finely foveolate	Tricolporopollenites sp. - indet., prolate, ovoid, thin	cf. Margocolporites sp. - indet.	tricolporate indet., ~spherical, large, thin, long colpi	Plicapollis? sp.	Tricolporites sp. - indet., large, foveolate, tectate, rhomboidal
P1	2005JEA160C	n											
P2	2005JEA237B	1											
P3	2005MBW415A					15							
P4	2005Z235A					5							
P5	2005Z165B					2							
P6	2005Z171B					1							
P7	2005LF124A	1				2							
P8	2005Z47B												
P9	2005MBW232A					n	1	n	n	n			
P10	2005MBW144A					7							
P11	2005JEA210C		2	n	n								
P12	2005LF105A					n							
P13	2005Z36C					1			3		21	n	n
P14	2005LF217D												
P15	2005Z229A												





## **Appendix F**

### **Energy and geochemical analyses of coal and coal ash**

Twenty-one samples of coal were collected for energy and geochemical analyses. The weathered layer was cleaned off of coal layers greater than 1 foot thick and a fresh channel sample was collected in doubled-up ziplock bags surrounded by packing tape. Sample information and apparent coal rank calculations are compiled in table F1. Coal energy analyses were performed to American Society of Testing Materials (ASTM) standards by R.L. Stull of Geochemical Testing (table F2). For information on ASTM standards, visit the ASTM website, <http://www.astm.org/>, or contact ASTM Customer Service at [service@astm.org](mailto:service@astm.org). For Annual Book of ASTM Standards volume information, refer to the standard's Document Summary page on the ASTM website. J.D. McCord at the USGS Energy Lab analyzed the major-, minor-, and trace-element composition of the coal and coal ash (table F3). Geochemical analyses were performed to American Society of Testing Materials (ASTM), International Standards Organization (ISO), Environmental Protection Agency (EPA), and USGS standards. Most elements were analyzed by inductively coupled plasma–mass spectroscopy (ICP–MS) or inductively coupled plasma–atomic emission spectroscopy (ICP–AES). Analytical methods and reporting limits are included in table F4.

This page has intentionally been left blank.

Table F1. Apparent coal rank calculations and supporting sample data from coal samples collected in the Liberty Bell area, Fairbanks A-4 Quadrangle, Alaska. Apparent coal rank calculations are based on the formulas and criteria from Wood and others (1983). Location coordinates were collected using a hand-held GPS unit (no differential correction was applied), and coordinates are presented in latitude and longitude (based on the NAD27 Alaska datum) and in UTM coordinates (based on the Clark 1866 spheroid, NAD27 datum, UTM zone 6 projection).

Map Location	Sample Number	Latitude	Longitude	UTM Easting	UTM Northing	Formation	Lithology	Apparent Thickness	Mineral-Matter-Free BTU	Matter-Free Fixed Carbon %	Apparent Coal Rank
C1	2005LF124A	64.035824	-148.678539	418008	7101889	Healy Creek	platey lignite coal beds, bed thickness is variable but mostly 8 cm thick	1.5 m	7692	46	Lignite A
C2	2005MBW232A	64.042121	-148.582048	422738	7102471	Healy Creek	black, breaks into smooth fractured pieces, interbedded with thin, light brown claystone	unknown	6957	46	Lignite A
C3	2005MBW266A	64.035915	-148.678463	418012	7101899	Healy Creek	black, breaks with smooth surface	>2.4 m	7879	45	Lignite A
C4	2005Z36B	64.125307	-148.752381	414676	7111956	Healy Creek	nearly horizontal seam of dark brown to black lignite	30 cm	6465	43	Lignite A
C5	2005Z38D	64.124866	-148.743541	415105	7111895	Healy Creek	seams vary from <1-cm-thick discontinuous partings up to 20-cm-thick traceable beds; at least 14 beds >5 cm thick; some coal with resin grains up to 6 mm	unknown	7284	43	Lignite A
C6	2005Z47A	64.102325	-148.734638	415470	7109372	Healy Creek	base of coal outcrop is not exposed, interbedded silty claystone 2 cm thick	>2.4 m	7996	42	Lignite A
C7	2005LF105A	64.040906	-148.639873	419910	7102406	Healy Creek	platey coal	0.6 m	8679	46	High-volatile Subbituminous C
C8	2005JEA160B	64.006314	-148.761612	413865	7098723	Lignite Creek	platey coal	76 cm	6767	39	Lignite A
C9	2005MBW245A	64.029164	-148.64557	419600	7101105	Suntrana	both burnt and unburnt coal are present; coal is black, planar bedded, and smooth and slightly shiny on broken surfaces	unknown	6972	41	Lignite A
C10	2005MBW415A	64.046366	-148.729501	415551	7103130	Suntrana	slightly conchoidal to mostly hackley fracturing coal; beds slightly folded	3.05 m	8068	43	Lignite A
C11	2005Z155A	64.011346	-148.662115	418738	7099142	Suntrana	coal seam	45 cm	7308	49	Lignite A
C12	2005Z167A	64.011991	-148.694866	417140	7099255	Suntrana	5.6-cm-thick coal seam located 1.4 m above this coal seam tops a fining upward cycle; base of bed is underwater	1.34 m	7707	44	Lignite A
C13	2005Z170A1	64.020545	-148.699498	416938	7100214	Suntrana	black lignite coal, top sample of three samples	2.5 m	7618	44	Lignite A
C14	2005Z170A2	64.020545	-148.699498	416938	7100214	Suntrana	thick black outcrop of lignite coal, middle sample of three samples	4 m	7975	44	Lignite A
C15	2005Z170A3	64.020545	-148.699498	416938	7100214	Suntrana	black lignite coal, bottom sample of three samples; lowermost sample is pretty clean, without obvious silt or ash layers; bed looks horizontal, lower contact is with siltstone below.	2-3 m	6856	43	Lignite A
C16	2005MBW254A	64.027424	-148.662007	418791	7100932	Suntrana	black, smoothly fracturing, layered coal with minor brown clay on partings	1.52 m	5973	40	Lignite B
C17	2005Z156C	64.013001	-148.667369	418487	7099332	Suntrana	sand above and silt below; coal has tree roots going through it	57 cm	5438	38	Lignite B
C18	2005Z165A	64.013015	-148.684044	417672	7099356	Suntrana	lignite coal crops out beneath 5-cm-thick soil cover	38 cm	6133	42	Lignite B
C19	2005Z171A	64.021726	-148.697523	417039	7100343	Suntrana	unit overlies a gray chocolate brown siltstone	unknown	6142	38	Lignite B
C20	2005Z171C	64.021726	-148.697523	417039	7100343	Suntrana	lignite coal	1.6 m	6261	39	Lignite B
C21	2005Z236A	64.005587	-148.726426	415578	7098584	Suntrana	3-m-thick coal bed with slight warp to coal/sandstone contact; slight ferricrete cementing of sandstone for 3-4 cm at upper contact	3 m	8371	45	High-volatile Subbituminous C

This page intentionally left blank.



Table F2. Raw coal energy data from samples collected in the Liberty Bell area, Fairbanks A-4 Quadrangle, Alaska. Analyses were performed to American Society of Testing Materials (ASTM) standards—continued.

	ASTM standard	2005JEA160B	2005LE105A	2005LE124A	2005MBW232A	2005MBW245A	2005MBW254A	2005MBW266A	2005MBW415A	2005Z155A	2005Z156C	2005Z165A	2005Z167A	2005Z170A1	2005Z170A2	2005Z170A3	2005Z171A	2005Z171C	2005Z236A	2005Z36B	2005Z38D	2005Z47A
<b>Heating Value (BTU/Lb)</b>	D5865																					
<b>As received</b>		4840	7613	6000	4520	6521	2441	5875	7823	5593	3334	5463	7345	6175	6261	4474	3236	3332	7671	5605	5738	5741
<b>Dry</b>		7008	10171	8403	6241	9837	3100	7973	11335	8062	4841	8661	11004	8662	8464	6217	4375	4531	10430	9116	8359	7677
<b>Dry Ash-Free</b>		11349	11994	11760	11308	10820	10195	11722	11818	11746	10103	10322	11773	11494	11580	11251	10752	11037	11657	11430	11734	11796
<b>FORMS OF SULFUR</b>	D2492																					
<b>As Received</b>																						
Sulfate Sulfur		0.01	0.01	0.01	0.01	0.01	0.01	0.02	0.01	0	0.01	0.01	0.02	0.02	0.02	0.01	0.02	0.01	0.01	0.01	0.02	0.01
Pyritic Sulfur		0.02	0.06	0.02	0.02	0.02	0.01	0.01	0.01	0.01	0.04	0.01	0.01	0.01	0.02	0.02	0.01	0.04	0.01	0.01	0.02	0.01
Organic Sulfur		0.27	0.19	0.14	0.12	0.18	0.2	0.13	0.14	0.27	0.07	0.11	0.08	0.17	0.28	0.16	0.17	0.13	0.18	0.65	0.62	0.13
<b>Dry</b>																						
Sulfate Sulfur		0.01	0.01	0.01	0.01	0.01	0.01	0.02	0.01	0	0.01	0.01	0.03	0.02	0.01	0.01	0.02	0.01	0.01	0.01	0.03	0.01
Pyritic Sulfur		0.03	0.08	0.03	0.02	0.03	0.01	0.01	0.01	0.02	0.05	0.02	0.01	0.01	0.01	0.03	0.01	0.05	0.01	0.01	0.02	0.01
Organic Sulfur		0.39	0.26	0.2	0.18	0.28	0.26	0.18	0.2	0.39	0.11	0.17	0.13	0.25	0.15	0.22	0.24	0.18	0.25	1.07	0.91	0.18
<b>Dry Ash Free</b>																						
Sulfate Sulfur		0.02	0.01	0.01	0.02	0.01	0.03	0.03	0.01	0	0.02	0.01	0.04	0.03	0.01	0.02	0.05	0.03	0.01	0.01	0.05	0.02
Pyritic Sulfur		0.05	0.09	0.04	0.04	0.04	0.03	0.02	0.01	0.03	0.11	0.03	0.01	0.01	0.01	0.06	0.03	0.13	0.01	0.01	0.03	0.02
Organic Sulfur		0.62	0.32	0.29	0.33	0.3	0.85	0.26	0.21	0.56	0.23	0.2	0.13	0.33	0.22	0.39	0.59	0.44	0.28	1.34	1.26	0.27
<b>Free Selling Index</b>	D720-91	0	0	0	0	0	0	0	0	0	0	0	0	0	0	0	0	0	0	0	0	0
<b>Equilibrium Moisture</b>	D1412-03	21.79	25.56	28.16	26.83	22.89	17.28	29.8	25.93	28.71	23.49	34.01	27.29	28.54	26.98	27.38	24.62	23.24	29.67	36.99	25.71	22.49

Table F3. Major-, minor-, and trace-element geochemical analyses of coal and coal ash from samples collected in the Liberty Bell area, Fairbanks A-4 Quadrangle, Alaska. Note: < RPT = value was less than reported limit.

Sample Number	Moisture %	Hg ppm	Se ppm	Cl ppm	S %	Al %	Ba ppm	Be ppm	Ca %	Co ppm	Cr ppm	Cu ppm	Fe %	K %
2005JEA160B	7.26	0.144	1.03	17.8	0.417	11.2	1380	3.39	5.2	14.5	168	179	2.3	1.07
2005LF105A	9.33	0.122	0.337	50.3	0.359	12.5	3510	5.47	6.74	51.2	185	201	3.06	1.24
2005LF124A	6.37	0.14	0.452	31.2	0.243	14.4	2340	4.09	3.07	43.2	215	111	1.85	2.08
2005MBW232A	6.49	0.175	0.472	13.4	0.202	13.2	3210	3.83	1.43	17.6	227	108	1.54	2.77
2005MBW245A	8.45	0.106	0.244	17.8	0.266	9.74	12000	7.29	16.9	61.7	135	151	5.55	0.87
2005MBW254A	2.85	0.355	0.313	23.2	0.267	10.1	784	2.09	0.402	4.26	24.6	10.8	0.93	2.53
2005MBW266A	6.13	0.14	0.466	10.8	0.213	14	2100	3.58	2.82	29.7	193	100	1.25	2.28
2005MBW415A	10.6	0.076	< RPT	12.6	0.202	9.04	6800	45.2	20.7	20.4	73.3	84.2	7.6	0.551
2005Z155A	7.21	0.258	1.03	10.7	0.436	7.2	2730	3.74	3.71	48.1	194	122	1.76	1.28
2005Z156C	7.7	1.25	1.41	19.1	0.142	11.9	2310	5.09	2.87	24.9	147	111	2.52	1.79
2005Z165A	9.43	0.125	< RPT	19.5	0.2	9.84	2900	3.12	12.3	29.6	137	116	4.19	1.04
2005Z167A	11.9	0.19	< RPT	17.8	0.134	5.57	6040	18.7	25.8	202	120	117	8.02	0.268
2005Z170A1	9.21	0.116	0.312	13.5	0.208	11.4	1890	3.16	6.75	28.3	163	150	2.47	1.27
2005Z170A2	10.1	0.123	0.31	10.6	0.187	11.4	1790	2.82	6.9	22.1	149	135	2.46	1.13
2005Z170A3	6.96	0.138	0.462	11	0.218	12	1150	3.18	3.04	16.7	155	112	3.02	1.51
2005Z171A	7.41	0.138	1.48	< RPT	0.223	11.8	1060	3.76	2.73	16.5	163	98.9	1.96	1.51
2005Z171C	5.75	0.145	1.54	12.4	0.199	11.2	1030	3.54	2.59	15.1	155	119	2.5	1.63
2005Z236A	10.3	0.11	0.24	10.4	0.209	9.15	3340	4.78	17.3	38.4	140	148	4.13	0.723
2005Z36B	9.82	0.178	2.9	61	0.974	8.67	3490	26.4	6.01	87.7	60.7	171	2.96	2.16
2005Z38D	9.4	0.24	1.76	26.8	0.902	11.5	6530	16.6	1.93	40.4	76.5	146	2.43	1.95
2005Z47A	6.12	0.18	< RPT	19.5	0.181	15.5	2850	3.37	1.77	8.3	39.1	30.7	2.66	2.52

Table F3. Major-, minor-, and trace-element geochemical analyses of coal and coal ash from samples collected in the Liberty Bell area, Fairbanks A-4 Quadrangle, Alaska. Note: < RPT = value was less than reported limit—continued.

Sample Number	Li ppm	Mg %	Mn ppm	Na %	Ni ppm	P %	S %	Sc ppm	Si %	Sr ppm	Th ppm	Ti %	V ppm	Y ppm
2005JEA160B	51.1	1.47	1010	0.226	45.4	0.0217	1.03	32.4	26.5	155	15.4	0.639	274	48.3
2005LF105A	69.3	1.1	467	0.0848	141	0.0319	2.18	43.2	23.7	949	30.5	0.615	302	57
2005LF124A	92.7	0.956	401	0.0974	174	0.0252	0.815	35.2	25.8	352	31.6	0.701	292	33.5
2005MBW232A	85.7	0.869	59.8	0.102	49.3	0.0235	0.468	31.8	27.9	272	23.9	0.626	344	30.4
2005MBW245A	66.3	1.22	244	0.038	98.4	0.0427	3.2	33.5	14.9	2460	24.8	0.453	229	91.2
2005MBW254A	33.5	0.433	152	0.0453	10.5	0.0285	0.199	6.86	33	69.7	13.7	0.222	34.6	11.1
2005MBW266A	81.1	0.984	218	0.1	88.4	0.0203	0.636	31.9	27.5	332	24.8	0.743	279	29.1
2005MBW415A	60.6	2.61	2190	0.0574	48.4	0.0502	5.14	24.8	10.4	2200	18.7	0.285	156	48.8
2005Z155A	56.2	0.889	199	0.0536	118	0.123	1.25	25.2	31.7	535	22.1	0.398	194	40.8
2005Z156C	45.2	0.68	656	0.14	34.4	0.0222	0.395	29.7	28.7	450	29.9	0.592	247	44.8
2005Z165A	50	1.68	2970	0.114	59.3	0.0273	1.28	31.4	22.3	1150	17.4	0.652	234	35.6
2005Z167A	48.8	3.76	4460	0.128	697	0.0338	3.04	21.5	10.2	2840	< RPT	0.486	137	102
2005Z170A1	48.2	1.35	1100	0.13	67.4	0.0388	1.15	31	25.3	563	14.6	0.615	276	34.8
2005Z170A2	46.7	1.32	868	0.102	60.2	0.0501	0.907	30.1	25.9	568	12.3	0.627	242	34.6
2005Z170A3	49	1.11	770	0.238	58.8	< RPT	0.641	27.7	28.6	249	10.1	0.577	230	30.4
2005Z171A	56.9	0.976	377	0.576	54.8	< RPT	0.48	28.8	29.7	183	11.1	0.669	248	41.8
2005Z171C	51.8	1.13	342	0.636	51.1	< RPT	0.444	28.2	28.9	177	11.7	0.594	247	39.7
2005Z236A	48.7	2.6	2860	0.114	79.5	0.0261	2.6	35.4	16.5	1860	20.9	0.534	253	54.7
2005Z36B	38.4	1.29	783	0.398	564	0.0439	3.88	36.4	24.7	423	33.5	0.257	255	295
2005Z38D	67.2	0.871	254	0.36	78.5	0.0558	1.35	35.3	28.6	227	36.8	0.546	336	133
2005Z47A	62.5	1.18	340	0.076	19.9	0.271	0.511	14.8	25.5	178	39.1	0.365	67	24.3

Table F3. Major-, minor-, and trace-element geochemical analyses of coal and coal ash from samples collected in the Liberty Bell area, Fairbanks A-4 Quadrangle, Alaska. Note: < RPT = value was less than reported limit—continued.

Sample Number	Ag ppm	As ppm	Au ppm	Bi ppm	Cd ppm	Cs ppm	Ga ppm	Ge ppm	Mo ppm	Nb ppm	Pb ppm	Rb ppm	Sb ppm	Sn ppm
2005JEA160B	< RPT	3.26	< RPT	0.284	0.229	8.12	18.4	2.57	4.61	7.02	17.3	85.9	1.14	4.13
2005LF105A	< RPT	2.73	< RPT	0.202	0.192	1.99	11.7	2.42	6.96	9.33	16.2	31.1	0.827	3.7
2005LF124A	< RPT	5.01	< RPT	0.297	0.328	11.3	25.7	2.88	1.8	9.7	18.6	157	1.66	6.05
2005MBW232A	< RPT	58.5	< RPT	0.772	1.04	8.52	34.4	4.6	7.59	9.06	37.3	80.2	6.05	8.32
2005MBW245A	< RPT	45.9	< RPT	1.12	2.57	14.8	33.7	7.11	8.54	13	52.8	105	12.4	9.71
2005MBW254A	< RPT	13.4	< RPT	1.11	1.6	24.2	36.1	8.01	4.25	17.1	70.1	147	13.9	11.2
2005MBW266A	< RPT	22.7	< RPT	0.88	1.75	31.3	35.7	7.14	3.99	15.2	49.9	253	11.8	10
2005MBW415A	< RPT	47.5	< RPT	0.853	0.81	6.27	22.3	7.54	12.3	8.45	42.5	65.8	38.1	6.14
2005Z155A	< RPT	37.1	< RPT	0.911	0.111	5.26	33	3.24	1.53	12.3	48.4	255	2.45	32.4
2005Z156C	< RPT	9.66	< RPT	1.03	0.686	26	34.1	7.31	3.29	16.8	47.3	160	8.48	12.2
2005Z165A	< RPT	144	< RPT	0.903	0.463	1.59	22.7	12.4	17.6	8.11	116	28.4	25	9.91
2005Z167A	< RPT	60.1	< RPT	1.42	0.787	5.82	21.3	5.8	8.89	9.62	51.6	82.7	19.3	7.23
2005Z170A1	< RPT	13.6	< RPT	1.18	0.879	20.9	33.4	10.8	8.1	13.1	60.7	138	12.8	10.2
2005Z170A2	< RPT	16.6	< RPT	0.627	0.323	5.83	24.6	6.2	8.28	9.6	34.1	71.2	8.22	6.42
2005Z170A3	< RPT	17.8	< RPT	0.299	1.38	0.158	11.7	3.36	4.12	6.49	12.4	7.56	2.4	4.38
2005Z171A	< RPT	14.3	< RPT	0.646	0.926	8.34	29.8	5.35	7.46	8.86	41.2	95.8	6.93	5.91
2005Z171C	< RPT	11.5	< RPT	0.566	0.655	6.56	30.3	3.26	4.1	8.19	31.8	71.6	4.64	5.49
2005Z236A	< RPT	13.8	< RPT	0.434	0.777	7.44	29.8	3.75	3.18	7.57	26.6	98	3.89	4.95
2005Z36B	< RPT	18.1	< RPT	0.434	0.895	7.02	30.9	6.32	3.5	9.03	26.6	95.3	4.73	6.22
2005Z38D	< RPT	18.8	< RPT	0.544	1.41	7.59	30.1	3.86	3.82	10.3	30	117	4.85	6.38
2005Z47A	< RPT	22.1	< RPT	0.752	0.772	3	21.9	6.38	16.9	9.24	37.5	35.2	13	6.58

Table F3. Major-, minor-, and trace-element geochemical analyses of coal and coal ash from samples collected in the Liberty Bell area, Fairbanks A-4 Quadrangle, Alaska. Note:  
 < RPT = value was less than reported limit—continued.

Sample Number	Te ppm	Tl ppm	U ppm	Zn ppm
2005JEA160B	0.206	0.663	2.93	63.5
2005LF105A	0.112	0.261	1.61	65.5
2005LF124A	0.185	1.04	2.76	177
2005MBW232A	0.391	0.978	5.72	87.2
2005MBW245A	0.373	1.48	11.5	126
2005MBW254A	0.334	1.45	12.3	287
2005MBW266A	0.295	1.98	7.58	43.1
2005MBW415A	0.496	0.762	12.3	82.7
2005Z155A	< RPT	1.8	10.3	31.2
2005Z156C	0.292	1.29	9.89	63.8
2005Z165A	0.365	1.16	7.26	35
2005Z167A	0.337	1.01	8.4	144
2005Z170A1	0.345	1.24	7.9	49.4
2005Z170A2	0.274	0.748	5.55	35.2
2005Z170A3	0.261	0.117	2.26	474
2005Z171A	0.371	0.917	5.43	61.1
2005Z171C	0.3	0.708	4.69	63.9
2005Z236A	0.235	0.974	4	93
2005Z36B	0.235	1.01	4.23	83.9
2005Z38D	0.284	1.17	4.88	116
2005Z47A	0.345	0.455	8.27	31.2

Table F4. Methodology and reported limits for major-, minor-, and trace-element geochemical analyses of coal and coal ash. Reported limits are at the 95 percent confidence level. Analytical methods include: ICP-MS/AES = Inductively Coupled Plasma with Mass Spectroscopy or Atomic Emission Spectroscopy and ICP-AES = Inductively Coupled Plasma with Atomic Emission Spectroscopy. Digestion: four acid digestion = HF-HNO<sub>3</sub>-HClO<sub>4</sub> and HCl leach. NOTE: — = not applicable.

Element	Reported Limits	Units	Digestion if applicable	Analytical Method	ASTM Standard	Comments
Moisture	—	percent	—	Furnace	D3173	
Hg	0.02	ppm	—	—	D6414-A	
Se	0.2	ppm	—	—	—	USGS in-house method
Cl	10	ppm	—	Combustion	D6721	Using TOX 100 Cl analyzer
S	0.05	percent	—	Combustion	D4239	Using LECO
Ashing	—	—	—	Furnace	D3174	ASTM method (750 °C) plus USGS method (525 °C)
Al	0.02	percent	four acid	ICP-AES	D6349	
Ba	2	ppm	four acid	ICP-AES	D6349	
Be	1	ppm	four acid	ICP-AES	D6349	
Ca	0.02	percent	four acid	ICP-AES	D6349	
Co	2	ppm	four acid	ICP-AES	D6349	
Cr	2	ppm	four acid	ICP-AES	D6349	
Cu	2	ppm	four acid	ICP-AES	D6349	
Fe	0.02	percent	four acid	ICP-AES	D6349	
K	0.02	percent	four acid	ICP-AES	D6349	
Li	4	ppm	four acid	ICP-AES	D6349	
Mg	0.02	percent	four acid	ICP-AES	D6349	
Mn	2	ppm	four acid	ICP-AES	D6349	
Na	0.02	percent	four acid	ICP-AES	D6349	
Ni	4	ppm	four acid	ICP-AES	D6349	
P	0.02	percent	four acid	ICP-AES	D6349	
S	0.02	percent	four acid	ICP-AES	D6349	
Sc	4	ppm	four acid	ICP-AES	D6349	
Si	0.02	percent	four acid	ICP-AES	D6349	
Sr	1	ppm	four acid	ICP-AES	D6349	
Th	8	ppm	four acid	ICP-AES	D6349	
Ti	0.02	percent	four acid	ICP-AES	D6349	
V	2	ppm	four acid	ICP-AES	D6349	
Y	1	ppm	four acid	ICP-AES	D6349	
Ag	2	ppm	four acid	ICP-MS/AES	D6721	
As	0.2	ppm	four acid	ICP-MS/AES	D6721	
Au	10	ppm	four acid	ICP-MS/AES	D6721	
Bi	0.1	ppm	four acid	ICP-MS/AES	D6721	
Cd	0.1	ppm	four acid	ICP-MS/AES	D6721	
Cs	0.1	ppm	four acid	ICP-MS/AES	D6721	
Ga	0.1	ppm	four acid	ICP-MS/AES	D6721	
Ge	0.1	ppm	four acid	ICP-MS/AES	D6721	
Mo	0.2	ppm	four acid	ICP-MS/AES	D6721	
Nb	0.1	ppm	four acid	ICP-MS/AES	D6721	
Pb	0.5	ppm	four acid	ICP-MS/AES	D6721	
Rb	0.1	ppm	four acid	ICP-MS/AES	D6721	
Sb	0.1	ppm	four acid	ICP-MS/AES	D6721	
Sn	3	ppm	four acid	ICP-MS/AES	D6721	
Te	0.1	ppm	four acid	ICP-MS/AES	D6721	
Tl	0.1	ppm	four acid	ICP-MS/AES	D6721	
U	0.1	ppm	four acid	ICP-MS/AES	D6721	
Zn	3	ppm	four acid	ICP-MS/AES	D6721	

This page intentionally left blank.

## **Appendix G**

### **Alaska Resource Data File occurrences in the southern half of the Fairbanks A-4 Quadrangle**

Alaska Resource Data File (ARDF) occurrences listed in Freeman and Schaefer (2001) and located in the Liberty Bell area were located in the field and described (table G1).

This page has intentionally been left blank.

Table G1. Mineral occurrence summaries from the southern half of the Fairbanks A-4 Quadrangle. Occurrence descriptions abstracted from Freeman and Schaefer (2001) and modified from work completed for this report and other sources as cited. Information that has been modified and additional information is displayed as italics and noted with an asterisk. Location coordinates in regular print are from the ARDF and locations in italics were collected using a hand-held GPS unit (no differential correction was applied). Coordinates are presented in latitude and longitude (based on the NAD27 Alaska datum) and in UTM coordinates (based on the Clark 1866 spheroid, NAD27 datum, UTM zone 6 projection).

ARDF Number	Latitude	Longitude	UTM Easting	UTM Northing	Occurrence Name	Deposit model, occurrence type, status	Major (Minor) Commodities	Ore and gangue minerals	Comments	Mineralized Samples (Athey and others, 2005)
FB126	64.050	-149.000	402359	7103922	Cody Creek	Placer Au occurrence, inactive	Au	Gold		
FB127	64.030	-148.970	403754	7101649	Moose Creek; Big Moose Creek; Keys; Triple Xs	Placer Au-PGE mine, inactive	Au (Hg, Pt, Sn, W)	Cassiterite, cinnabar, gold, platinum, scheelite		
FB128	64.030	-148.950	404731	7101619	Little Moose Creek	Placer Au mine, inactive	Au	Gold, scheelite		
FB129	64.050	-148.940	405287	7103832	Rambler; Barlow; Koska	Simple Sb deposit prospect, inactive	Au*, Ag, As, Sb, (Pb)*	Arsenopyrite*, galena, gold, stibnite in quartz veins	<i>Mineralized float of quartz-arsenopyrite vein, quartz vein in altered granite, and hornfelsed carbonaceous material was found 1,200 feet west of ARDF location</i>	2005MBW363A
FB130	64.073	-148.864	409092	7106300	Unnamed (near Spruce Creek)		Au (Ag, Pb, Sb)	Arsenopyrite, gold, jamesonite, scorodite in quartz veins*	<i>Several prospect pits in the headwaters area of Spruce Creek contain arsenopyrite and scorodite mineralized quartz veins; no locality was found at the ARDF location.</i>	2005JEA49A
FB131	64.048	-148.927	405897	7103538	Moose Creek		Au, Ag*, As*, Cu*	Arsenopyrite, pyrite in granodiorite*	<i>New coordinates are for a mineralized dike sample. Local placer miners report that gold is recoverable by processing quartz-tourmaline veins with a small crusher and gravity separation.</i>	2005MBW50A
FB132	64.050	-148.840	410168	7103687	Liberty Bell	<i>Au skarn, polymetallic vein*</i> mine, inactive	Ag, Au, Bi, Cu, As*	Arsenopyrite, bismuthinite, bornite, chalcopyrite, covellite, enargite, galena, gold, kobellite, loellingite, malachite, pyrrhotite, pyrite, sphalerite, tennantite, ullmannite in actinolite and phlogopite skarn and quartz tourmaline veins	<i>Of the described occurrences in the ARDF only selected mineralized areas in the Northwest Copper zone were sampled for trace-metal geochemistry.</i>	2005LF228A, 2005LF230A
FB133	64.040	-148.830	410624	7102559	Eva Creek	Placer Au mine, inactive	Au (W)	Gold, scheelite, wolframite		
FB134	64.100	-148.830	410816	7109243	Rex Creek	Placer Au mine, inactive	Au (Cu, Sb)	Chalcopyrite, gold, pyrite, stibnite		
FB135	64.070	-148.720	416086	7105751	Unnamed (near California Creek)	Simple Sb deposit prospect, inactive	Sb (W)	Ferberite, stibnite, wolframite in quartz vein	<i>The occurrence described in the ARDF was not found</i>	
FB136	64.060	-148.720	416056	7104637	California; Danzinger	Polymetallic vein mine, inactive	Au, As* (Ag, Bi, Cu, Pb, Sb)	Arsenopyrite, bismuthinite, chalcopyrite, galena, gold, jamesonite, pyrite, stibnite in quartz (tourmaline) vein*	<i>The occurrence described in the ARDF was not found, but several occurrences of shear zones with quartz (tourmaline) arsenopyrite (pyrite) veins were sampled in the immediate vicinity.</i>	2005MBW292A, 2005MBW296B, 2005MBW298A, 2005MBW303A, 2005MBW407A
FB137	64.050	-148.720	416026	7103523	California Creek	Placer Au-PGE mine, inactive	Au (Hg, Pt)	Cinnabar, gold, platinum group metals		
FB138	64.030	-148.690	417431	7101256	McAdam Creek	Placer Au mine, inactive	Au	Gold		
FB139	64.050	-148.620	420907	7103395	Unnamed (at head of Eagle Creek)	Simple Sb deposit occurrence, inactive	Sb (Ag, Au)	Stibnite, galena, gold, (pyrite) in quartz	<i>The occurrence described in the ARDF was not found</i>	
FB140	64.100	-148.520	425922	7108846	Daniels Creek	Placer Au mine, inactive	Au			
FB141	64.090	-148.490	427357	7107697	Totatlanika River	Placer Au mines, undetermined	Au			

Table G1. Mineral occurrence summaries from the southern half of the Fairbanks A-4 Quadrangle. Occurrence descriptions abstracted from Freeman and Schaefer (2001) and modified from work completed for this report and other sources as cited. Information that has been modified and additional information is displayed as italics and noted with an asterisk. Location coordinates in regular print are from the ARDF and locations in italics were collected using a hand-held GPS unit (no differential correction was applied). Coordinates are presented in latitude and longitude (based on the NAD27 Alaska datum) and in UTM coordinates (based on the Clark 1866 spheroid, NAD27 datum, UTM zone 6 projection)—continued.

ARDF Number	Latitude	Longitude	UTM Easting	UTM Northing	Occurrence Name	Deposit model, occurrence type, status	Major (Minor) Commodities	Ore and gangue minerals	Comments	Mineralized Samples (Athey and others, 2005)
FB142	64.050	-148.550	424324	7103310	Unnamed (head of Fourth of July Creek)	Polymetallic vein	<i>Ag*, Sb, Au, Pb*</i>	<i>Stibnite, cerusite, stibiconite in quartz veins*</i>	<i>Scattered veins in multiple locations on ridges north and west of the headwaters of Fourth of July Creek.</i>	2005MBW169A, 2005MBW174A, 2005MBW224A
FB143	64.030	-148.540	424759	7101070	Fourth of July Creek;	Placer Au mine, inactive	Au (Ag, Pb, Sb)	Gold, jamesonite		
FB144	64.000	-148.550	424189	7097740	Homestake Creek	Placer Au mine, inactive	Au	Gold		
<i>new*</i>	<i>64.085</i>	<i>-148.586</i>	<i>422664</i>	<i>7107253</i>	<i>Unnamed (head of Daniels Creek)*</i>	<i>Polymetallic vein prospect, inactive</i>	<i>Au, Ag (As, Bi, Pb, Sb)</i>	<i>Arsenopyrite, pyrite, stibnite in quartz-tourmaline veins</i>	<i>Veins widespread in Paleozoic metasedimentary rocks associated with Cretaceous granite dikes on the ridges around headwaters of Daniels Creek. Several trenches and hand-dug pits are the result of exploration work by Cominco, Inc. and NERCO in late 1980s (L.K. Freeman, written communication, 2006)</i>	<i>2005JEA121B, 2005LF61B, 2005LF75B, 2005LF75C, 2005LF75E, 2005LF77A, 2005LF78A, 2005LF79B</i>
<i>new*</i>	<i>64.066</i>	<i>-148.501</i>	<i>426738</i>	<i>7105041</i>	<i>Unnamed, (near mouth of Buzzard Creek)*</i>	<i>Simple Sb deposit occurrence, inactive*</i>	<i>Sb*</i>	<i>Stibnite in quartz vein*</i>	<i>Vein in cliff on east side of Totatlanika River just above flood plain.</i>	<i>2005LF141B</i>